Supporting Information

Tuning intramolecular charge transfer and spin-orbit coupling of AIE-active type-I photosensitizers for photodynamic therapy

Ravinder Singh, Deng-Gao Chen, Chun-Hsiang Wang, Chi-Chi Wu, Chao-Hsien Hsu, Chi-Hua Wu, Tai-Ying Lai, Pi-Tai Chou* and Chao-Tsen Chen*

* Department of Chemistry, National Taiwan University, Taipei 10617, Taiwan
Email: chenct@ntu.edu.tw, chop@ntu.edu.tw

List of contents:

1. Experimental section ---------- page S2-S13

2. Experimental description of ROS generation, imaging, and PDT ----- page S13-S16

3. Table S1 & Fig. S1 ---------- page S17

4. Figs. S2 & S3 ---------- page S18

5. Table S2 & Fig. S4 ---------- page S19-S26

6. Table S3-S10 ---------- page S20-S27

7. Figs. S5 & S6 ---------- page S28

8. Computational section (CS) & Fig. S7 ---------- page S29-S31

9. NMR (^{1}H & ^{13}C) (Figs. S8 to S26) ---------- pages S32-S50

10. HRMS data (Figs. S27 to S45) ---------- pages S51-S69

11. References ---------- pages S70

Experimental section

Materials and characterization. All the reagents and starting materials were commercially purchased with high purities and the solvents were dried by distillation methods under appropriate drying agents. In general, the progress of the reactions was monitored by TLC plates (i.e., Merck silica gel 60 F_{254}) and the desired compounds were purified by flash column chromatography on silica gel 60 (230-400 mesh ASTM). The precursors and the target compounds were characterized by using ^{1}H and ^{13}C NMR spectra (i.e., recorded on a Bruker AVIII 400MHz spectrometer, and samples were dissolved in either $CDCl_3$ or DMSO-d_6 depending on the solubility). The chemical shifts were expressed in ppm and the coupling constants (*J*) in Hz. The splitting patterns were abbreviated as: singlet (s), doublet (d), triplet (t), quartet (q), multiplet (m), and broad peaks (bs). High resolution of mass spectra (HRMS) was obtained on WATERS LCT Premier Xe. UV-Vis absorption and fluorescence spectra were measured on Perkin-Elmer and Hitachi F-4500 fluorescence spectrophotometers, respectively. The crystal of **TPE-*1*CUM** and reference compound **6-NEt$_2$-CUM** were grown by the vapor diffusion method, where the vapors of volatile pentane solvent were diffused into the solution of **TPE-*1*CUM** and **6-NEt$_2$-CUM** in CH_2Cl_2. The single-crystal structure was solved by SHELXL-97. Scanning electron microscope (SEM) images were taken on a S4800 (Hitachi, Japan) scanning electron microscope. SEM and fluorescent image samples were prepared by drop-casting onto Si wafers and glass plates at room temperature, respectively. Dynamic light scattering (DLS) analyses were performed by using Malvern instruments-Zetasizer Nano ZS90. The electron paramagnetic resonance (EPR) measurements were carried out on Bruker ELEXSYS-II E500 in X-band. Confocal laser scanning microscope (CLSM) characterizations were performed with a Zeiss Axiovert 200 inverted microscope

equipped with a 100x oil immersion objective with a numerical aperture of 1.4 and an Ebq 100 Isolated electronic ballast for mercury vapor compressed-arc lamps.

Syntheses of ethyl 2-(benzo[d]thiazol-2-yl) acetate (B) and (4-hydroxyphenyl)(4-methoxyphenyl)methanone (4) were conducted by following the reported procedures, respectively.[1,2]

General synthetic procedures of McMurry condensation to obtain hydroxyl and methoxy functionalized tetraphenylethylene precursors 1a-1f. Zinc dust was added in a cleaned dry 500 mL three-necked round-bottomed flask followed by the addition of dry THF (100 mL) at room temperature and purged with argon gas for 10 min. The reaction mixture was cooled to -5 to 0°C with an ice-salt bath, then titanium tetrachloride ($TiCl_4$) was added slowly drop-wise up to 10-15 min and allowed to reflux at 74°C for 4 h. The reaction mixture was cooled to -5 to 0°C again, and precursors with diverse functionalities in THF solution (15 mL) were added slowly for their corresponding desired compounds. After refluxing overnight, the reaction was cooled to room temperature, quenched with a 10% HCl aqueous solution, and extracted with ethyl acetate (200 mL). The organic layer was washed with brine solution (100 mL x 2) and dried over anhydrous $MgSO_4$. After filtration and solvent evaporation, the crude residue was purified by flash column chromatography (silica gel, hexane/ethyl acetate) to obtain white coloured solids of the desired compounds.

Synthesis of 4-(1,2,2-triphenylvinyl)phenol (1a). 1a was synthesized by following the aforementioned general synthetic procedure of McMurry Condensation, using benzophenone (**1**) (4.0 g, 21.95 mmol), 4-hydroxy benzophenone (**2**) (5.22 g, 26.34 mmol), $TiCl_4$ (9.54 mL, 48.29 mmol), Zn dust (6.31 g, 98.58 mmol), and dry THF (100 mL). The crude residue was subjected to

the flash column chromatography (silica gel, hexane/ethyl acetate: 9/1 to 8/2, R_f = 0.5) to afford as a white color solid (yield = 5.35 g, 70%). ESI-HRMS calcd for $C_{26}H_{21}O$ (M^++1) 349.1582, found 349.1587; Melting point (mp) = 219-221°C; ^{1}H NMR (400 MHz, $CDCl_3$) δ 7.01-7.12 (m, 15H), 6.89 (d, *J* = 8.0 Hz, 2H), 6.56 (d, *J* = 8.0 Hz, 2H), 4.66 (s, 1H); $^{13}C\{^1H\}$ NMR (100 MHz, $CDCl_3$) δ 160.39, 142.93, 139.93, 136.35, 134.86, 131.10, 128.10, 126.97, 120.26, 117.29.

Synthesis of 4-(1-(4-methoxyphenyl)-2,2-diphenylvinyl)phenol (1b). 1b was synthesized using benzophenone (**1**) (4.0 g, 21.95 mmol), (4-hydroxyphenyl)(4-methoxyphenyl)methanone (**4**) (6.01 g, 26.34 mmol), $TiCl_4$ (9.54 mL, 48.29 mmol), Zn dust (6.31 g, 98.58 mmol), and dry THF (100 mL). The crude residue was subjected to the flash column chromatography (silica gel, hexane/ethyl acetate: 9/1 to 8/2, R_f = 0.65) to afford as a white color solid (yield = 4.56 g, 55%). ESI-HRMS calcd for $C_{27}H_{23}O_2$ (M^++1) 379.1695, found 379.1693; Melting point (mp) = 86-88°C;^{1}H NMR (400 MHz, $CDCl_3$) δ 7.01-7.11 (m, 10H), 6.88-6.95 (m, 4H), 6.63 (d, *J* = 8.0 Hz, 2H), 6.56 (d, *J* = 8.0 Hz, 2H), 4.70 (s, 1H), 3.74 (s, 3H);$^{13}C\{^1H\}$ NMR (100 MHz, $CDCl_3$) δ 158.01, 154.20, 144.87, 144.29, 140.07, 139.29, 136.41, 132.77, 132.59, 131.37, 128.49, 128.37, 127.68, 126.09, 114.60, 113.05, 55.12.

Synthesis of 4-(2-(4-methoxyphenyl)-1,2-diphenylvinyl)phenol (1c). 1c was synthesized using 4,4'-dimethoxy benzophenone (**5**) (4.0 g, 20.18 mmol), 4,4'-dihydroxy benzophenone (**3**) (5.23 g, 24.31 mmol), $TiCl_4$ (8.77 mL, 44.39 mmol), Zn dust (5.81 g, 88.79 mmol), and dry THF (100 mL). The crude residue was subjected to the flash column chromatography (silica gel, hexane/ethyl acetate: 9/1 to 7/3, R_f = 0.55) to afford as a white color solid (yield = 6.23 g, 75%). ESI-HRMS calcd for $C_{28}H_{25}O_4$ (M^++1) 425.1732, found 425.1747; Melting point (mp) = 242-243°C;^{1}H NMR (400 MHz, $CDCl_3$) δ 8.38 (s, 1H), 6.36-6.43 (m, 8H), 6.62-6.74 (m, 12H), 3.55 (m, 3H); $^{13}C\{^1H\}$ NMR (100 MHz, $CDCl_3$) δ 157.20, 155.11, 138.93, 136.90, 135.20, 132.13, 114.33, 112.58, 54.70.

Synthesis of 4,4'-(2,2-bis(4-methoxyphenyl)ethene-1,1-diyl)diphenol (1d). 1d was synthesized using benzophenone (**1**) (4.0 g, 21.95 mmol), 4,4'-dihydroxy benzophenone (**3**) (5.63 g, 26.34 mmol), $TiCl_4$ (9.54 mL, 48.29 mmol), Zn dust (6.31 g, 98.58 mmol), and dry THF (100 mL). The crude residue was subjected to the flash column chromatography (silica gel, hexane/ethyl acetate: 9/1 to 6/4, R_f = 0.35) to afford as a white color solid (yield = 4.0 g, 50%). ESI-HRMS calcd for $C_{26}H_{21}O_2$ (M^++1) 365.1547, found 365.1536; Melting point (mp) = 224-225°C;^{1}H NMR (400 MHz, $CDCl_3$) δ 9.24-9.30 (bs, 1H), 7.01-7.13 (m, 16H), 6.93 (d, *J* = 8.0 Hz, 2H), 6.73 (d, *J* = 8.0 Hz, 2H), 6.48 (d, *J* = 8.0 Hz, 2H); $^{13}C\{^1H\}$ NMR (100 MHz, $CDCl_3$) δ 155.14, 134.68, 132.09, 130.86, 127.04, 125.26, 114.16.

Synthesis of 4-(2,2-bis(4-methoxyphenyl)-1-phenylvinyl)phenol (1e). 1e was synthesized using 4-hydroxy benzophenone (**2**) (6.0 g, 30.27 mmol), 4,4'-dihydroxy benzophenone (**3**) (5.0 g, 26.34 mmol), $TiCl_4$ (13.15 mL, 66.59 mmol), Zn dust (8.71 g, 133.19 mmol), and dry THF (100 mL). The crude residue was subjected to the flash column chromatography (silica gel, hexane/ethyl acetate: 9/1 to 4/6, R_f = 0.30) to afford as a white color solid (yield = 6.05 g, 55%). ESI-HRMS calcd for $C_{26}H_{21}O_3$ (M^++1) 381.1474, found 381.1485; Melting point (mp) = 286-287°C; ^{1}H NMR (400 MHz, $CDCl_3$) δ 10.96 (t, *J* = 8.0 Hz, 3H), 9.64 (t, *J* = 8.0 Hz, 3H), 7.16-7.25 (m, 9H), 7.02 – 7.05 (m, 2H), 6.74 - 6.82 (m, 3H); $^{13}C\{^1H\}$ NMR (100 MHz, $CDCl_3$) δ 155.57, 155.44, 144.52, 139.14, 137.69, 134.68, 134.62, 134.50, 131.96, 131.91, 131.86, 130.77, 127.57, 125.75, 114.58, 114.50.

Synthesis of 4,4',4'',4'''-(ethene-1,1,2,2-tetrayl) tetraphenol (1f). 1f was synthesized using 4,4'-dihydroxy benzophenone (**3**) (5.0 g, 26.34 mmol), $TiCl_4$ (9.50 mL, 48.26 mmol), Zn dust (6.45 g, 98.73 mmol), and dry THF (100 mL). The crude residue was subjected to the flash column chromatography (silica gel, hexane/ethyl acetate: 9/1 to 3/7, R_f = 0.2) to afford as a white color

solid (yield = 5.35 g, 45 %). ESI-HRMS calcd for $C_{26}H_{21}O_4$ (M^++1) 397.1423, found 397.1434; Melting point (mp) = 190-192^{o}C;^{1}H NMR (400 MHz, DMSO-d_6) δ 9.19 (bs, 4H), 6.71 (d, J = 8.0 Hz, 8H), 6.48 (d, J = 8.0 Hz, 8H); ^{13}C{^{1}H} NMR (100 MHz, DMSO-d_6) δ 155.36, 135.07, 131.96, 128.88, 114.50.

General synthetic procedures of duff reaction to afford aldehyde functionalized tetraphenylethylene precursors. The prepared precursors **2a-2f** and hexamethylenetetramine (HMTA) were placed in a cleaned dry 100 mL three-necked round-bottomed flask followed by the addition of glacial acetic acid/trifluoroacetic acid (TFA) (20 mL) at room temperature under nitrogen atmosphere. The resulting reaction mixture was refluxed for 6-8 h. The colour of the reaction mixture changed from light yellow to dark reddish colour. Progress of the reaction was monitored by TLC. After the reaction completion, the reaction mixture was cooled to room temperature and hydrolysed with H_2O (100 mL), and allowed to stir for 20-30 min. Subsequently, the reaction mixture was diluted with ethyl acetate (100 mL) and washed with brine solution (100 mL x 2). Organic layer was separated and dried over $MgSO_4$, filtered, and evaporated to get the crude residue, which was subjected to the flash column chromatography (silica gel, hexane/ethyl acetate) to afford yellowish colored solids of the desired compounds.

Synthesis of 2-hydroxy-5-(1,2,2-triphenylvinyl) benzaldehyde (2a). 2a was synthesized using 4-(1,2,2-triphenylvinyl)phenol (**1a**) (4.0 g, 11.47 mmol), hexamethylenetetramine (HMTA) (1.6 g, 11.47 mmol), and glacial acetic acid (20 mL). The crude residue was subjected to the flash column chromatography (silica gel, hexane/ethyl acetate: 9/1 to 8/2, R_f = 0.70) to afford as a yellowish color solid (yield = 2.59 g, 60%). ESI-HRMS calcd for $C_{27}H_{21}O_2$ (M^++1) 377.1548, found 377.1536; Melting point (mp) = 160-161^{o}C;^{1}H NMR (400 MHz, $CDCl_3$) δ 10.91 (s, 1H), 9.58 9s, 1H), 7.11-7.19 (m, 2H), 6.99-7.13 (m, 15H), 6.71 (d, J = 8.0 Hz, 1H); ^{13}C{^{1}H} NMR (100

MHz, $CDCl_3$) δ 196.37, 160.07, 143.26, 142.96, 141.35, 139.96, 138.80, 136.29, 135.48, 131.23, 131.16, 131.12, 128.42, 128.05, 127.95, 127.85, 127.65, 127.56, 126.74, 126.64, 126.53, 120.05, 116.86.

Synthesis of 2-hydroxy-5-(1-(4-methoxyphenyl)-2,2-diphenylvinyl)benzaldehyde (2b). 2b was synthesized using 4-(1-(4-methoxyphenyl)-2,2-diphenylvinyl)phenol (**1e**) (4.0 g, 10.57 mmol), hexamethylenetetramine (HMTA) (1.48 g, 10.57 mmol), and glacial acetic acid (20 mL). The crude residue was subjected to the flash column chromatography (silica gel, hexane/ethyl acetate: 9/1, R_f = 0.75) to afford as a yellowish color solid (yield = 2.36 g, 55%). ESI-HRMS calcd for $C_{28}H_{23}O_3$ (M^++1) 407.1659, found 407.1642; Melting point (mp) = 222-223°C; ^{1}H NMR (400 MHz, $CDCl_3$) δ (under process); $^{13}C\{^1H\}$ NMR (100 MHz, $CDCl_3$) δ 196.75, 160.33, 158.61, 143.85, 140.78, 140.38, 138.67, 136.68, 136.11, 135.56, 132.76, 131.50, 128.20, 128.01, 126.81, 126.66, 120.35, 117.09, 113.54, 55.34.

Synthesis of 5,5'-(2,2-bis(4-methoxyphenyl)ethene-1,1-diyl)bis(2-hydroxybenzaldehyde) (2c). 2c was synthesized using 4-(2-(4-methoxyphenyl)-1,2-diphenylvinyl)phenol (**1c**) (4.0 g, 10.57 mmol), hexamethylenetetramine (HMTA) (1.48 g, 10.57 mmol), and glacial acetic acid (20 mL). The crude residue was subjected to the flash column chromatography (silica gel, hexane/ethyl acetate: 9/1, R_f = 0.65) to afford as a yellowish color solid (yield = 2.36 g, 65%). ESI-HRMS calcd for $C_{30}H_{25}O_6$ (M^++1) 481.1637, found 481.1646; Melting point (mp) = 202-203°C;^{1}H NMR (400 MHz, $CDCl_3$) δ 10.93 (s, 1H), 9.62 (s, 1H), 7.21 (m, 4H), 6.93 (d, *J* = 8.0 Hz, 4H), 6.74 (m, 2H), 6.56 (d, *J* = 8.0 Hz, 4H), 3.75 (s, 6H); $^{13}C\{^1H\}$ NMR (100 MHz, $CDCl_3$) δ 196.42, 160.14, 158.44, 141.17, 140.06, 136.27, 135.51, 135.43, 135.01, 132.45, 120.33, 117.28, 113.42, 55.12.

Synthesis of 5,5'-(2,2-diphenylethene-1,1-diyl)bis(2-hydroxybenzaldehyde) (2d). 2d was synthesized using 4,4'-(2,2-diphenylethene-1,1-diyl)diphenol (**1d**) (4.0 g, 10.97 mmol),

hexamethylenetetramine (HMTA) (3.07 g, 21.95 mmol), and glacial acetic acid (20 mL). The crude residue was subjected to the flash column chromatography (silica gel, hexane/ethyl acetate: 9/1 to 8/2, R_f = 0.65) to afford as a yellowish color solid (yield = 2.53 g, 55%). ESI-HRMS calcd for $C_{28}H_{21}O_4$ (M^++1) 421.1434, found 421.1434; Melting point (mp) = 185-186^{o}C; ^{1}H NMR (400 MHz, $CDCl_3$) δ 10.94 (s, 2H), 9.60 (s, 2H), 7.19-7.21 (m, 4H), 7.13-7.15 (m, 6H), 7.02 (d, *J* = 8.0 Hz, 4H), 6.75 (d, *J* = 8.0 Hz, 2H); ^{13}C{^{1}H} NMR (100 MHz, $CDCl_3$) δ 196.34, 160.39, 142.93, 139.93, 136.35, 134.86, 131.10, 128.10, 126.97, 120.26, 117.29.

Synthesis of 6,6',6''-(2-phenylethene-1,1,2-triyl)tris(3-(benzo[d]thiazol-2-yl)-2H-chromen-2-one) (2e). 2e was synthesized using 4-(2,2-bis(4-methoxyphenyl)-1-phenylvinyl)phenol (**1e**) (4.0 g, 10.97 mmol), hexamethylenetetramine (HMTA) (3.07 g, 21.95 mmol), and TFA (20 mL). The crude residue was subjected to the flash column chromatography (silica gel, hexane/ethyl acetate: 9/1 to 8/2, R_f = 0.60) to afford as a yellowish color solid (yield = 2.30 g, 50%). ESI-HRMS calcd for $C_{28}H_{21}O_4$ (M^++1) 421.1434, found 421.1434; Melting point (mp) = 215-216^{o}C; ^{1}H NMR (400 MHz, $CDCl_3$) δ 10.91 (s, 1H), 9.58 9s, 1H), 7.11-7.19 (m, 2H), 6.99-7.13 (m, 15H), 6.71 (d, *J* = 8.0 Hz, 1H); ^{13}C{^{1}H} NMR (100 MHz, $CDCl_3$) δ 196.39, 196.31, 160.80, 160.67, 142.53, 140.00, 139.92, 137.43, 136.41, 136.26, 134.95, 134.74, 134.62, 131.28, 128.54, 127.55, 120.60, 120.49, 120.43, 117.95, 117.69, 117.58.

Synthesis of 5,5',5'',5'''-(ethene-1,1,2,2-tetrayl)tetrakis(2-hydroxybenzaldehyde) (2f). 2f was synthesized using 4,4',4'',4'''-(ethene-1,1,2,2-tetrayl)tetraphenol (**1f**) (4.0 g, 10.09 mmol), hexamethylenetetramine (HMTA) (5.65 g, 40.36 mmol), and TFA (20 mL). The crude residue was subjected to the flash column chromatography (silica gel, hexane/ethyl acetate: 9/1 to 8/2, R_f = 0.55) to afford as a yellowish color solid (yield = 2.05 g, 40%). ESI-HRMS calcd for $C_{30}H_{21}O_8$ (M^++1) 509.1214, found 509.1231; Melting point (mp) = 158-159^{o}C;^{1}H NMR (400 MHz, $CDCl_3$)

δ 10.99 (s, 4H), 9.65 (s, 4H), 7.23 (m, 8H), 6.80 (d, *J* = 8.0 Hz, 4H); $^{13}C\{^{1}H\}$ NMR (100 MHz, $CDCl_3$) δ 196.59, 160.02, 132.48, 132.42, 131.32, 131.29, 131.24, 127.96, 127.85, 127.66, 126.63, 126.54, 113.37, 113.09.

General synthetic procedures of Knoevenagel condensation to obtain C-6-substituted TPE-*n*CUM compounds. The prepared precursors **2a-2f** were placed in a cleaned dry 100 mL three-necked round-bottomed flask followed by the addition of MeOH (20 mL) at room temperature under a nitrogen atmosphere. Ethyl 2-(benzo[d]thiazol-2-yl) acetate (B) was then subjected to the above reaction mixture in one portion at room temperature and allowed to stir for 5 min. Subsequently, piperidine was added dropwise into the above reaction mixture at room temperature. The resulting reaction mixture was stirred at room temperature for 4-6 h. Progress of the reaction was monitored by TLC. After completion, the reaction mixture was cooled to room temperature and directly filtered on a Buckner funnel, washed with MeOH (100 mL x 2), and dried under a vacuum to furnish the desired compound.

Synthesis of 3-(benzo[d]thiazol-2-yl)-6-(1,2,2-triphenylvinyl)-2H-chromen-2-one (TPE-*1*CUM). The title compound was synthesized using 2-hydroxy-5-(1,2,2-triphenylvinyl) benzaldehyde (**2a**) (0.5 g, 1.32 mmol), MeOH (20 mL), ethyl 2-(benzo[d]thiazol-2-yl)acetate (B) (0.45 g, 1.98 mmol), and piperidine (0.17 mL, 1.98 mmol). **TPE-*1*CUM** was obtained as a light yellowish color solid (yield = 0.56 g, 80 %). ESI-HRMS calcd for $C_{36}H_{24}NO_2S$ (M^++1) 534.1505, found 534.1522; Melting point (mp) = 270-271 ^{o}C; ^{1}H NMR (400 MHz, $CDCl_3$) δ 8.81(s, 1H), 8.04 (d, *J* = 8.0 Hz, 1H), 7.96 (d, *J* = 8.0 Hz, 1H), 7.50 (t, *J* = 8.0 Hz, 1H), 7.37-7.42 (m, 2H), 7.32 (d, *J* = 8.0 Hz, 1H), 7.06-7.17 (m, 16H); $^{13}C\{^{1}H\}$ NMR (100 MHz, $CDCl_3$) δ 159.88, 152.32, 143.05, 142.93, 142.53, 142.52, 141.53, 138.62, 136.77, 136.48, 131.76, 131.26, 131.17, 128.12, 128.02, 127.76, 127.07, 126.95, 126.84, 126.45, 125.35, 122.84, 121.73, 120.03, 118.53, 116.03.

Synthesis of 3-(benzo[d]thiazol-2-yl)-6-(1-(4-methoxyphenyl)-2,2-diphenylvinyl)-2H-chromen-2-one (*gem*-OMe-TPE-*1*CUM). The title compound was synthesized using 2-hydroxy-5-(1-(4-methoxyphenyl)-2,2-diphenylvinyl)benzaldehyde (**2b**) (0.5 g, 1.23 mmol), MeOH (20 mL), ethyl 2-(benzo[d]thiazol-2-yl)acetate (B) (0.41 g, 1.84 mmol), and piperidine (0.18 mL, 1.84 mmol). ***gem*-OMe-TPE-*1*CUM** was obtained as a yellowish color solid (yield = 0.55 g, 80 %). ESI-HRMS calcd for $C_{37}H_{26}NO_3S$ (M^++1) 564.1605, found 564.1628; Melting point (mp) = 260-261 ^oC; ^1H NMR (400 MHz, $CDCl_3$) δ 8.84 (s, 1H), 8.04 (d, *J* = 8.0 Hz, 1H), 7.97 (d, *J* = 8.0 Hz, 1H), 7.53 (t, *J* = 8.0 Hz, 1H), 7.43 (t, *J* = 8.0 Hz, 1H), 7.32 (d, *J* = 8.0 Hz, 1H), 7.18 (s, 1H), 7.12-7.15 (m, 6H), 7.03-7.07 (m, 4H), 6.95 (d, *J* = 8.0 Hz, 2H), 6.68 (d, *J* = 8.0 Hz, 2H), 3.77 (s, 3H); $^{13}C\{^1H\}$ NMR (100 MHz, $CDCl_3$) δ 160.07, 158.66, 152.54, 152.48, 143.56, 143.37, 141.79, 141.75, 141.68, 138.41, 136.94, 136.75, 135.48, 132.69, 132.00, 131.50, 131.36, 128.27, 128.02, 127.08, 126.86, 126.62, 125.51, 123.03, 121.90, 120.15, 118.68, 116.16, 113.62, 55.33.

Synthesis of 6,6'-(2,2-bis(4-methoxyphenyl)ethene-1,1-diyl)bis(3-(benzo[d]thiazol-2-yl)-2H-chromen-2-one) (*gem-2*OMe-TPE-*2*CUM). The title compound was synthesized using 5,5'-(2,2-bis(4-methoxyphenyl)ethene-1,1-diyl)bis(2-hydroxybenzaldehyde) (**2c**) (0.5 g, 1.23 mmol), MeOH (20 mL), ethyl 2-(benzo[d]thiazol-2-yl)acetate (B) (0.41 g, 1.84 mmol), and piperidine (0.18 mL, 1.84 mmol). ***gem-2*OMe-TPE-*2*CUM** was obtained as a yellowish color solid (yield = 0.54 g, 79 %). ESI-HRMS calcd for $C_{48}H_{31}N_2O_6S_2$ (M^++1) 795.1619, found 795.1618; Melting point (mp) = 360-361 ^oC; ^1H NMR (400 MHz, $CDCl_3$) δ 8.87 (s, 2H), 7.94-8.04 (m, 4H), 7.33-7.54 (m, 8H), 7.20 (d, *J* = 8.0 Hz, 2H), 6.96 (t, *J* = 8.0 Hz, 4H), 6.71 (t, *J* = 8.0 Hz, 4H), 3.77 (d, *J* = 8.0 Hz, 6H); $^{13}C\{^1H\}$ NMR (100 MHz, $CDCl_3$) δ 160.02, 159.01, 152.62, 152.56, 143.63, 141.52, 141.33, 137.02, 136.65, 135.00, 134.57, 132.84, 131.91, 126.72, 125.64, 123.10, 121.98, 120.52, 119.08, 116.74, 113.80, 55.37.

Synthesis of 6,6'-(2,2-diphenylethene-1,1-diyl)bis(3-(benzo[d]thiazol-2-yl)-2H-chromen-2-one) (*gem*-TPE-*2*CUM). The title compound was synthesized using 5,5'-(2,2-diphenylethene-1,1-diyl)bis(2-hydroxybenzaldehyde) (**2d**) (0.5 g, 1.19 mmol), MeOH (20 mL), ethyl 2-(benzo[d]thiazol-2-yl)acetate (B) (0.78 g, 3.56 mmol), and piperidine (0.35 mL, 3.56 mmol). ***gem*-TPE-*2*CUM** was obtained as a yellowish color solid (yield = 0.67 g, 77 %). ESI-HRMS calcd for $C_{46}H_{27}N_2O_4S_2$ (M^++1) 735.1376, found 735.1407; Melting point (mp) = 367-368 ^oC; ^1H NMR (400 MHz, $CDCl_3$) δ 8.84(s, 2H), 8.02 (d, *J* = 8.0 Hz, 2H), 7.97 (d, *J* = 8.0 Hz, 2H), 7.52 (t, *J* = 8.0 Hz, 2H), 7.41 (t, *J* = 8.0 Hz, 2H), 7.33 (d, *J* = 8.0 Hz, 2H), 7.22 (d, *J* = 8.0 Hz, 2H), 7.16-7.18 (m, 6H), 7.06-7.09 (m, 4H); $^{13}C\{^1H\}$ NMR (100 MHz, $CDCl_3$) δ 159.62, 152.49, 152.32, 144.12, 142.25, 141.10, 140.34, 136.75, 136.26, 136.16, 131.67, 131.09, 128.27, 127.47, 126.45, 125.39, 122.84, 121.69, 120.38, 118.77, 116.44.

Synthesis of 6,6',6''-(2-phenylethene-1,1,2-triyl)tris(3-(benzo[d]thiazol-2-yl)-2H-chromen-2-one) (TPE-*3*CUM). The title compound was synthesized using 5,5',5''-(2-phenylethene-1,1,2-triyl)tris(2-hydroxybenzaldehyde) (**2e**) (0.5 g, 1.19 mmol), MeOH (20 mL), ethyl 2-(benzo[d]thiazol-2-yl)acetate (B) (0.78 g, 3.56 mmol), and piperidine (0.35 mL, 3.56 mmol). **TPE-*3*CUM** was obtained as a yellowish color solid (yield = 0.65 g, 75 %). ESI-HRMS calcd for $C_{56}H_{30}N_3O_6S_3$ (M^++1) 936.1248, found 936.1291; Melting point (mp) = 232-233 ^oC; ^1H NMR (400 MHz, $CDCl_3$) δ 8.83- 8.84 (m, 3H), 7.94-8.03 (m, 6H), 7.22-7.53 (m, 18H), 7.08-7.11 (m, 2H); $^{13}C\{^1H\}$ NMR (100 MHz, $CDCl_3$) δ 159.57, 152.80, 152.73, 152.18, 141.75, 141.08, 140.93, 139.86, 139.75, 139.60, 137.79, 136.74, 136.01, 135.95, 131.68, 131.11, 128.66, 128.07, 126.58, 125.55, 122.85, 121.76, 120.58, 119.17, 118.95, 117.08, 116.72.

Synthesis of 6,6',6'',6'''-(ethene-1,1,2,2-tetrayl)tetrakis(3-(benzo[d]thiazol-2-yl)-2H-chromen-2-one) (TPE-*4*CUM). The title compound was synthesized using 5,5',5'',5'''-(ethene-

1,1,2,2-tetrayl)tetrakis(2-hydroxybenzaldehyde) (**2f**) (0.25 g, 0.49 mmol), MeOH (20 mL), ethyl 2-(benzo[d]thiazol-2-yl)acetate (**B**) (0.65 g, 2.94 mmol), and piperidine (0.26 mL, 2.94 mmol). **TPE-*4*CUM** was obtained as a yellowish color solid (yield = 0.39 g, 70 %). ESI-HRMS calcd for $C_{66}H_{33}N_4O_8S_4$ (M^++1) 1137.1128, found 1137.1176; Melting point (mp) = 278-280 ^oC; ^1H NMR (400 MHz, $CDCl_3$) δ 8.87 (s, 4H), 7.95-8.01(m, 8H), 7.47-7.51 (m, 8H), 7.37-7.43(m, 8H), 7.31 (d, J = 8.0 Hz, 4H); $^{13}C\{^1H\}$ NMR (100 MHz, $CDCl_3$) δ 159.51, 153.17, 152.59, 140.77, 139.56, 139.30, 139.60, 137.05, 135.84, 131.78, 126.77, 125.77, 123.14, 121.97, 121.29, 119.48, 117.42.

Synthesis of 2,2'-((2Z,2'Z)-6,6'-(2,2-diphenylethene-1,1-diyl)bis(2-(2-phenylhydrazono)-2H-chromene-6,3-diyl))bis(benzo[d]thiazole) (*gem*-TPE-*2*CUM-2PH).[3] **2d** (0.25 g, 0.60 mmol) was placed in a cleaned dry 100 mL three-necked round-bottomed flask followed by the addition of MeOH (20 mL) at room temperature under a nitrogen atmosphere. 2-(Benzo[d]thiazol-2-yl)acetonitrile (0.25 g, 1.43 mmol) was then subjected to the above reaction mixture in one portion at room temperature. Subsequently, piperidine (0.17 mL, 1.78 mmol) was added dropwise into the above reaction mixture at room temperature. After completion of the reaction, the reaction mixture was directly filtered on Buckner funnel, washed with MeOH (100 mL x 2), and obtained crude compound 6,6'-(2,2-diphenylethene-1,1-diyl)bis(3-(benzo[d]thiazol-2-yl)-2H-chromen-2-imine (**2d'**). Without purification, **2d'** (0.20 g, 0.27 mmol) and phenylhydrazine (0.073 g, 0.67 mmol) were placed in a cleaned dry 100 mL three-necked round-bottomed flask followed by the addition of acetic acid (20 mL) at room temperature. Subsequently, sodium acetate (0.055g, 0.67 mmol) was added to the above reaction mixture at room temperature and stirred at room temperature for 1 h. The product precipitated from the reaction mixture and was collected by filtration on Buckner funnel, washed with MeOH (100 mL x 2), and dried under vacuum to furnish a reddish color solid (yield = 0.20 g, 79%). ESI-HRMS calcd for $C_{58}H_{39}N_6O_2S_2$ (M^++1) 915.2528, found 915.2570;

Melting point (mp) = 246-247°C;^{1}H NMR (400 MHz, DMSO-d_6) δ 9.64(s, 1H, NH-proton), 8.21 (d, J = 8.0 Hz, 2H), 8.01-8.03 (m, 3H), 7.54 (t, J = 8.0 Hz, 2H), 7.46 (t, J = 8.0 Hz, 2H), 7.14-7.35 (m, 16H), 7.06 (d, J = 8.0 Hz, 4H), 6.78 (t, J = 8.0 Hz, 1H); ^{13}C{^{1}H} NMR (100 MHz, DMSO-d_6) δ 159.33, 151.25, 150.66, 144.97, 142.48, 138.57, 137.16, 135.81, 130.38, 128.80, 127.75, 126.53, 126.24, 125.09, 122.31, 121.83, 121.41, 119.28, 118.59, 114.37, 112.51.

Photostability measurements

UV-VIS absorption spectra absorption spectra (UH5700 HITACHI spectrophotometer) of **TPE-*n*CUMs** show various degrees of degradation after different time of UV irradiation (light source: Xeon lamp, wavelength: 350 nm ± 5 nm, photon flux: 1.1x10^{17}photon/second). All measurements were made using a 1-cm quartz cuvette in spectral grade THF at a concentration of 10μM.

Experimental description of ROS generation, imaging and PDT

Hydrolysis process of DCHF-DA. Prepare 1 mM stock solution of 2'-7'-dichlorofluorescin diacetate (DCFH-DA) in 1 mL EtOH and 1mM stock solution of NaOH in 2 mL water separately. Then, mixing the 0.5 mL solution of 1mM DCFH-DA with 2 mL solution of 1mM NaOH, the resulting solution was allowed to stir for 30 min at room temperature. 7.5 mL PBS buffer (10mM) was added to the above solution for neutralization. The final concentration of the above hydrolyzed DCFH solution becomes 50 μM and is ready to use for the ROS generation experiment.

Total ROS detection. The ROS produced by the respective **TPE-*n*CUMs** was measured using the ROS indicator (DCFH-DA). **TPE-*n*CUMs** (5 μM, e.g. 20 μL from 500 μM stock solution in DMSO) and hydrolyzed DCFH (5μM, e.g. 200 μL from 50μM stock solution) were added to the cuvette containing PBS/DMSO (v/v = 99:1) solution (2 mL) and then irradiated with a white light

(50 mW cm^{-2}) at different times, and the FL emission spectra of DCFH dye excited at 490 nm (λ_{em} = 525 nm) were immediately measured.

Singlet oxygen detection ($^1O_2$). The detection of $^1O_2$ in **TPE-*n*CUMs** after the white-light irradiation was measured by using a $^1O_2$-indicator-9,10-anthracinadipropanoic acid (ABDA). **TPE-*n*CUMs** (5 μM, e.g. 10 μL from 1 mM stock solution in DMSO) and ABDA (50 μM, e.g. 10μL from 10 mM stock solution in DMSO) were added to the cuvettes containing a 2 mL solution of PBS/DMSO (v/v = 99:1) and irradiated with white light (50 mW cm^{-2}) at different times for up to 20 minutes, and the absorption spectra from 350 to 800 nm were collected. For $^1O_2$-generation control experiments, the sample of Rose Bengal dye (5 μM, e.g. 10 μL from 1 mM stock solution in DMSO) and ABDA (50 μM) was added to the cuvettes containing a 2 mL solution of PBS/DMSO (v/v = 99:1) which was irradiated with white light for 20 mins and measured the absorption spectra.

Type-I superoxide radical ($^{\bullet}O_2^-$) detection. The superoxide radical ($^{\bullet}O_2^-$) produced by **TPE-*n*CUMs** was detected by mixing the fluorescent probe dihydrorhodamine 123 (DHR123) and radical scavenger vitamin C (V_C). **TPE-*n*CUMs** (5 μM, e.g. 10 μL from 1 mM stock solution in DMSO) and DHR 123 (10 μM, e.g.10 μL from 2 mM stock solution in DMSO) were added to the cuvettes containing a 2 mL solution of PBS/DMSO (v/v = 99:1) and irradiated with white light (50 mW cm^{-2}) at different times, and the FL emission spectra of DHR123 dye were collected. Further evidence of the free radical generation, **TPE-*n*CUMs** (5 μM), DHR 123 (10 μM, e.g. 5 μL from 4 mM stock solution in DMSO), and vitamin C (Vc) (10 μM, e.g. 5 μL from 4 mM stock solution in DMSO) were added into the cuvette containing PBS/DMSO (v / v = 99: 1) solution (2 mL). Then irradiated the sample with white light for 15 min and the FL emission spectra were collected. To further confirm the free-radical ROS generation in **TPE-*n*CUMs**, the electron

paramagnetic resonance (EPR) spin-trapping technique using 5, 5-dimethyl-1-pyrroline-*N*-oxide (DMPO) as a spin-trap agent in air-saturated PBS/DMSO; v/v = 99:1 solution was conducted. DMPO (25 μM) and **gem-*2*OMe-TPE-*2*CUM** (10 μM, e.g. 10 μL from 1mM stock solution in DMSO) in air-saturated PBS/DMSO; v/v = 99:1 solution was irradiated with white-light (50 mW cm^{-2}) for 20 min, and a free radical signal could be measured by the EPR spectrometer.

Cell imaging. HeLa cells were cultured in Dulbecco's modified eagle medium (DMEM) containing 10% fetal bovine serum at 37°C in a humidified environment containing 5% CO_2. Initially, HeLa cells were subcultured into different cell culture dishes (35*12mm) for 24 h at 37°C and 5% CO_2, then cultured with ***gem*-OMe-TPE-*1*CUM** (5 μM) in 1% DMSO solution of 10% FBS DMEM medium (e.g. added 50 mL) for 24 h at 37°C and 5% CO_2. The subcellular distribution uptakes of ***gem*-OMe-TPE-*1*CUM** in the cells were assessed by co-localization analysis, where first the above-cultured cells with ***gem*-OMe-TPE-*1*CUM** (5μM) were washed with the PBS solution (500 μL x 3) and simultaneously incubated with commercially available bio-probes for subcellular structures such as Lyso-Tracker Deep Red (50 nM), and Mito-Tracker Deep Red (100 nM) for 30 min at 37°C and 5% CO_2. Thereafter, the culture media of each well were washed with PBS solution (500 μL x 3) and replaced with 1000 μL of new culture media DMEM/F-12, No Phenol Red is used in cell culture processing of confocal laser scanning microscopy (CLSM) images.

Cell viability. The cytotoxicity of ***gem*-OMe-TPE-*1*CUM** was assessed by WST-1 method. HeLa cells were firstly seeded into a 24-well plate at a density of 0.05 x 10^6 cells per well in DMEM and incubated for 24 h at 37°C and 5% CO_2. Then the medium was washed with PBS solution (500 μL X3) and replaced with 1% DMSO solution of 10% FBS DMEM by the different concentrations of ***gem*-OMe-TPE-*1*CUM** (0, 2, 4, 6, 8, 10, 20, and 30 μM) and the cells were incubated for another

24 h at 37 °C and 5% CO_2. After incubation, for DARK-Categorized samples, the culture media of each well were removed, washed with PBS solution (500 μL x 3), filled with 500μL of new culture media containing WST (10%) and incubated for an additional 2 h at 37 °C and 5% CO_2. For LIGHT-Categorized samples, firstly, the samples were irradiated with white light (50 mW cm^{-2}) for 20 min, and then the culture media of each well were removed, washed with PBS solution (500 μL x 3), filled with 500 μL of new culture media containing WST (10%) and incubated for an additional 2 h at 37 °C and 5% CO_2. Then, the OD450 value (Abs.) of each well was measured by a microplate reader immediately. Cell viability was expressed by the ratio of OD450 values of the cells incubated with the ***gem*-OMe-TPE-*1*CUM** suspension to that of the cells incubated with culture medium only.

Intracellular ROS detection. HeLa cells were incubated into different groups such as; incubated with DCFH-DA (only)-w/o light), DCFH-DA (only)-w/light), ***gem*-OMe-TPE-*1*CUM** (30 μM)/DCFH-DA (5 μM)-w/o light, and ***gem*-OMe-TPE-*1*CUM** (30 μM)/DCFH-DA-w/light). Noted that, ***gem*-OMe-TPE-*1*CUM** (30 μM) was first incubated for 24 h, and later DCFH-DA (5 μM) probe was incubated for 30 min with free-FBS DMEM medium at 37°C and 5% CO_2. After incubation, for DARK-Categorized samples, the culture media of each well were removed, washed with PBS solution (500 μL x 3), and filled with 500 μL of new culture media DMEM/F-12, No Phenol Red is used in cell culture processing of CLSM images applications. For LIGHT-Categorized samples, firstly, the samples were irradiated with white light (50 mW cm^{-2}) for 20 min, and then the culture media of each well were removed, washed with PBS solution (500 μL X3), and filled with 500 μL of new culture media DMEM/F-12, No Phenol Red is used in cell culture processing of CLSM images applications. A green fluorescence was observed in ***gem*-OMe-TPE-*1*CUM** (30 μM)/DCFH-DA-w/ light) using CLSM with the excitation wavelength

of 488 nm, and emission wavelength was collected from 500 to 550 nm.

Table S1 Photophysical properties of **TPE-*1*CUM**, ***gem*-OMe-TPE-*1*CUM**, ***gem*-*2*OMe-TPE-*2*CUM**, ***gem*-TPE-*2*CUM**, **TPE-*3*CUM**, and **TPE-*4*CUM** in THF.

Compound	Solvent	λ^a_{max} (nm)	λ^b_{max} (nm)	ε($M^{-1}cm^{-1}$)[c]	$\Delta\nu$ (cm^{-1})[d]	ϕ_f (%)[e]	τ_{obs} (ns)[f]	κ_r ($x10^7 s^{-1}$)[g]	κ_{nr} ($x10^8 s^{-1}$)[h]
TPE-*1*CUM	THF	350	542	31118	10121	8.70	3.33	2.61	2.74
***gem*-OMe-TPE-*1*CUM**	THF	350	579	42668	10872	2.83	2.28	1.24	4.26
***gem*-OMe-TPE-*2*CUM**	THF	356	590	65032	11140	3.95	2.5	1.58	3.84
gem-TPE-2CUM	THF	356	534	64962	9363	9.56	3.42	2.80	2.64
TPE-*3*CUM	THF	357	526	88326	8999	13.19	3.14	4.20	2.76
TPE-*4*CUM	THF	359	519	121616	8092	18.59	3.11	5.98	2.62

λ^a_{max} = Absorbance, λ^b_{max} = Emission at excitation equal to λ^a_{max}, **($M^{-1}cm^{-1}$)[c]** =Molar extinction coefficient, $\Delta\nu$ **(cm^{-1})[d]** = Stokes shift, ϕ_f **(%)[e]** = Quantum yield, τ_{obs} **(ns)[f]** = Life time, κ_r **($x10^7 s^{-1}$)[g]** = ϕ_f **(%)[e]/** τ_{obs} **(ns)[f]**, and κ_{nr} **($x10^8 s^{-1}$)[h]** = **1 -** ϕ_f **(%)[e]/** τ_{obs} **(ns)[f]**.

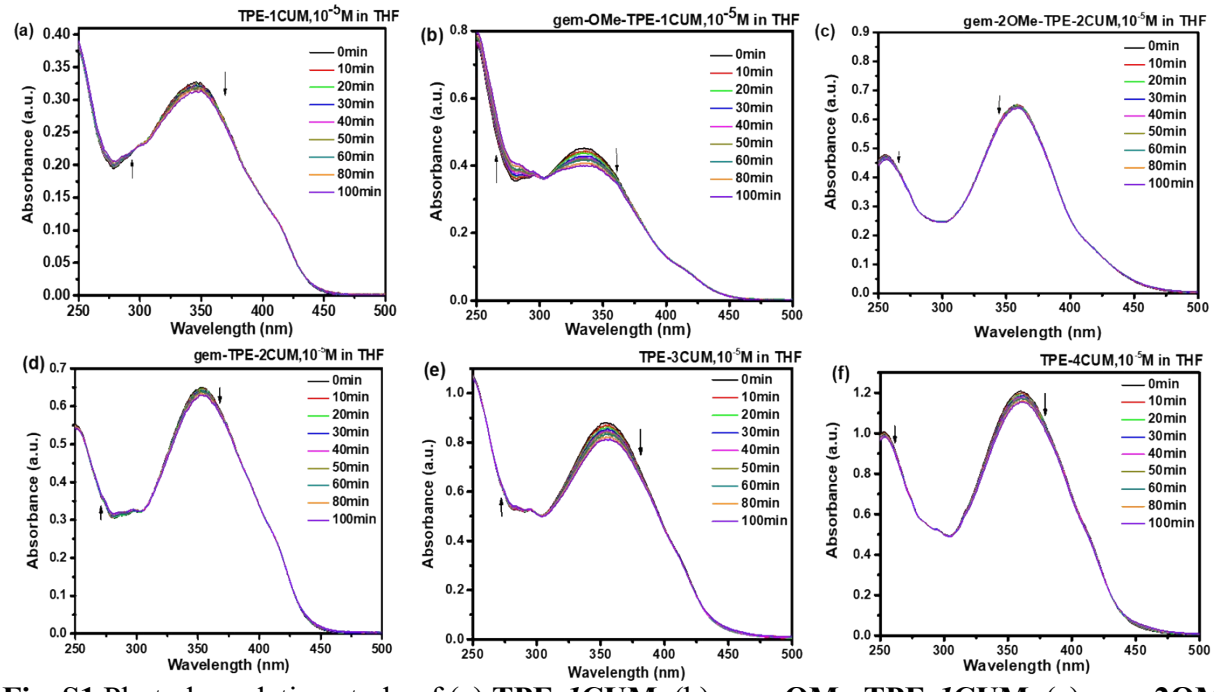

Fig. S1 Photodegradation study of (a) **TPE-*1*CUM**, (b) ***gem*-OMe-TPE-*1*CUM**, (c) ***gem*-2OMe-TPE-*2*CUM**, (d) ***gem*-TPE-*2*CUM**, (e) **TPE-*3*CUM**, and (f) **TPE-*4*CUM**. UV-VIS absorption spectra (10μM, tetrahydrofuran) were measured in a 1-cm quartz cuvette, continuously irradiated with UV light (350 nm, $1.1x10^{17}$photon/second).

.

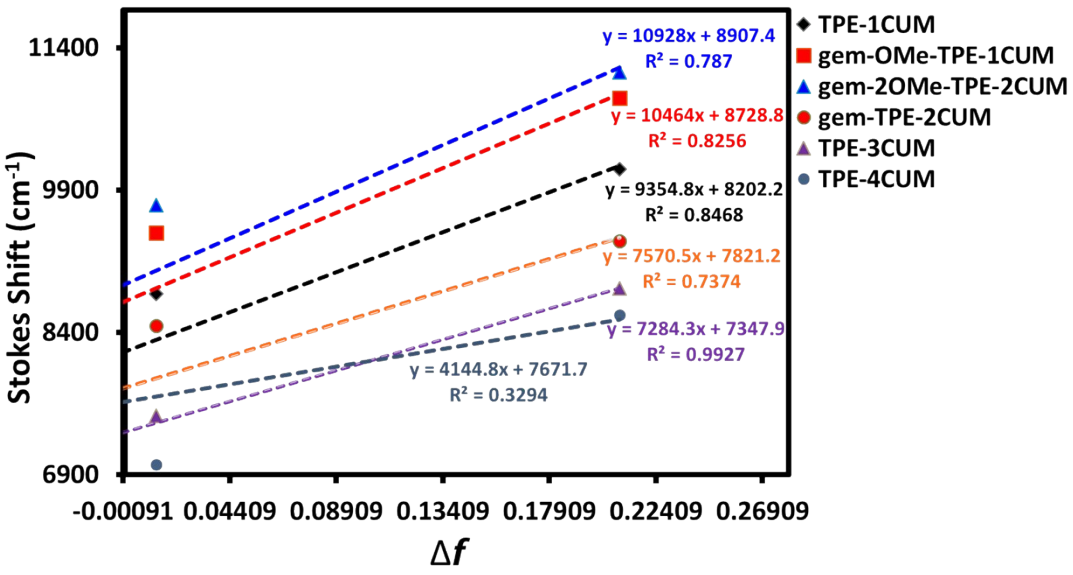

Fig. S2 Correlation of orientation polarizability (Δ*f*) of different solvents polarity with stokes shift of **TPE-*n*CUMs**.

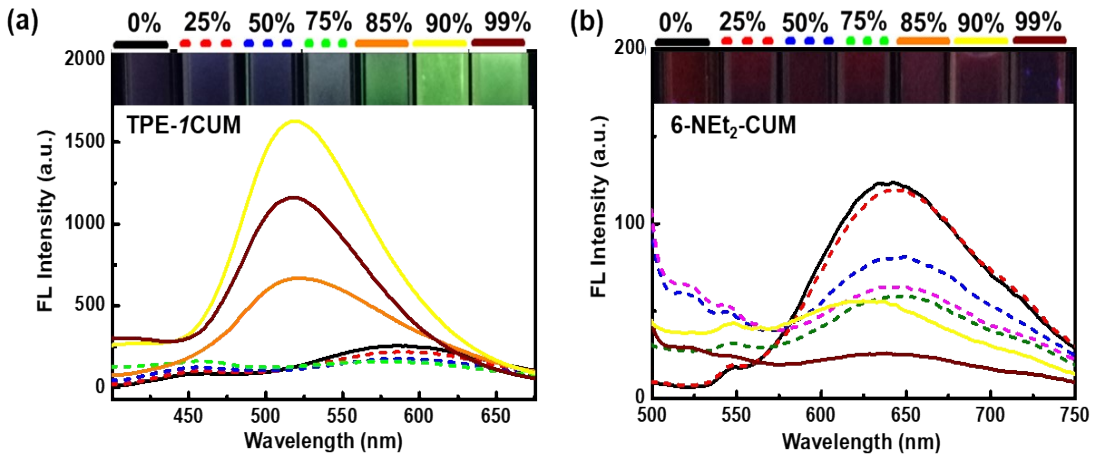

Fig. S3 FL spectra with increasing glycerol fractions: 0, 25, 50, 75, 85, 90, and 99%; (a) **TPE-*1*CUM** and (b) **6-NEt$_2$-CUM**; Insets: their corresponding FL photoimages with increasing glycerol fractions: 0, 25, 50, 75, 85, 90, and 99% under UV-lamp. (λ_{ex} = 350 and 469 nm for **TPE-*1*CUM** and **6-NEt$_2$-CUM**, respectively)

Table S2 Fluorescence quantum yields of **TPE-*n*CUMs** in both aggregation and solid-states.

Compound	In aggregation state ϕ_f (%)	In Solid-State ϕ_f (%)
TPE-*1*CUM	6.5% (at 90% H_2O in THF)	47%
***gem*-OMe-TPE-*1*CUM**	9.8% (at 80% H_2O in THF)	35%
***gem*-2OMe-TPE-*2*CUM**	8.3% (at 90% H_2O in THF) 4.8% (at 99% H_2O in THF)	55%
gem-TPE-2CUM	3.5% (at 60% H_2O in THF) 9.9% (at 80% H_2O in THF)	16%
TPE-*3*CUM	13% (at 90% H_2O in THF)	32%
TPE-*4*CUM	4.8% (at 50% H_2O in THF) 9.2% (at 80% H_2O in THF)	10%

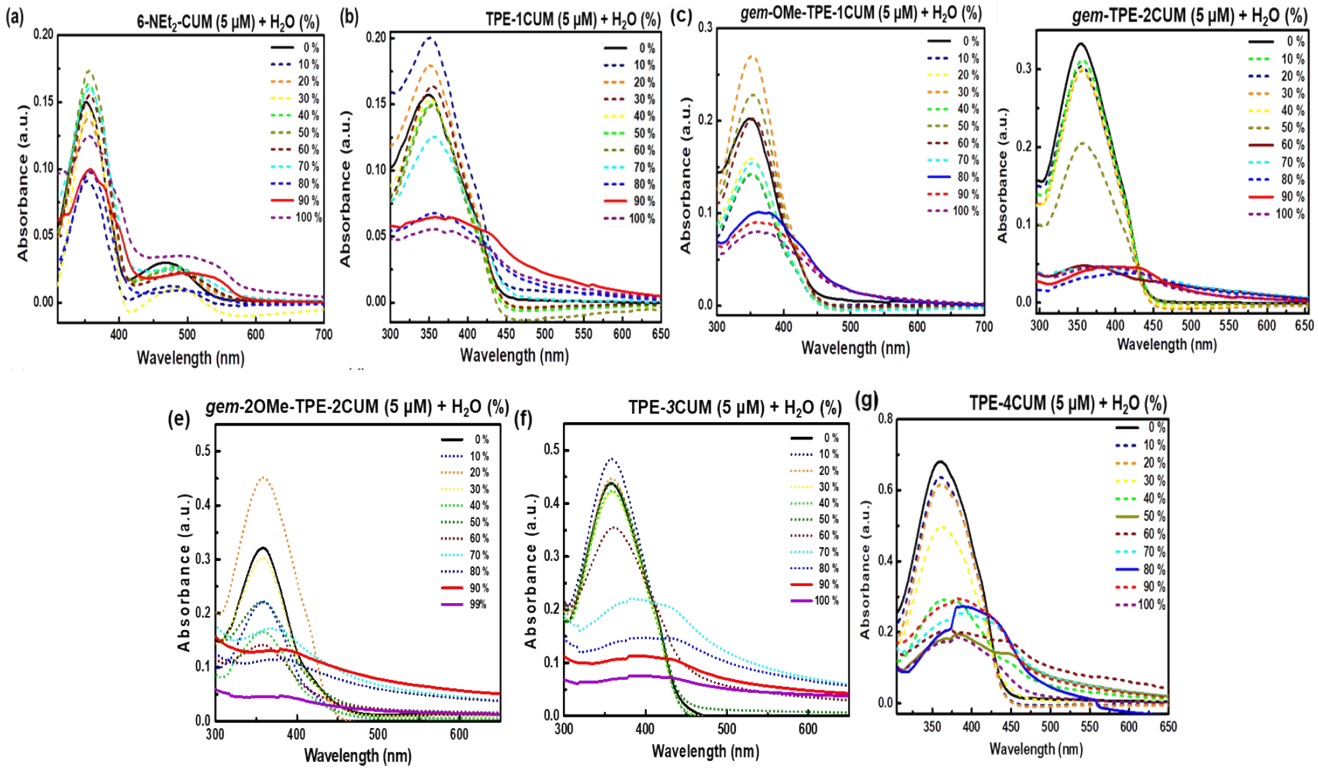

Fig. S4 UV-Visible spectra with increasing water fractions: 0, 10, 20, 30, 40, 50, 60, 70, 80, 90, and 100%; (a) **6-NEt$_2$-CUM** (b) **TPE-*1*CUM** (c) ***gem*-OMe-TPE-*1*CUM** (d) ***gem*-TPE-*2*CUM** (e) ***gem*-2OMe-TPE-*2*CUM** (f) **TPE-*3*CUM** and (g) **TPE-*4*CUM**.

Table S3 Crystal data and structure refinement for **TPE-*1*CUM** (ic19018).

Identification code	ic19018	
Empirical formula	C36 H23 N O2 S	
Formula weight	533.61	
Temperature	150(2) K	
Wavelength	1.54178 Å	
Crystal system	Monoclinic	
Space group	C 1 2/c 1	
Unit cell dimensions	a = 29.846(2) Å	a= 90°.
	b = 16.8082(12) Å	b= 99.761(6)°.
	c = 10.7713(7) Å	g = 90°.
Volume	5325.3(6) Å^3	
Z	8	
Density (calculated)	1.331 Mg/m^3	
Absorption coefficient	1.352 mm^{-1}	
F(000)	2224	
Crystal size	0.40 x 0.30 x 0.01 mm^3	
Theta range for data collection	3.00 to 67.98°.	
Index ranges	-31<=h<=35, -19<=k<=20, -12<=l<=9	
Reflections collected	9816	
Independent reflections	4839 [R(int) = 0.0630]	
Completeness to theta = 67.98°	99.7 %	
Absorption correction	Semi-empirical from equivalents	
Max. and min. transmission	1.00000 and 0.80827	
Refinement method	Full-matrix least-squares on F^2	
Data / restraints / parameters	4839 / 0 / 361	
Goodness-of-fit on F^2	1.341	
Final R indices [I>2sigma(I)]	R1 = 0.0897, wR2 = 0.2720	
R indices (all data)	R1 = 0.1550, wR2 = 0.3067	
Largest diff. peak and hole	0.405 and -0.387 e.Å^{-3}	

Table S4 Atomic coordinates (x 10^4) and equivalent isotropic displacement parameters (Å^{2}x 10^3) for **TPE-*1*CUM** (ic19018). U(eq) is defined as one-third of the trace of the orthogonalized U^{ij} tensor.

	x	y	z	U(eq)

S(1)	1674(1)	3196(1)	4425(2)	59(1)
O(1)	1711(2)	2070(3)	2555(4)	58(1)
O(2)	2265(1)	1811(3)	1484(4)	53(1)
N(1)	2505(2)	3714(3)	4896(5)	51(1)
C(1)	1810(2)	3893(4)	5604(6)	55(2)
C(2)	1538(3)	4232(4)	6398(7)	67(2)
C(3)	1728(3)	4777(5)	7288(7)	70(2)
C(4)	2185(3)	4973(4)	7408(7)	68(2)
C(5)	2461(3)	4646(4)	6633(6)	61(2)
C(6)	2270(2)	4101(4)	5725(6)	53(2)
C(7)	2234(2)	3224(4)	4156(6)	48(2)
C(8)	2095(2)	2213(4)	2427(6)	51(2)
C(9)	2402(2)	2791(4)	3179(5)	46(2)
C(10)	2826(2)	2892(4)	2942(6)	50(2)
C(11)	2992(2)	2469(4)	1957(6)	50(2)
C(12)	3424(2)	2570(4)	1675(6)	54(2)
C(13)	3560(2)	2180(4)	666(6)	56(2)
C(14)	3261(2)	1648(4)	2(6)	52(2)
C(15)	2826(2)	1525(4)	264(6)	55(2)
C(16)	2698(2)	1935(4)	1245(6)	48(2)
C(17)	4023(2)	2290(5)	334(6)	57(2)
C(18)	4276(2)	2968(4)	513(6)	55(2)
C(19)	4082(2)	3729(4)	897(6)	58(2)
C(20)	3724(2)	4094(5)	134(7)	62(2)
C(21)	3548(3)	4812(5)	477(9)	76(2)
C(22)	3733(3)	5150(5)	1623(10)	81(3)
C(23)	4088(3)	4805(5)	2367(10)	86(3)
C(24)	4269(3)	4098(5)	2028(7)	71(2)
C(25)	4752(3)	3007(5)	304(7)	66(2)
C(26)	4896(3)	3661(6)	-317(8)	90(3)
C(27)	5332(3)	3700(7)	-561(10)	107(3)
C(28)	5641(3)	3122(7)	-150(10)	95(3)
C(29)	5513(3)	2496(5)	536(10)	87(3)
C(30)	5074(2)	2435(5)	741(8)	70(2)
C(31)	4195(2)	1590(5)	-319(6)	61(2)
C(32)	4286(2)	1682(5)	-1541(7)	70(2)
C(33)	4449(3)	1038(6)	-2142(8)	83(3)
C(34)	4529(3)	322(6)	-1531(9)	83(3)
C(35)	4437(3)	220(5)	-316(8)	76(2)
C(36)	4263(2)	864(5)	274(7)	66(2)

Table S5 Bond lengths [Å] and angles [°] for **TPE-*1*CUM** (ic19018).

S(1)-C(1)	1.725(7)
S(1)-C(7)	1.743(6)
O(1)-C(8)	1.203(7)
O(2)-C(16)	1.375(7)
O(2)-C(8)	1.386(7)
N(1)-C(7)	1.322(8)
N(1)-C(6)	1.387(8)
C(1)-C(2)	1.398(9)
C(1)-C(6)	1.401(9)
C(2)-C(3)	1.376(10)
C(3)-C(4)	1.388(11)

C(4)-C(5)	1.383(9)
C(5)-C(6)	1.389(9)
C(7)-C(9)	1.438(8)
C(8)-C(9)	1.480(9)
C(9)-C(10)	1.344(8)
C(10)-C(11)	1.434(8)
C(11)-C(12)	1.383(8)
C(11)-C(16)	1.390(9)
C(12)-C(13)	1.389(9)
C(13)-C(14)	1.374(9)
C(13)-C(17)	1.495(9)
C(14)-C(15)	1.392(9)
C(15)-C(16)	1.369(8)
C(17)-C(18)	1.362(10)
C(17)-C(31)	1.505(9)
C(18)-C(25)	1.477(9)
C(18)-C(19)	1.491(10)
C(19)-C(20)	1.376(10)
C(19)-C(24)	1.395(10)
C(20)-C(21)	1.391(10)
C(21)-C(22)	1.386(12)
C(22)-C(23)	1.347(12)
C(23)-C(24)	1.381(11)
C(25)-C(30)	1.386(10)
C(25)-C(26)	1.392(11)
C(26)-C(27)	1.372(11)
C(27)-C(28)	1.361(13)
C(28)-C(29)	1.378(12)
C(29)-C(30)	1.368(11)
C(31)-C(36)	1.377(10)
C(31)-C(32)	1.397(9)
C(32)-C(33)	1.390(11)
C(33)-C(34)	1.372(12)
C(34)-C(35)	1.393(12)
C(35)-C(36)	1.401(10)
C(1)-S(1)-C(7)	89.5(3)
C(16)-O(2)-C(8)	122.4(5)
C(7)-N(1)-C(6)	110.9(5)
C(2)-C(1)-C(6)	120.2(7)
C(2)-C(1)-S(1)	129.7(6)
C(6)-C(1)-S(1)	110.0(5)
C(3)-C(2)-C(1)	119.0(7)
C(2)-C(3)-C(4)	120.3(7)
C(5)-C(4)-C(3)	121.8(7)
C(4)-C(5)-C(6)	118.2(7)
N(1)-C(6)-C(5)	124.9(6)
N(1)-C(6)-C(1)	114.6(6)
C(5)-C(6)-C(1)	120.5(6)
N(1)-C(7)-C(9)	120.1(6)
N(1)-C(7)-S(1)	115.0(5)
C(9)-C(7)-S(1)	124.8(5)
O(1)-C(8)-O(2)	117.5(6)
O(1)-C(8)-C(9)	125.6(6)
O(2)-C(8)-C(9)	116.9(5)
C(10)-C(9)-C(7)	122.2(6)
C(10)-C(9)-C(8)	119.6(6)

C(7)-C(9)-C(8)	118.2(6)
C(9)-C(10)-C(11)	122.2(6)
C(12)-C(11)-C(16)	118.8(6)
C(12)-C(11)-C(10)	123.5(6)
C(16)-C(11)-C(10)	117.6(6)
C(11)-C(12)-C(13)	121.5(7)
C(14)-C(13)-C(12)	117.6(6)
C(14)-C(13)-C(17)	120.0(6)
C(12)-C(13)-C(17)	122.3(7)
C(13)-C(14)-C(15)	122.5(6)
C(16)-C(15)-C(14)	118.2(6)
C(15)-C(16)-O(2)	117.5(6)
C(15)-C(16)-C(11)	121.2(6)
O(2)-C(16)-C(11)	121.3(5)
C(18)-C(17)-C(13)	125.5(6)
C(18)-C(17)-C(31)	119.7(6)
C(13)-C(17)-C(31)	114.7(6)
C(17)-C(18)-C(25)	122.7(6)
C(17)-C(18)-C(19)	121.7(6)
C(25)-C(18)-C(19)	115.6(6)
C(20)-C(19)-C(24)	118.6(7)
C(20)-C(19)-C(18)	121.0(7)
C(24)-C(19)-C(18)	120.4(7)
C(19)-C(20)-C(21)	121.2(8)
C(22)-C(21)-C(20)	118.7(8)
C(23)-C(22)-C(21)	120.5(8)
C(22)-C(23)-C(24)	121.2(9)
C(23)-C(24)-C(19)	119.7(8)
C(30)-C(25)-C(26)	117.3(7)
C(30)-C(25)-C(18)	123.2(7)
C(26)-C(25)-C(18)	119.5(7)
C(27)-C(26)-C(25)	120.7(9)
C(28)-C(27)-C(26)	121.1(10)
C(27)-C(28)-C(29)	119.0(8)
C(30)-C(29)-C(28)	120.3(9)
C(29)-C(30)-C(25)	121.4(8)
C(36)-C(31)-C(32)	119.9(7)
C(36)-C(31)-C(17)	120.7(6)
C(32)-C(31)-C(17)	119.4(7)
C(33)-C(32)-C(31)	119.5(8)
C(34)-C(33)-C(32)	120.4(8)
C(33)-C(34)-C(35)	120.8(8)
C(34)-C(35)-C(36)	118.6(8)
C(31)-C(36)-C(35)	120.7(7)

Symmetry transformations used to generate equivalent atoms:

Table S6 Anisotropic displacement parameters ($Å^2 x\ 10^3$) for **TPE-*1*CUM** (ic19018). The anisotropic displacement factor exponent takes the form:$-2p^2[h^2\ a^{*2}U^{11} + ..+ 2\ h\ k\ a^*\ b^*\ U^{12}]$

	U^{11}	U^{22}	U^{33}	U^{23}	U^{13}	U^{12}
S(1)	62(1)	63(1)	53(1)	-2(1)	16(1)	3(1)
O(1)	56(3)	66(3)	54(3)	-4(2)	15(2)	-10(2)

O(2)	62(3)	54(3)	42(2)	-3(2)	11(2)	-2(2)
N(1)	64(3)	48(3)	44(3)	6(3)	19(2)	2(3)
C(1)	71(4)	49(4)	49(4)	9(3)	19(3)	8(3)
C(2)	77(5)	66(5)	66(5)	2(4)	32(4)	4(4)
C(3)	93(6)	66(5)	60(5)	-5(4)	33(4)	10(4)
C(4)	111(7)	41(4)	54(4)	-4(3)	25(4)	2(4)
C(5)	80(5)	56(4)	48(4)	4(3)	18(4)	3(4)
C(6)	70(4)	49(4)	43(3)	5(3)	20(3)	0(3)
C(7)	58(4)	43(3)	45(4)	10(3)	13(3)	-1(3)
C(8)	60(4)	49(4)	43(3)	4(3)	8(3)	1(3)
C(9)	58(4)	46(4)	36(3)	5(3)	10(3)	4(3)
C(10)	56(4)	50(4)	42(3)	-1(3)	8(3)	-6(3)
C(11)	60(4)	56(4)	37(3)	7(3)	13(3)	5(3)
C(12)	64(4)	58(4)	42(3)	-2(3)	14(3)	-5(3)
C(13)	66(4)	61(4)	45(4)	9(3)	18(3)	9(4)
C(14)	68(4)	44(4)	47(4)	-1(3)	19(3)	6(3)
C(15)	76(5)	52(4)	38(3)	-5(3)	13(3)	0(3)
C(16)	55(4)	48(4)	44(3)	1(3)	11(3)	-1(3)
C(17)	62(4)	73(5)	38(3)	2(3)	14(3)	12(4)
C(18)	55(4)	65(5)	45(4)	0(3)	13(3)	4(3)
C(19)	56(4)	69(5)	55(4)	-4(4)	23(3)	-10(4)
C(20)	59(4)	75(5)	54(4)	1(4)	20(3)	5(4)
C(21)	77(5)	67(5)	91(6)	8(5)	34(5)	8(4)
C(22)	73(6)	66(5)	111(7)	-22(5)	36(5)	-4(4)
C(23)	86(6)	83(6)	97(7)	-38(6)	35(5)	-21(5)
C(24)	63(4)	82(6)	69(5)	-12(4)	14(4)	-11(4)
C(25)	69(4)	79(5)	54(4)	3(4)	20(4)	6(4)
C(26)	72(5)	111(8)	92(6)	42(6)	31(5)	14(5)
C(27)	84(6)	134(9)	112(8)	38(7)	44(6)	5(6)
C(28)	62(5)	114(8)	115(8)	-8(7)	28(5)	6(6)
C(29)	65(5)	82(6)	111(7)	-18(6)	7(5)	18(5)
C(30)	65(5)	74(5)	72(5)	7(4)	13(4)	4(4)
C(31)	64(4)	73(5)	48(4)	-2(4)	13(3)	11(4)
C(32)	70(5)	93(6)	51(4)	-7(4)	23(3)	10(4)
C(33)	77(5)	114(8)	63(5)	-9(5)	23(4)	12(5)
C(34)	81(6)	88(7)	85(6)	-28(5)	27(5)	8(5)
C(35)	77(5)	74(6)	78(6)	-8(5)	14(4)	6(4)
C(36)	73(5)	70(5)	59(4)	-2(4)	19(4)	2(4)

Table S7 Crystal data and experimental details for **6-NEt$_2$-CUM** (ic20004).

Crystal data		
Empirical formula	C20.50 H20 N2 O2.50 S	
Formula weight	366.44	
Crystal system	Monoclinic	
Space group	$P2_1/n$	
Unit cell dimensions	a = 4.66470(10) Å	a= 90°.
	b = 20.4684(8) Å	b= 96.234(3)°.
	c = 19.0563(8) Å	g = 90°.
Volume	1808.72(11) Å^3	
Z	4	
F(000)	772	

Density (calculated)	1.346 Mg/m^3
Wavelength	0.71073 Å
Cell parameters reflections used	3999
Theta range for Cell parameters	3.3660 to 28.4960°.
Absorption coefficient	0.199 mm^{-1}
Temperature	100(2) K
Crystal size	0.25 x 0.10 x 0.10 mm^3
Data collection	
Diffractometer	Xcalibur, Atlas, Gemini
Absorption correction	Semi-empirical from equivalents
Max. and min. transmission	1.00000 and 0.98383
No. of measured reflections	9600
No. of independent reflections	4005 [R(int) = 0.0374]
No. of observed [I>2_igma(I)]	3004
Completeness to theta = 25.242°	99.8 %
Theta range for data collection	2.930 to 27.500°.
Refinement	
Final R indices [I>2sigma(I)]	R1 = 0.0524, wR2 = 0.1482
R indices (all data)	R1 = 0.0757, wR2 = 0.1694
Goodness-of-fit on F^2	1.073
No. of reflections	4005
No. of parameters	264
No. of restraints	40
Largest diff. peak and hole	0.700 and -0.263 e.$Å^{-3}$

Table S8 Atomic coordinates (x 10^4) and equivalent isotropic displacement parameters ($Å^2$x 10^3) for **6-NEt_2-CUM** (ic20004). U(eq) is defined as one third of the trace of the orthogonalized U^{ij} tensor.

	x	y	z	U(eq)
S(1)	8116(1)	4137(1)	8202(1)	22(1)
O(1)	4808(3)	3111(1)	8456(1)	26(1)
O(2)	1261(3)	2634(1)	7794(1)	20(1)
N(1)	6403(4)	4459(1)	6901(1)	22(1)
N(2)	-5439(4)	2188(1)	5236(1)	22(1)
C(1)	9760(4)	4796(1)	7842(1)	25(1)
C(2)	11989(5)	5188(1)	8159(1)	29(1)
C(3)	12957(5)	5690(1)	7762(2)	33(1)
C(4)	11729(5)	5805(1)	7076(2)	35(1)
C(5)	9549(5)	5414(1)	6756(2)	31(1)
C(6)	8555(4)	4898(1)	7148(1)	23(1)
C(7)	5946(4)	4042(1)	7395(1)	20(1)
C(8)	3763(4)	3525(1)	7290(1)	18(1)
C(9)	2121(4)	3444(1)	6665(1)	19(1)
C(10)	-41(4)	2944(1)	6574(1)	17(1)
C(11)	-1746(4)	2830(1)	5934(1)	19(1)
C(12)	-3821(4)	2328(1)	5870(1)	18(1)
C(13)	-4198(4)	1970(1)	6488(1)	19(1)
C(14)	-2547(4)	2083(1)	7124(1)	20(1)
C(15)	-443(4)	2562(1)	7159(1)	18(1)
C(16)	3392(4)	3094(1)	7886(1)	20(1)

C(17)	-7195(5)	1601(1)	5159(1)	26(1)
C(18)	-5433(6)	976(1)	5122(1)	36(1)
C(19)	-4712(5)	2490(1)	4584(1)	26(1)
C(20)	-6228(5)	3132(1)	4422(2)	35(1)
O(3)	4320(30)	4681(6)	5417(5)	79(3)
C(21)	7090(40)	4447(10)	5333(9)	98(5)
O(4)	6520(20)	4897(5)	4926(5)	68(3)
C(22)	8780(40)	5330(8)	4894(7)	81(4)

Table S9 Bond lengths [Å] and angles [°] for **6-NEt$_2$-CUM** (ic20004).

S(1)-C(1)	1.729(2)
S(1)-C(7)	1.758(2)
O(1)-C(16)	1.208(3)
O(2)-C(16)	1.366(3)
O(2)-C(15)	1.381(2)
N(1)-C(7)	1.304(3)
N(1)-C(6)	1.391(3)
N(2)-C(12)	1.382(3)
N(2)-C(17)	1.453(3)
N(2)-C(19)	1.461(3)
C(1)-C(6)	1.394(3)
C(1)-C(2)	1.397(3)
C(2)-C(3)	1.381(4)
C(3)-C(4)	1.388(4)
C(4)-C(5)	1.383(4)
C(5)-C(6)	1.401(3)
C(7)-C(8)	1.467(3)
C(8)-C(9)	1.355(3)
C(8)-C(16)	1.465(3)
C(9)-C(10)	1.434(3)
C(10)-C(15)	1.392(3)
C(10)-C(11)	1.402(3)
C(11)-C(12)	1.407(3)
C(12)-C(13)	1.415(3)
C(13)-C(14)	1.383(3)
C(14)-C(15)	1.385(3)
C(17)-C(18)	1.526(4)
C(19)-C(20)	1.507(4)
O(3)-C(21)	1.401(15)
O(4)-C(22)	1.383(15)
C(1)-S(1)-C(7)	88.72(11)
C(16)-O(2)-C(15)	121.81(17)
C(7)-N(1)-C(6)	110.32(19)
C(12)-N(2)-C(17)	120.59(19)
C(12)-N(2)-C(19)	119.97(18)
C(17)-N(2)-C(19)	116.40(18)
C(6)-C(1)-C(2)	121.9(2)
C(6)-C(1)-S(1)	109.99(16)
C(2)-C(1)-S(1)	128.1(2)
C(3)-C(2)-C(1)	117.6(2)

C(2)-C(3)-C(4)	121.1(2)
C(5)-C(4)-C(3)	121.7(2)
C(4)-C(5)-C(6)	118.1(3)
N(1)-C(6)-C(1)	115.2(2)
N(1)-C(6)-C(5)	125.1(2)
C(1)-C(6)-C(5)	119.7(2)
N(1)-C(7)-C(8)	122.6(2)
N(1)-C(7)-S(1)	115.75(16)
C(8)-C(7)-S(1)	121.62(17)
C(9)-C(8)-C(16)	120.4(2)
C(9)-C(8)-C(7)	121.7(2)
C(16)-C(8)-C(7)	117.91(19)
C(8)-C(9)-C(10)	121.1(2)
C(15)-C(10)-C(11)	119.37(19)
C(15)-C(10)-C(9)	117.26(19)
C(11)-C(10)-C(9)	123.4(2)
C(10)-C(11)-C(12)	121.2(2)
N(2)-C(12)-C(11)	122.2(2)
N(2)-C(12)-C(13)	120.92(19)
C(11)-C(12)-C(13)	116.90(19)
C(14)-C(13)-C(12)	122.4(2)
C(13)-C(14)-C(15)	119.0(2)
O(2)-C(15)-C(14)	117.05(19)
O(2)-C(15)-C(10)	121.88(18)
C(14)-C(15)-C(10)	121.06(19)
O(1)-C(16)-O(2)	117.1(2)
O(1)-C(16)-C(8)	125.4(2)
O(2)-C(16)-C(8)	117.46(19)
N(2)-C(17)-C(18)	113.40(18)
N(2)-C(19)-C(20)	113.35(19)

Symmetry transformations used to generate equivalent atoms:

Table S10 Anisotropic displacement parameters ($Å^2 x\ 10^3$) for **6-NEt$_2$-CUM** (ic20004). The anisotropic displacement factor exponent takes the form: $-2p^2[\ h^2\ a^{*2}U^{11} + ..+ 2\ h\ k\ a^*\ b^*\ U^{12}\ ]$

	U^{11}	U^{22}	U^{33}	U^{23}	U^{13}	U^{12}
S(1)	21(1)	24(1)	23(1)	-3(1)	2(1)	-1(1)
O(1)	24(1)	33(1)	20(1)	3(1)	-1(1)	-3(1)
O(2)	22(1)	22(1)	16(1)	3(1)	1(1)	-1(1)
N(1)	22(1)	17(1)	27(1)	1(1)	6(1)	1(1)
N(2)	24(1)	25(1)	17(1)	1(1)	1(1)	-4(1)
C(1)	22(1)	20(1)	34(1)	-6(1)	9(1)	0(1)
C(2)	23(1)	27(1)	38(1)	-12(1)	7(1)	1(1)
C(3)	25(1)	22(1)	53(2)	-13(1)	11(1)	-3(1)
C(4)	31(1)	19(1)	58(2)	-4(1)	19(1)	-4(1)
C(5)	29(1)	23(1)	41(2)	-1(1)	10(1)	1(1)
C(6)	20(1)	18(1)	32(1)	-3(1)	6(1)	2(1)
C(7)	19(1)	20(1)	21(1)	-1(1)	4(1)	3(1)
C(8)	17(1)	17(1)	21(1)	-2(1)	4(1)	3(1)
C(9)	20(1)	18(1)	20(1)	3(1)	6(1)	4(1)
C(10)	17(1)	17(1)	19(1)	1(1)	3(1)	4(1)
C(11)	21(1)	21(1)	16(1)	1(1)	5(1)	2(1)
C(12)	18(1)	21(1)	17(1)	-2(1)	3(1)	4(1)

C(13)	18(1)	17(1)	23(1)	-1(1)	5(1)	0(1)
C(14)	23(1)	19(1)	19(1)	4(1)	6(1)	2(1)
C(15)	17(1)	21(1)	15(1)	0(1)	1(1)	4(1)
C(16)	17(1)	22(1)	21(1)	-1(1)	3(1)	3(1)
C(17)	26(1)	28(1)	22(1)	0(1)	-1(1)	-6(1)
C(18)	49(2)	29(1)	28(1)	-4(1)	0(1)	0(1)
C(19)	26(1)	33(1)	18(1)	-1(1)	3(1)	-7(1)
C(20)	36(1)	40(2)	31(1)	13(1)	4(1)	-4(1)
O(3)	124(8)	75(7)	34(5)	-3(5)	-9(5)	-1(6)
C(21)	156(11)	72(9)	56(8)	-20(7)	-33(9)	1(9)
O(4)	124(7)	44(5)	30(4)	-14(4)	-14(5)	11(5)
C(22)	148(10)	76(8)	22(6)	7(6)	18(7)	43(8)

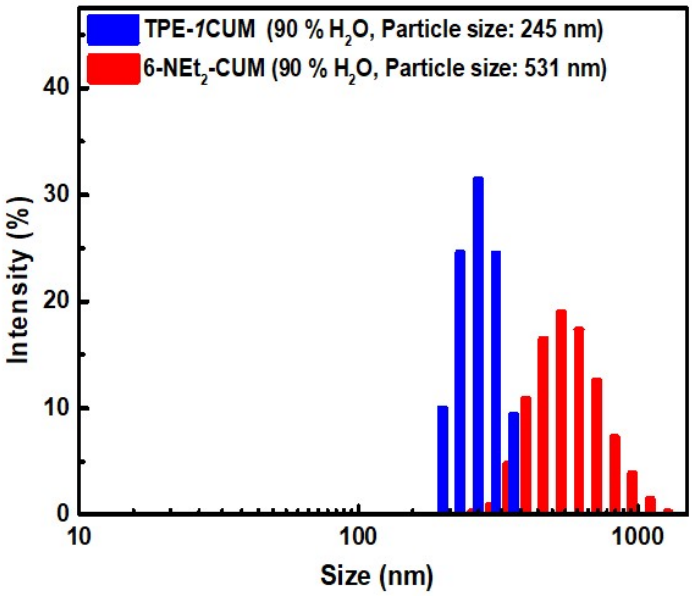

Fig. S5 DLS measurements of **TPE-*1*CUM** and **6-NEt$_2$-CUM** at similar water contents (f_w =90%) in THF.

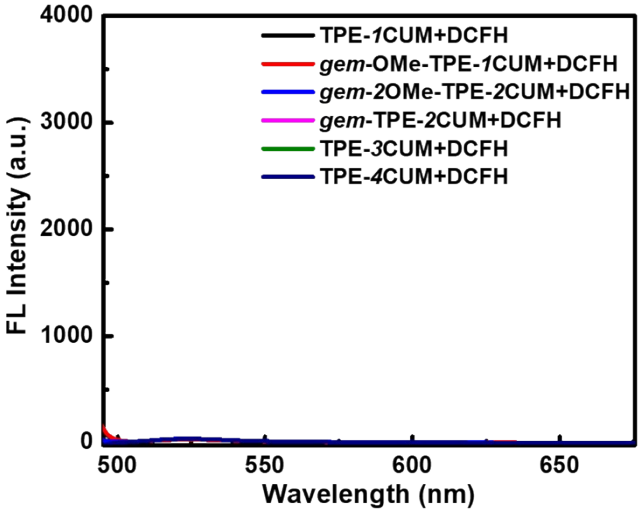

Fig. S6 ROS generation in the mixtures of DCFH (5 μM) and **TPE-*n*CUMs** (5 μM) in molecular-state (DMSO only) after white-light irradiation (50 mW cm^{-2}, 20 min). (λ_{ex} = 490 nm for DCFH)

Computational Section (CS)

Density functional theory (DFT) and time-dependent density functional theory (TDDFT) calculations of **TPE-*n*CUMs** were conducted at the B3LYP/6-311+G** level by Gaussian 16 program to understand the correlation between structural and the optical properties. The solvent effects were considered using the polarizable continuum model (PCM) with the cyclohexane solvent (dielectric constant ε=2.02)

Table CS-1 The computed optical excitations and molecular orbital contributions for the S_0-optimized structures of **TPE-*n*CUMs**.

	State	E/eV	nm	f	Contribution	weight
TPE-*4*CUM	S_1	2.76	448.4	0.2267	HOMO→LUMO	97%
	S_2	2.86	434.0	0.0051	HOMO→LUMO+1	97%
	T_1	2.12	585.4	0	HOMO-2→LUMO+1	36%
					HOMO-1→LUMO	29%
					HOMO→LUMO	16%
	T_2	2.12	583.3	0	HOMO-2→LUMO	38%
					HOMO-1→LUMO+1	29%

					HOMO→LUMO+1	18%
TPE-*3*CUM	S_1	2.74	452.2	0.236	HOMO→LUMO	98%
	S_2	2.83	437.6	0.0341	HOMO→LUMO+1	97%
	T_1	2.12	583.3	0	HOMO-2→LUMO	31%
					HOMO-2→LUMO+1	21%
					HOMO-1→LUMO	15%
					HOMO→LUMO	17%
	T_2	2.13	580.5	0	HOMO-2→LUMO	19%
					HOMO-1→LUMO+1	41%
					HOMO→LUMO+1	19%
***gem*-TPE-*2*CUM**	S_1	2.71	456.9	0.0655	HOMO→LUMO	99%
	S_2	2.90	427.2	0.1083	HOMO→LUMO+1	98%
	T_1	2.13	581.1	0	HOMO-1→LUMO	66%
					HOMO→LUMO	19%
	T_2	2.38	521.8	0	HOMO-2→LUMO+1	38%
					HOMO→LUMO	8%
					HOMO→LUMO+1	21%
					HOMO→LUMO+2	11%
***gem*-OMe-TPE-*1*CUM**	S_1	2.49	497.8	0.0281	HOMO→LUMO	99%
	S_2	3.15	393.4	1.0051	HOMO-1→LUMO	97%
	T_1	2.14	580.0	0	HOMO-1→LUMO	70%
					HOMO→LUMO	19%
	T_2	2.37	524.0	0	HOMO-1→LUMO	11%
					HOMO→LUMO	68%
					HOMO→LUMO+1	12%
TPE-*1*CUM	S_1	2.68	462.3	0.0781	HOMO→LUMO	99%
	S_2	3.18	389.5	0.9504	HOMO-1→LUMO	97%
	T_1	2.14	578.4	0	HOMO-1→LUMO	69%
					HOMO→LUMO	21%
	T_2	2.48	499.2	0	HOMO→LUMO	43%
					HOMO→LUMO+1	41%
***gem*-2OMe-TPE-*2*CUM**	S_1	2.42	512.0	0.0337	HOMO→LUMO	99%
	S_2	2.61	474.8	0.064	HOMO→LUMO+1	99%
	T_1	2.11	588.5	0	HOMO-1→LUMO	52%
					HOMO→LUMO	33%
	T_2	2.28	544.7	0	HOMO-2→LUMO+1	10%
					HOMO-1→LUMO	10%
					HOMO→LUMO	29%

	HOMO→LUMO+1	20%
	HOMO→LUMO+2	14%

	HOMO-2	HOMO-1	HOMO	LUMO	LUMO+1	LUMO+2
TPE-*4*CUM	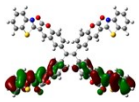	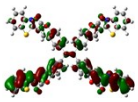	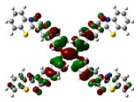	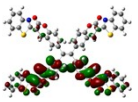		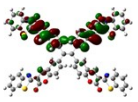
TPE-*3*CUM	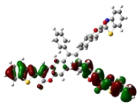	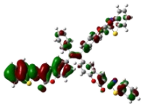	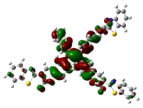	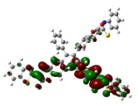	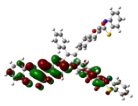	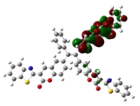
gem-TPE-*2*CUM	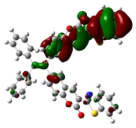	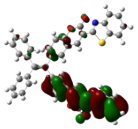	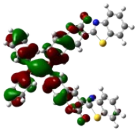	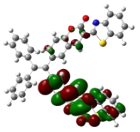	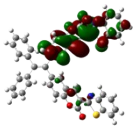	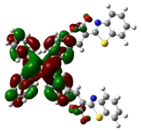
gem-OMe-TPE-*1*CUM	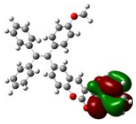	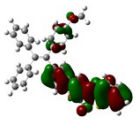	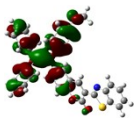	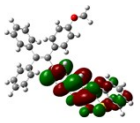	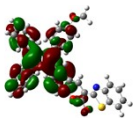	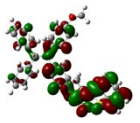
TPE-*1*CUM	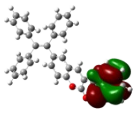	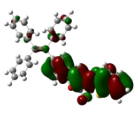	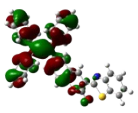	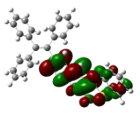	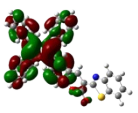	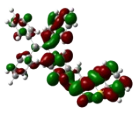
gem-2OMe-TPE-*2*CUM	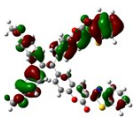	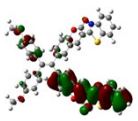	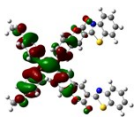	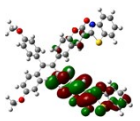	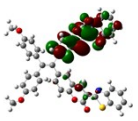	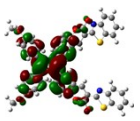

Fig. CS-1 Frontier molecular orbitals of **TPE-*n*CUMs** are associated with major optical transitions.

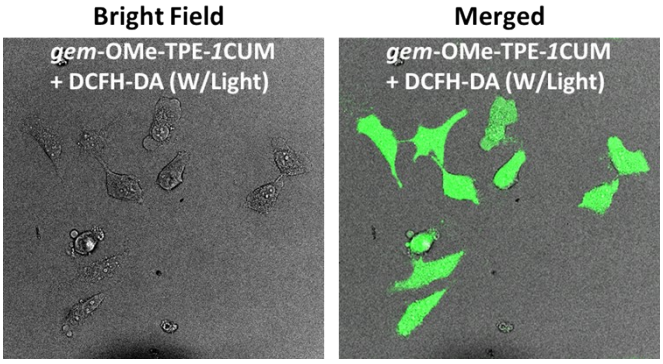

Fig. S7 the separate/merged fluorescence with bright-field images of ***gem*-OMe-TPE-*1*CUM+DCFH-DA (W/light)**.

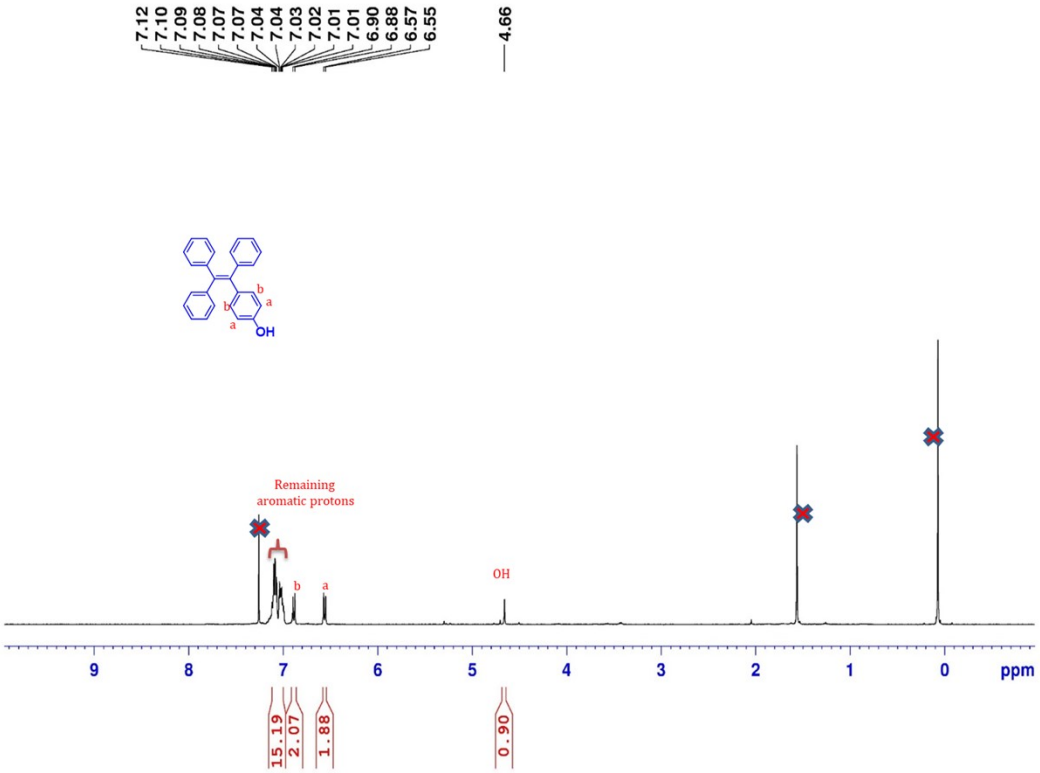

Fig. S8.1 ^{1}H-NMR of **1a**.

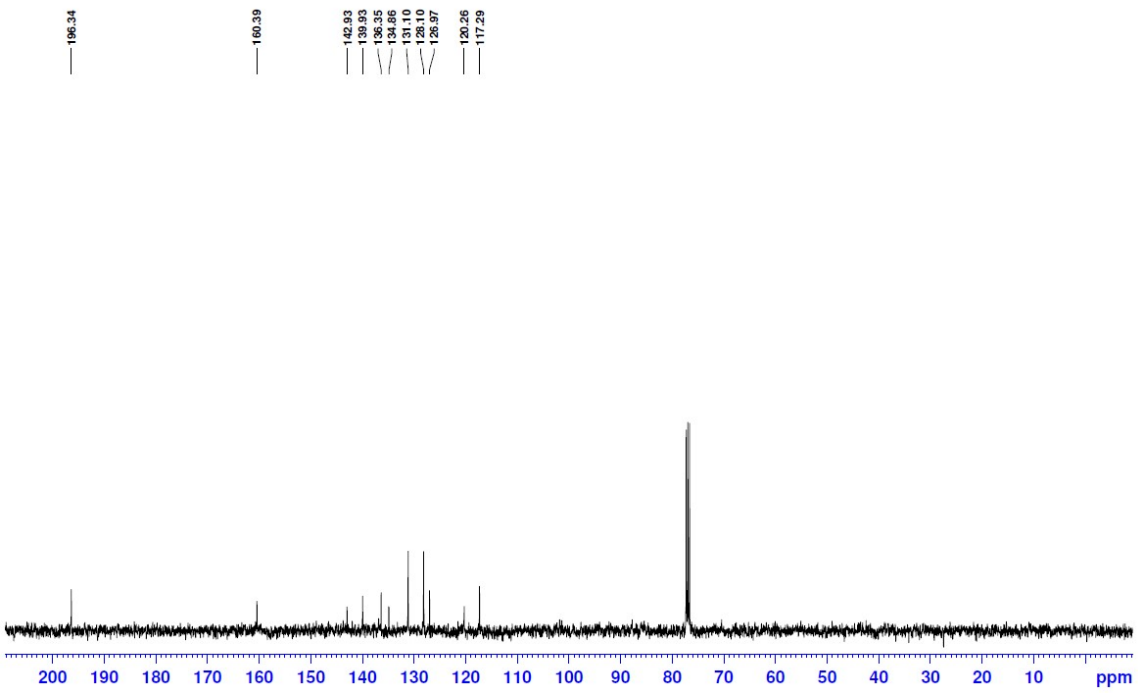

Fig. S8.2 ^{13}C-NMR of **1a**.

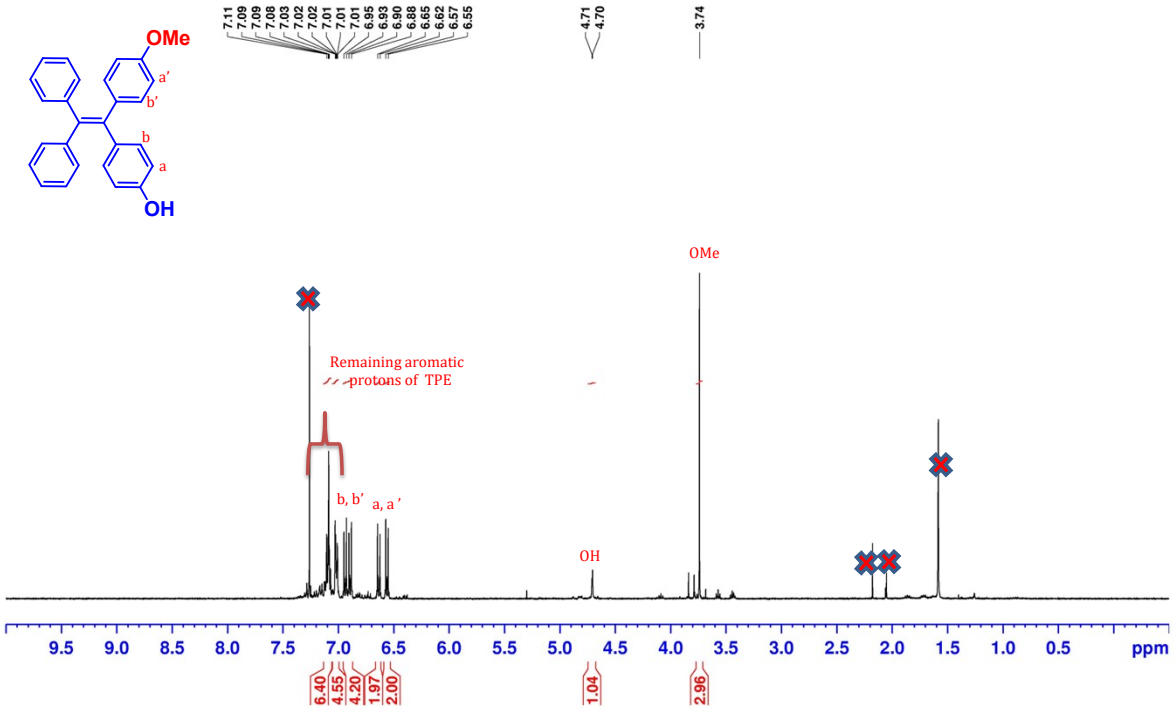

Fig. S9.1 ^{1}H-NMR of **1b**.

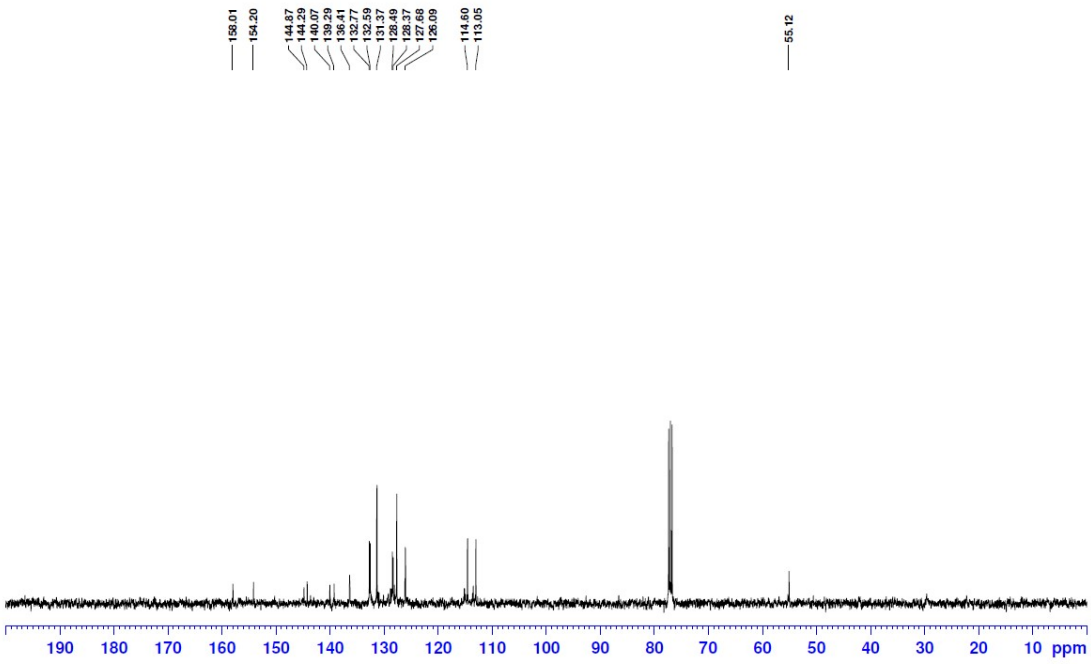

Fig. S9.2 ^{13}C-NMR of **1b**.

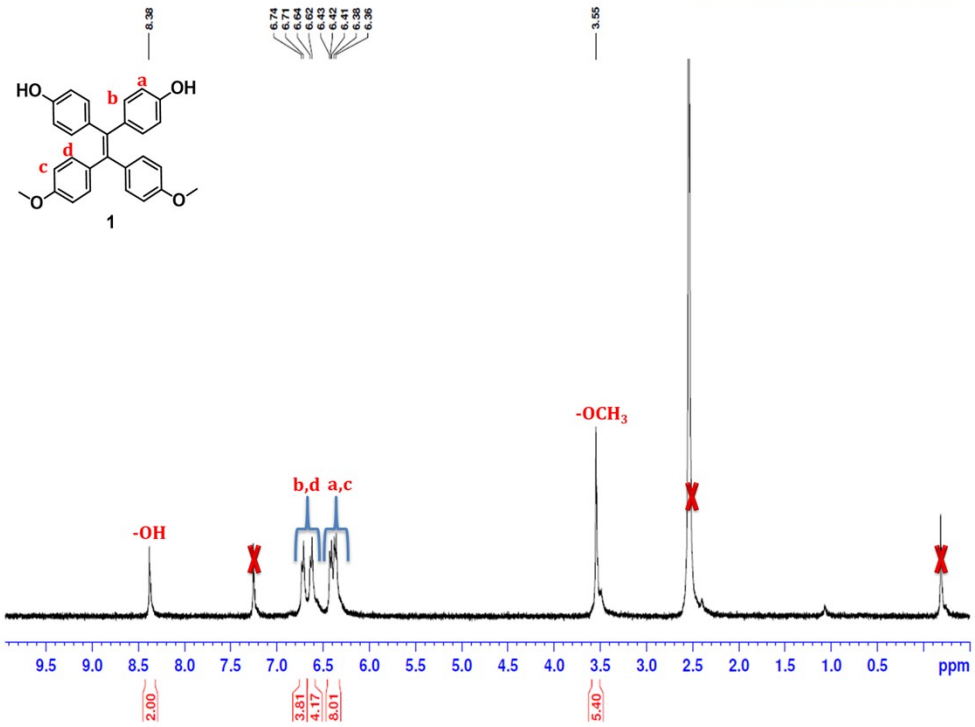

Fig. S10.1 ^{1}H-NMR of **1c**.

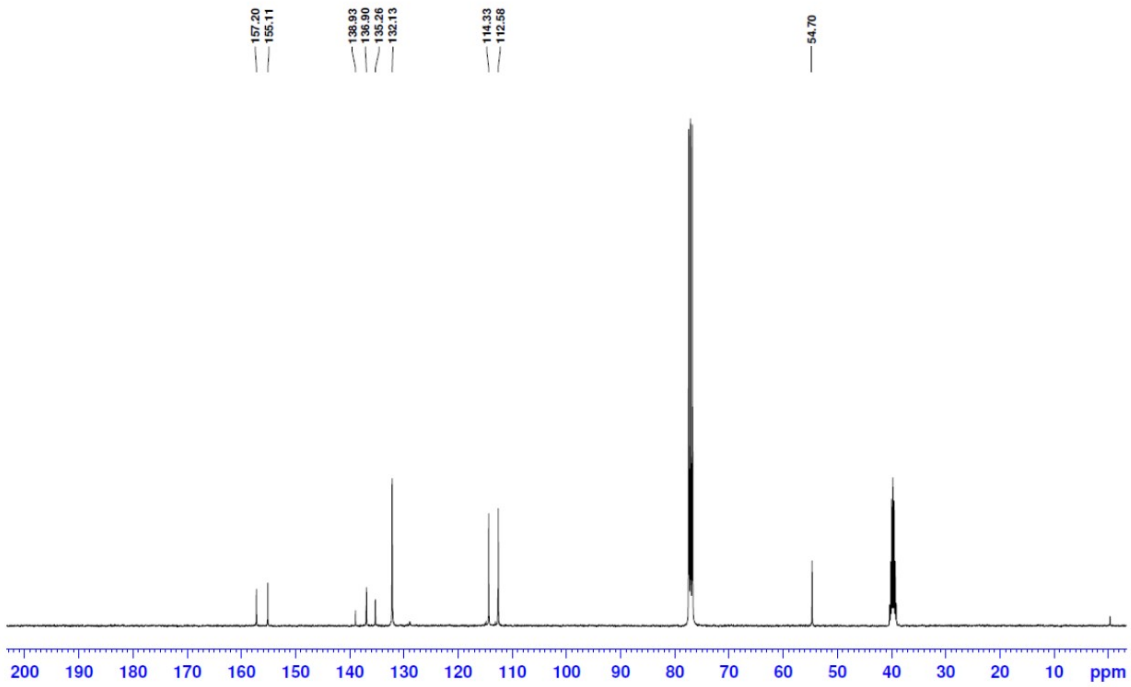

Fig. S10.2 ^{13}C-NMR of **1c**.

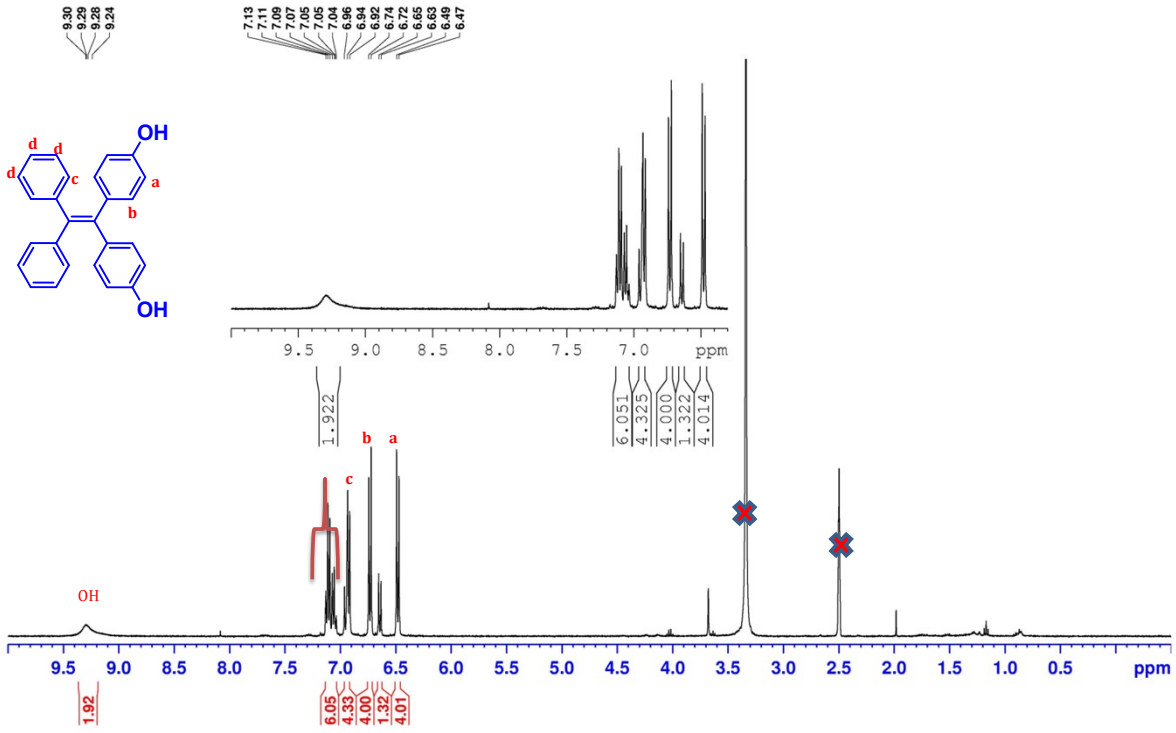

Fig. S11.1^{1}H-NMR of **1d**.

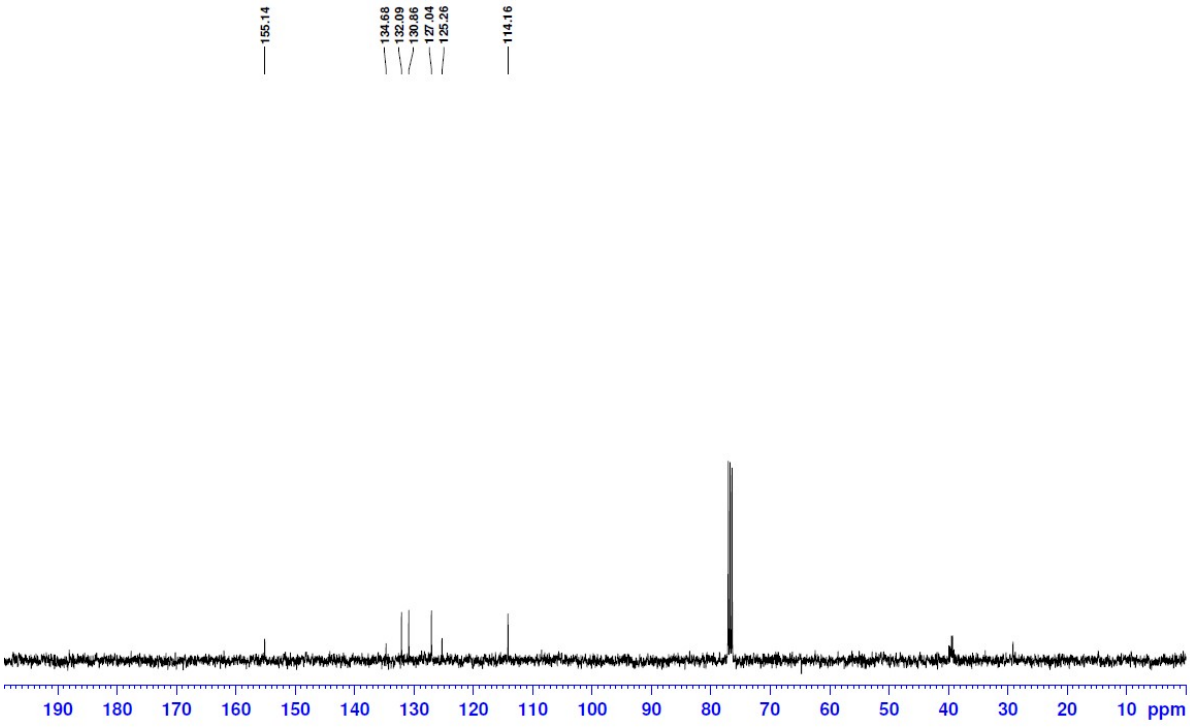

Fig. S11.2[13]C-NMR of **1d**.

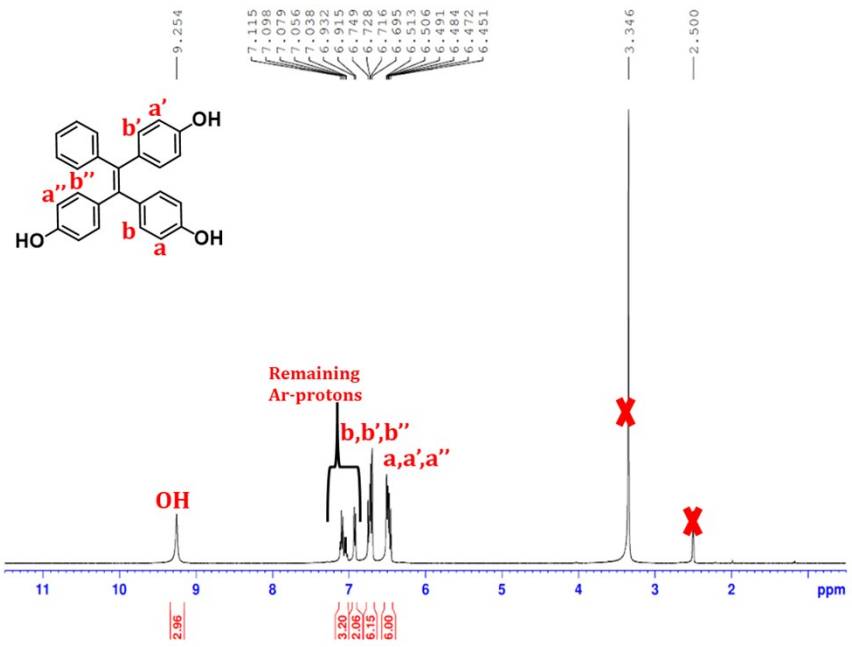

Fig. S12.1[1]H-NMR of **1e**.

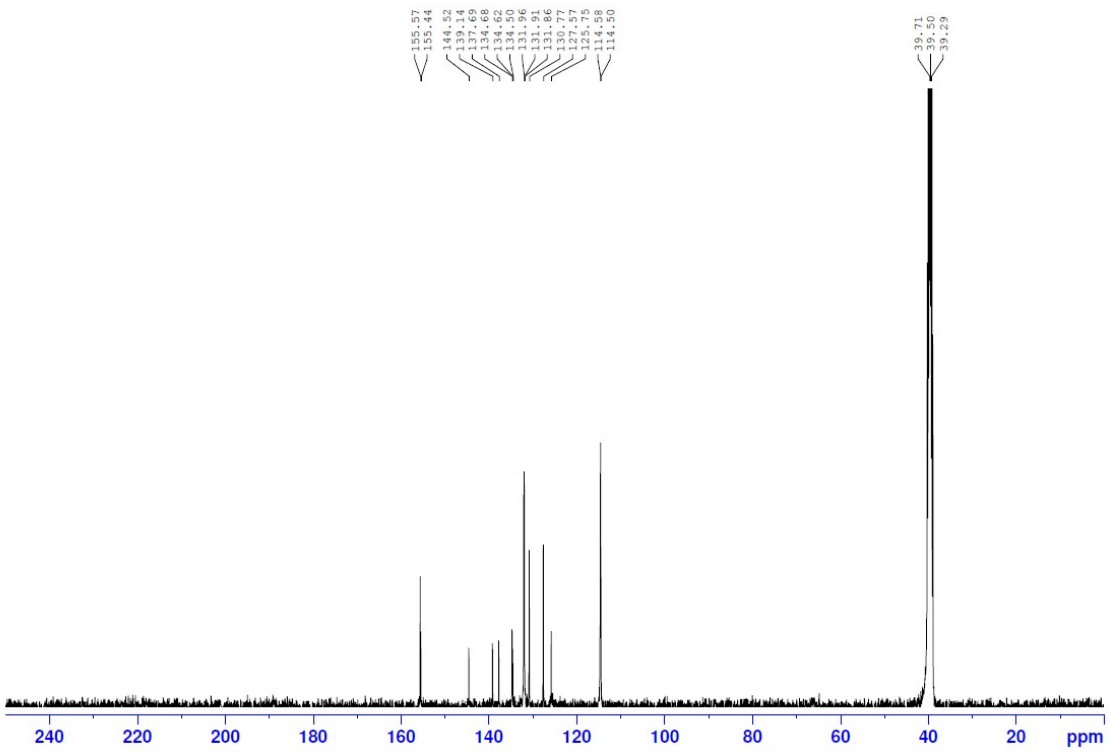

Fig. S12.2 ^{13}C-NMR of **1e**.

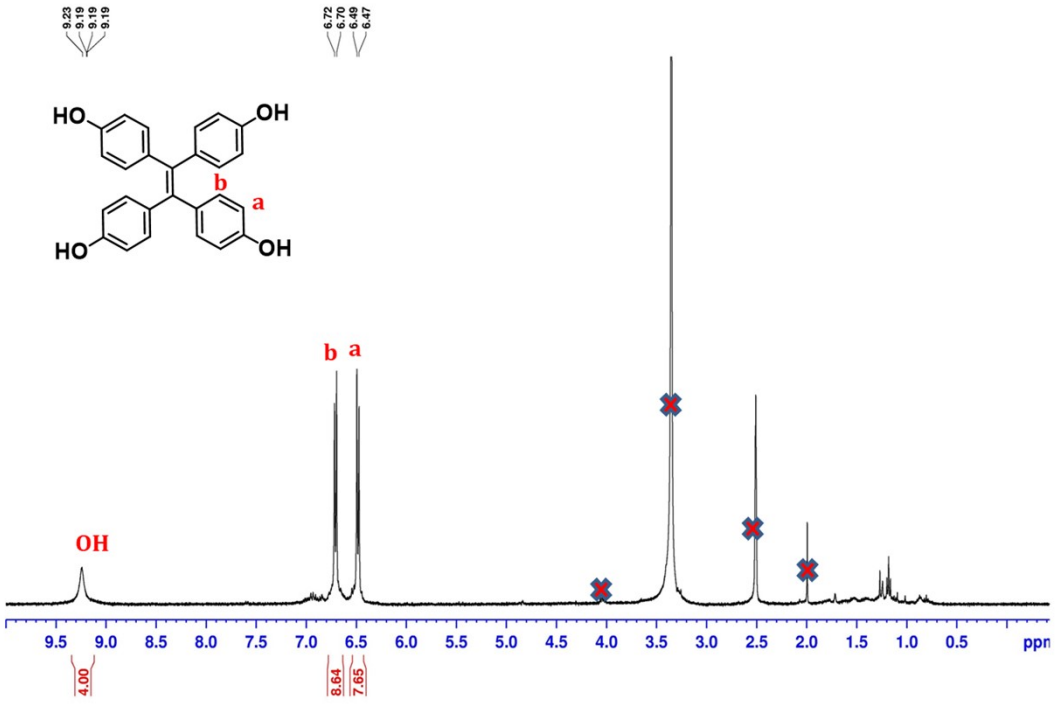

Fig. S13.1 ^{1}H-NMR of **1f**.

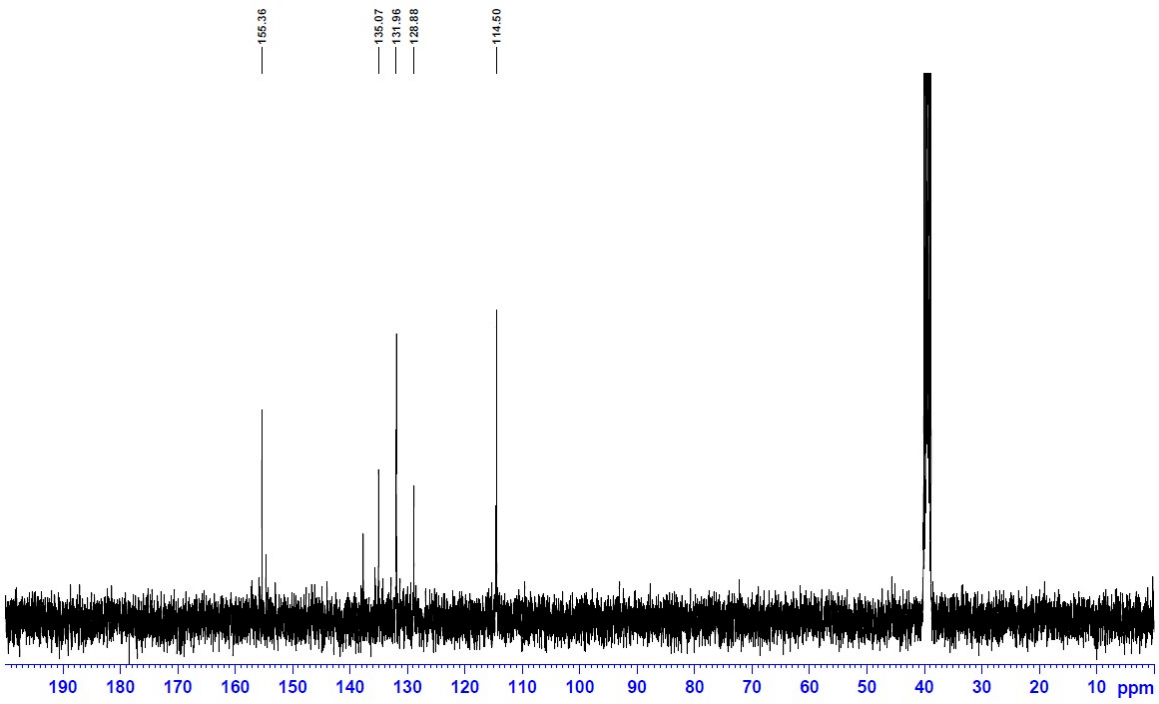

Fig. S13.2 ^{13}C-NMR of **1f**.

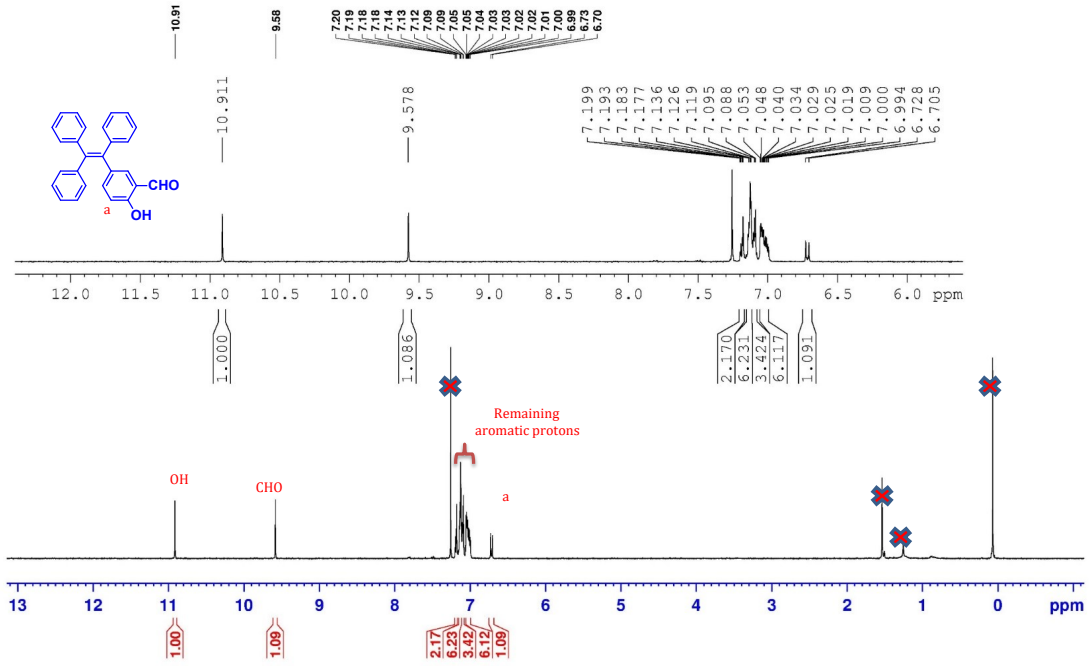

Fig. S14.1 ^{1}H-NMR of **2a**.

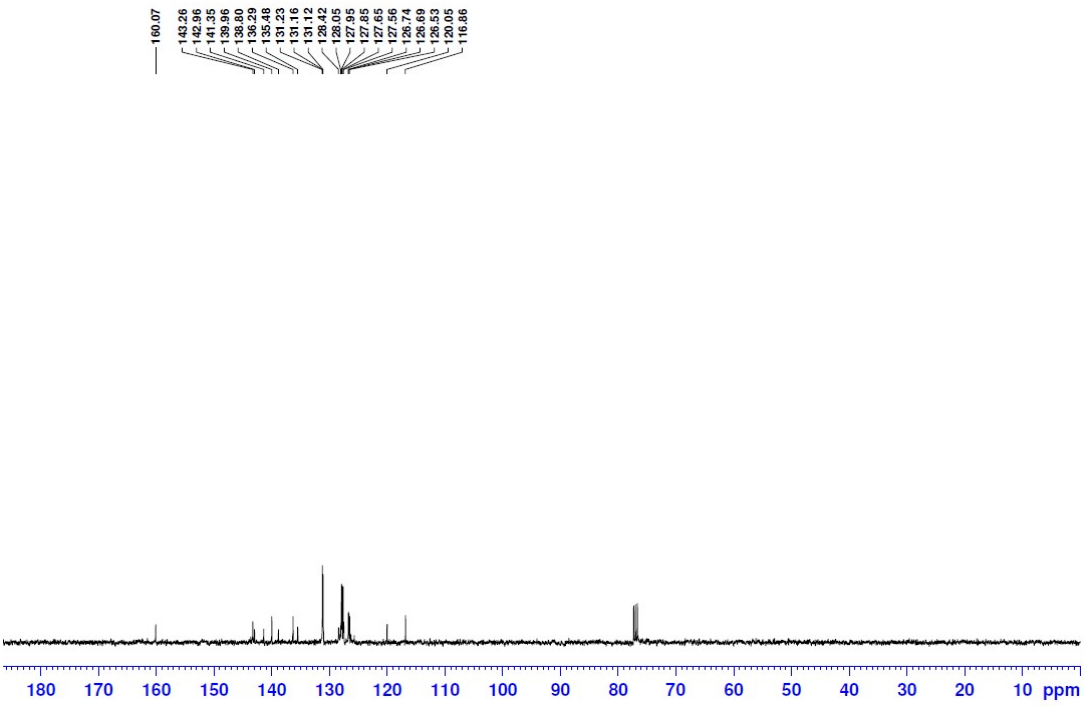

Fig. S14.2 ^{13}C-NMR of **2a**.

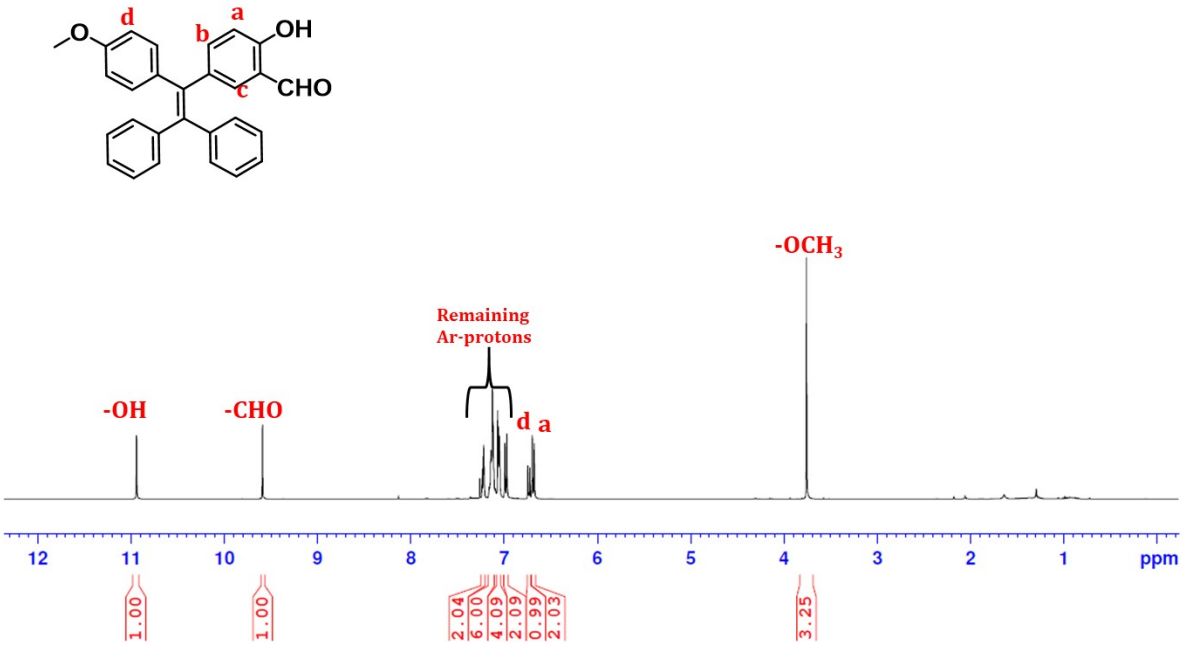

Fig. S15.1 ^{1}H-NMR of **2b**.

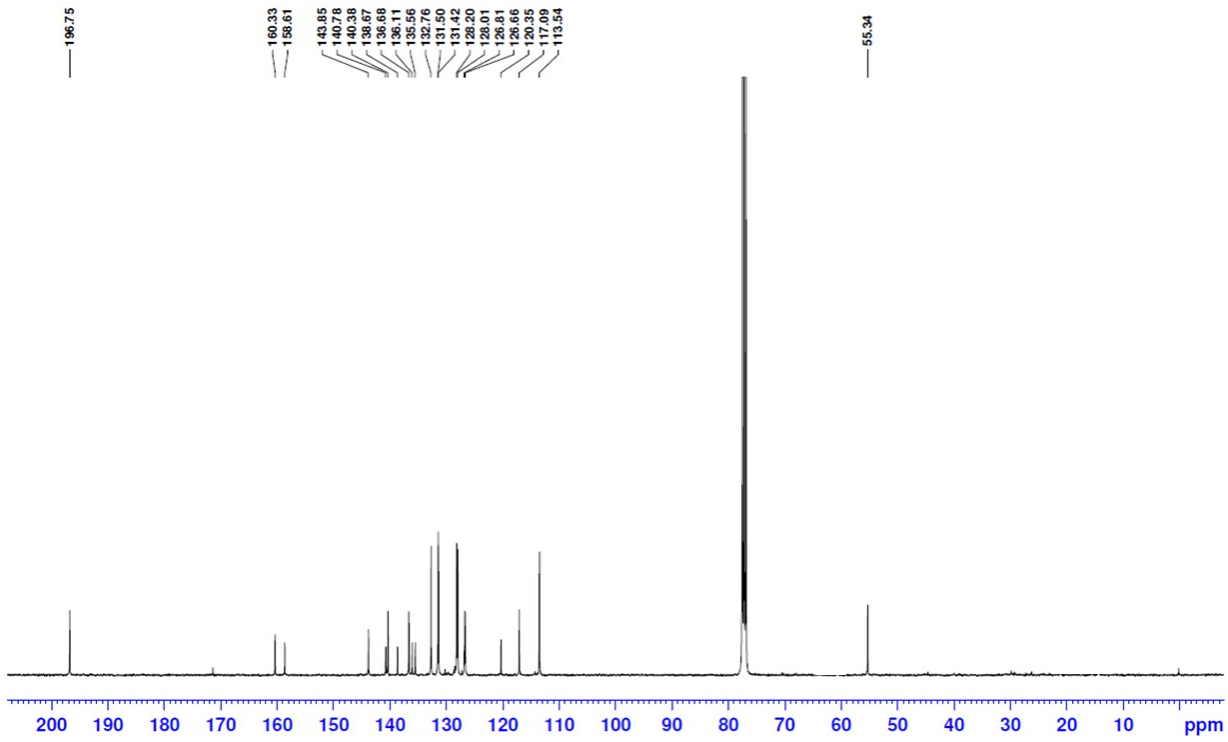

Fig. S15.2 ^{13}C-NMR of **2b**.

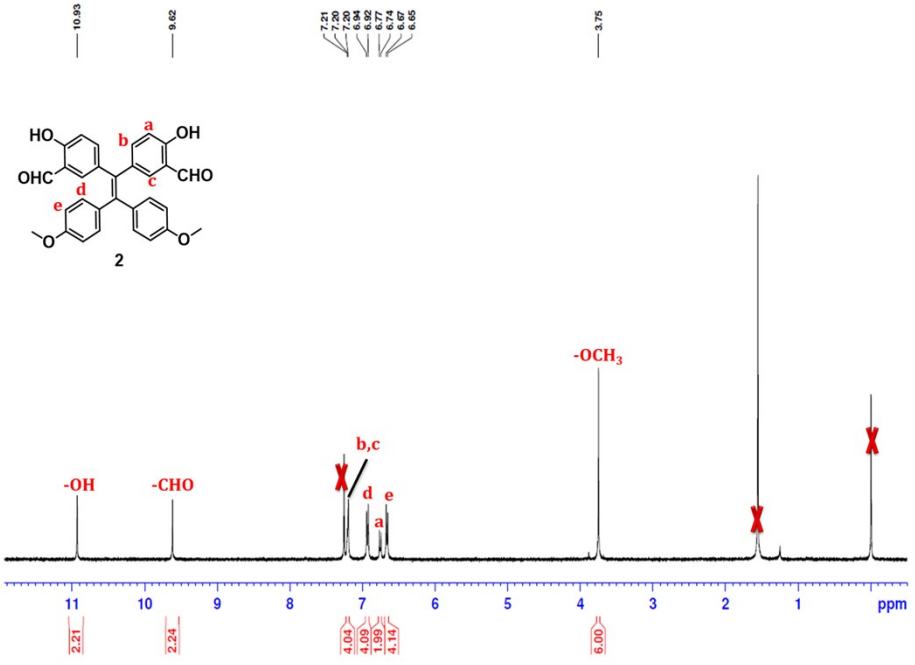

Fig. S16.1 ^{1}H-NMR of **2c**.

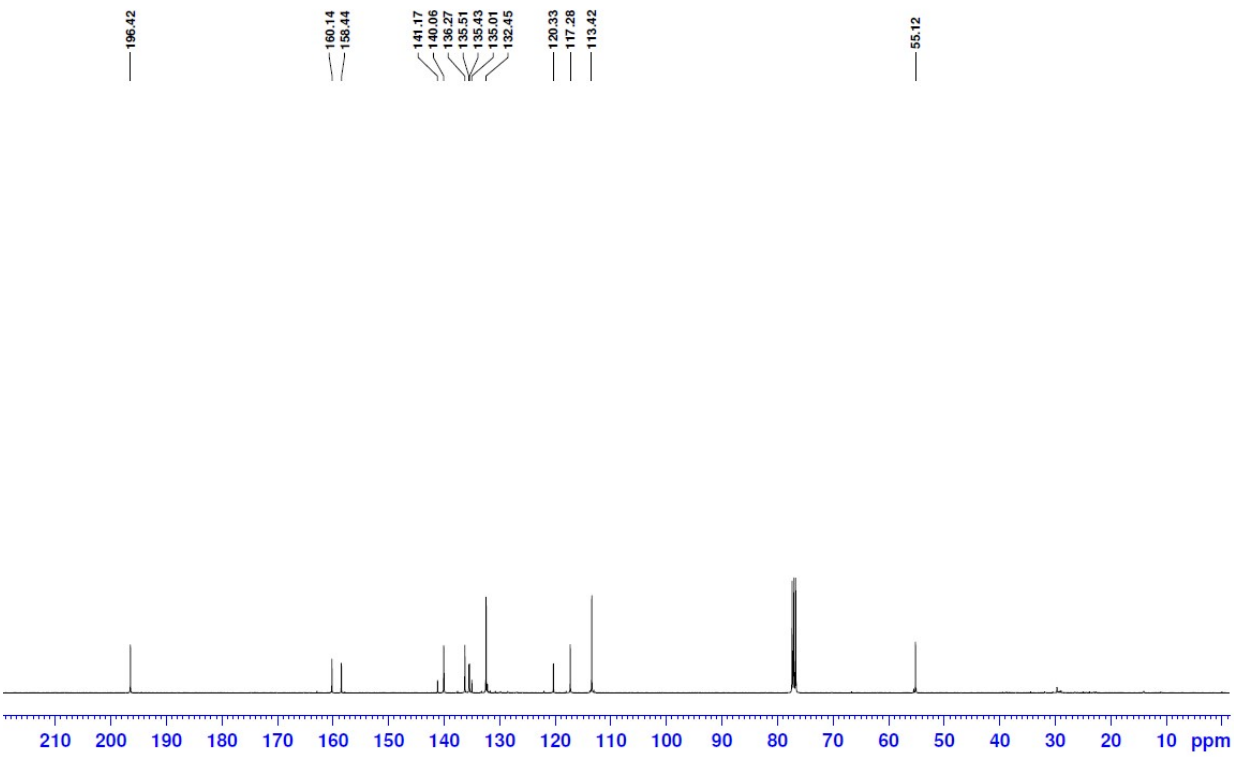

Fig. S16.2 ^{13}C-NMR of **2c**.

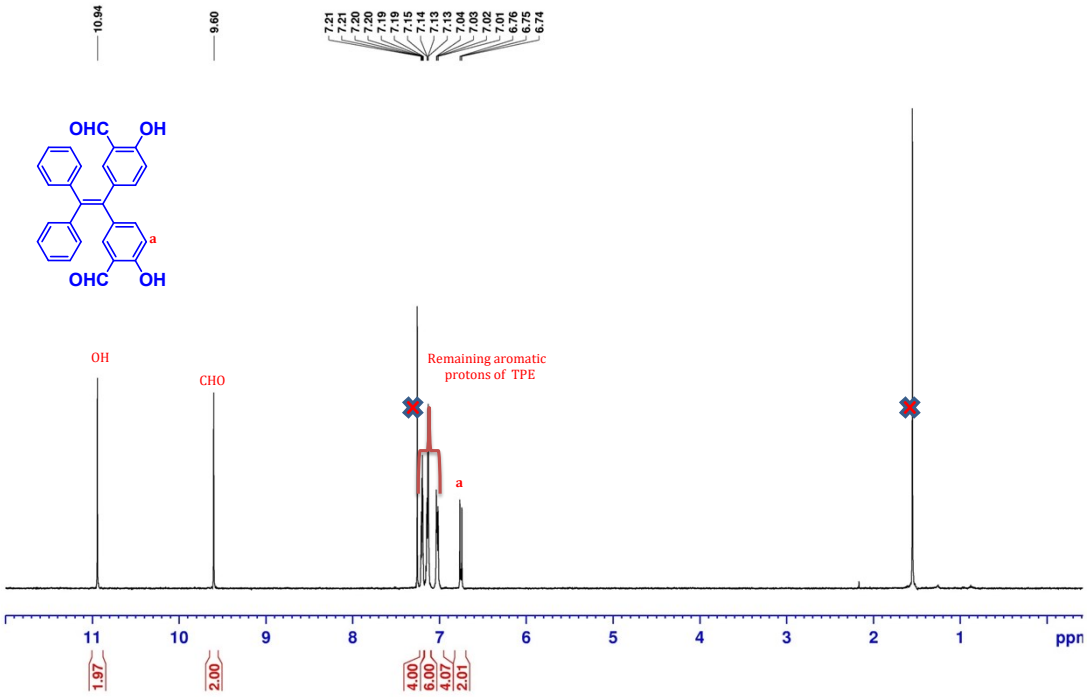

Fig. S17.1 ^{1}H-NMR of **2d**.

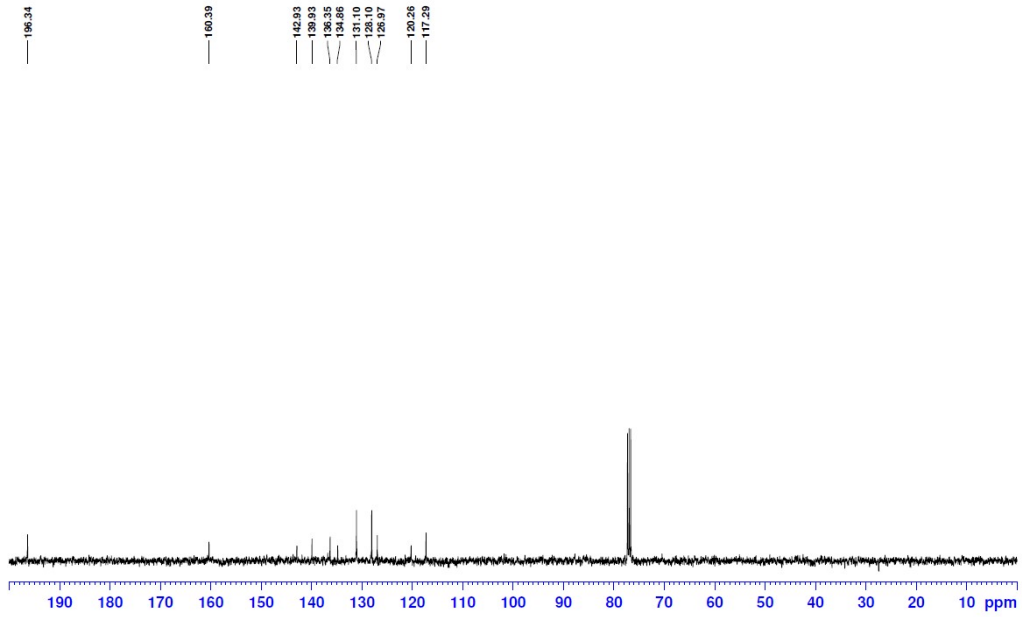

Fig. S17.2 ^{13}C-NMR of **2d**.

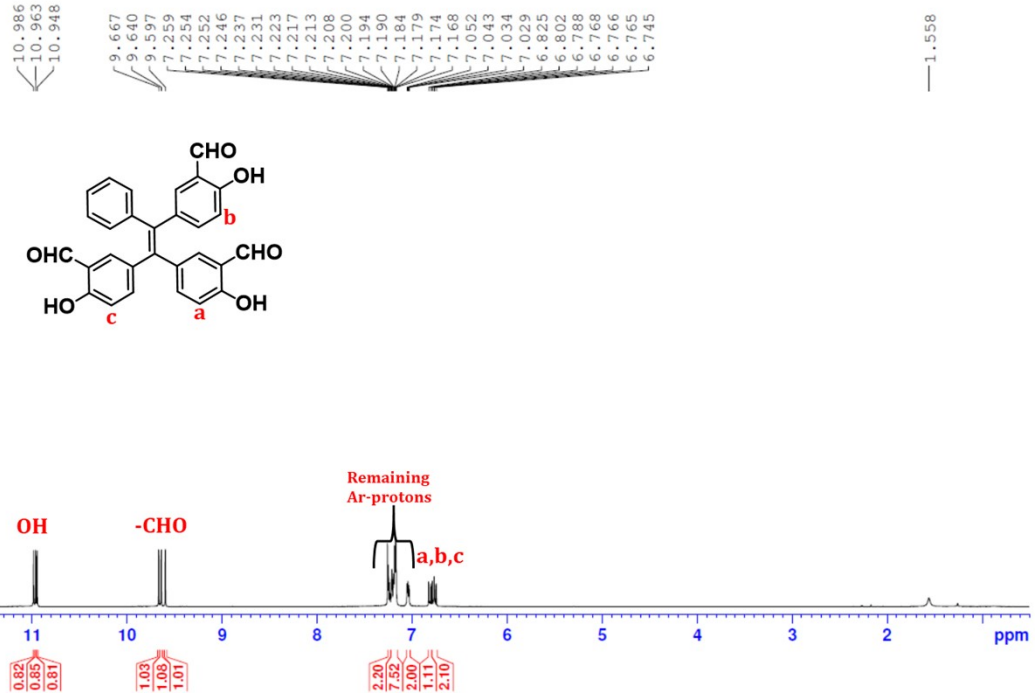

Fig. S18.1 ^{1}H-NMR of **2e**.

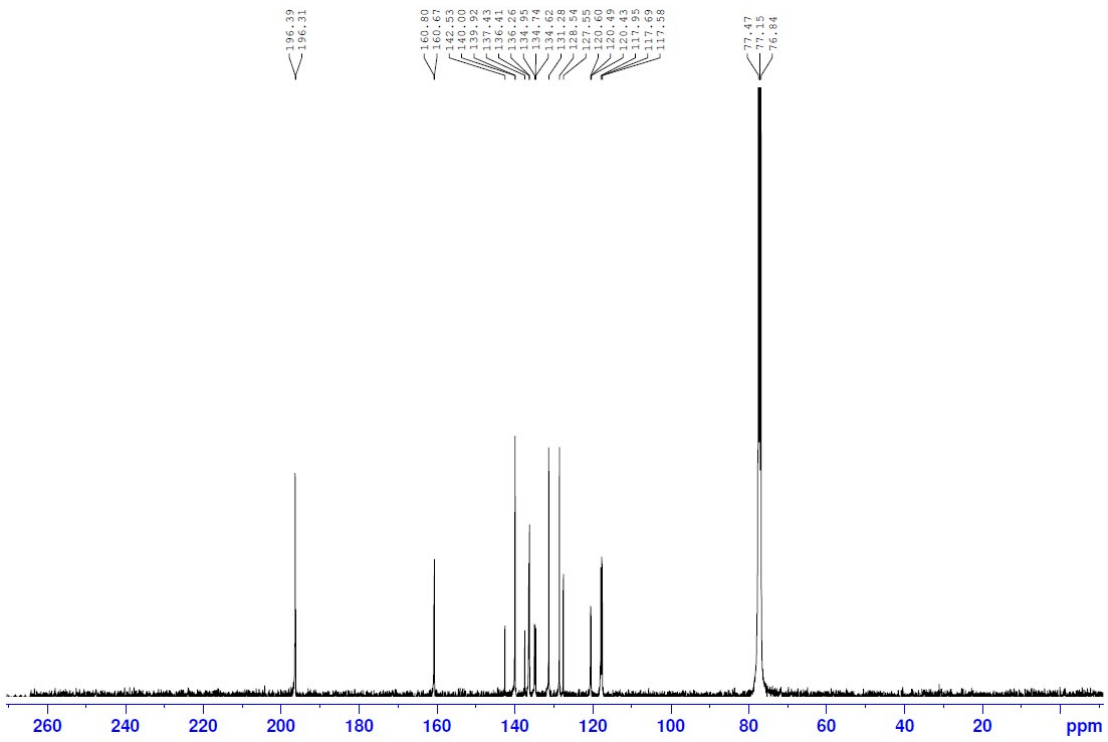

Fig. S18.2 ^{13}C-NMR of **2e**.

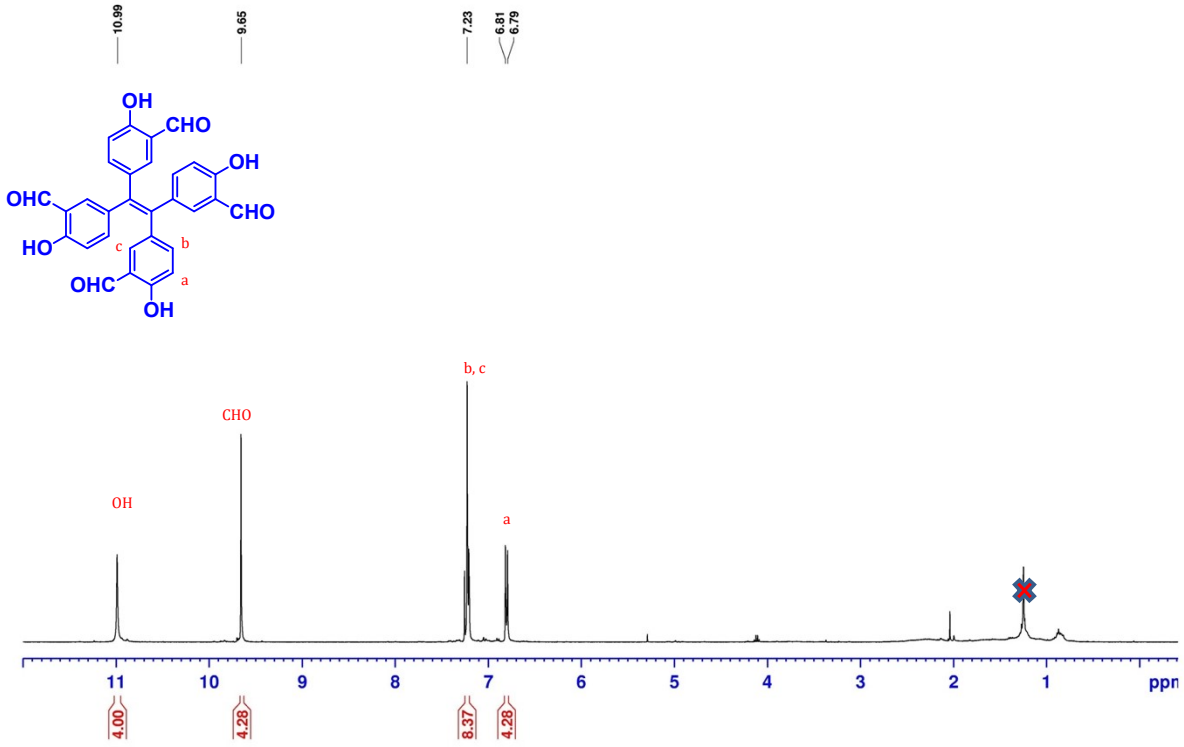

Fig. S19.1 [1]H-NMR of **3f**.

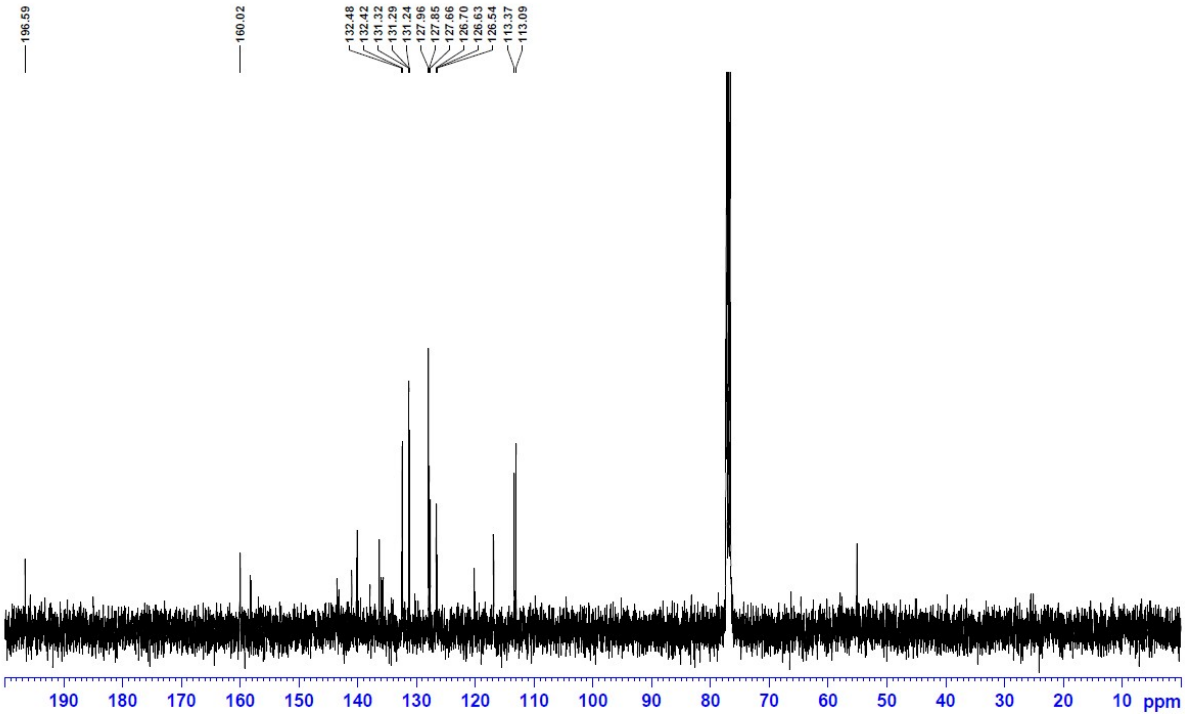

Fig. S19.2 [13]C-NMR of **3f**.

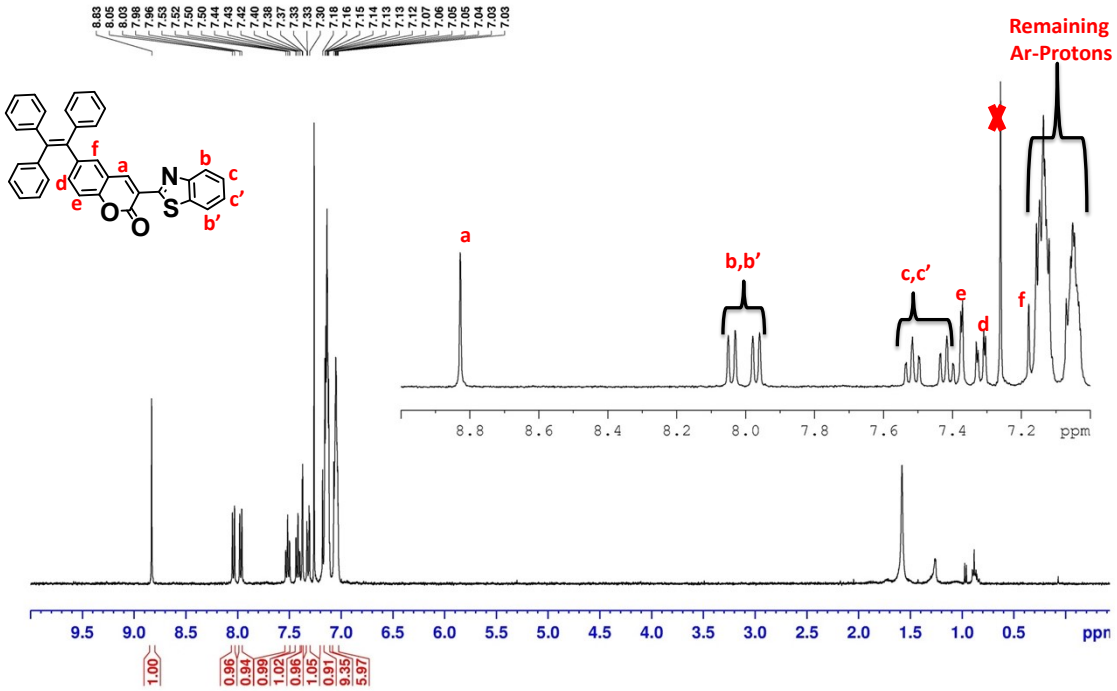

Fig. S20.1 [1]H-NMR of **TPE-*1*CUM**.

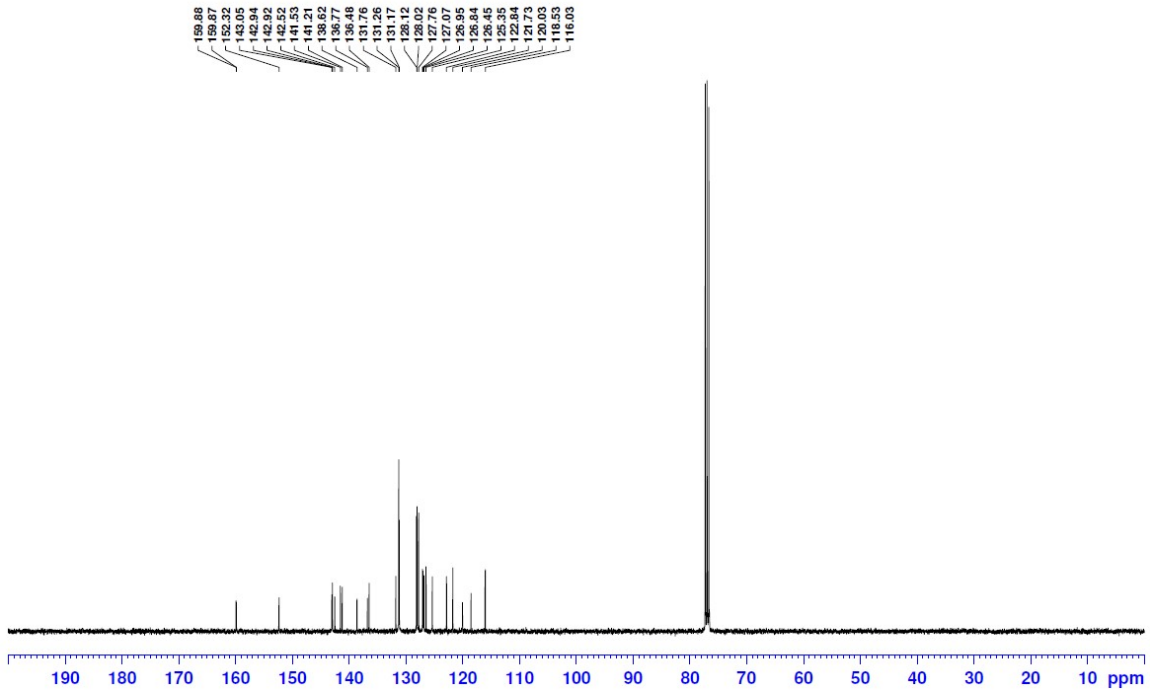

Fig. S20.2 ^{13}C-NMR of **TPE-*1*CUM**.

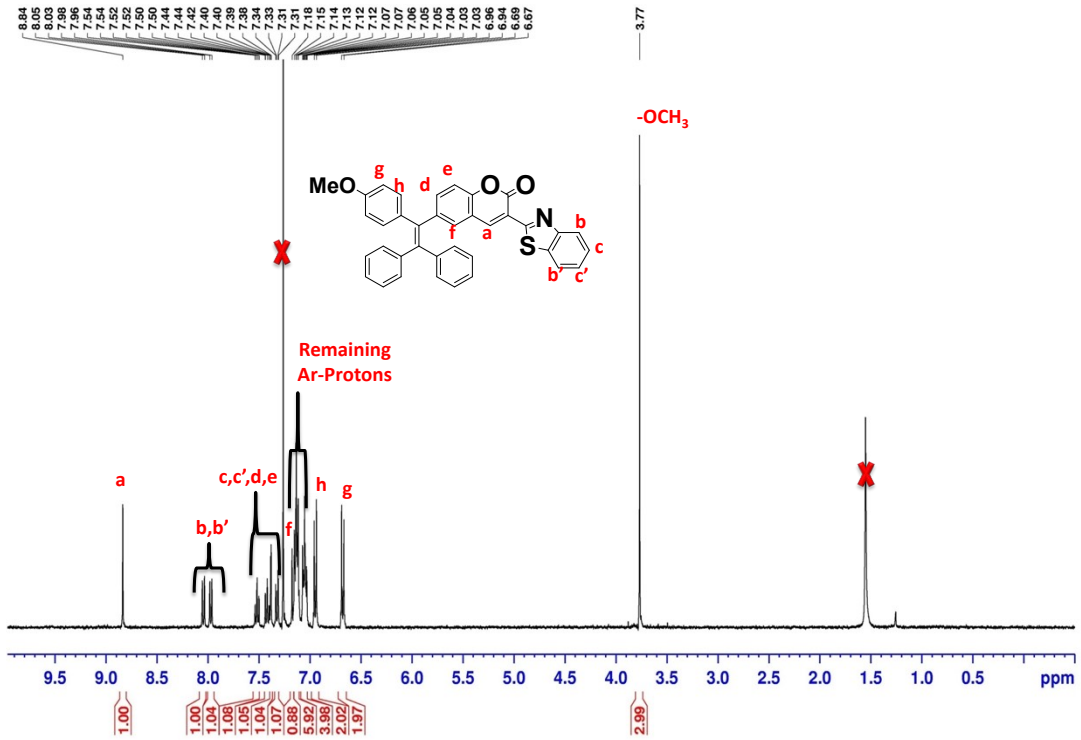

Fig. S21.1 ^{1}H-NMR of ***gem*-OMe-TPE-*1*CUM**.

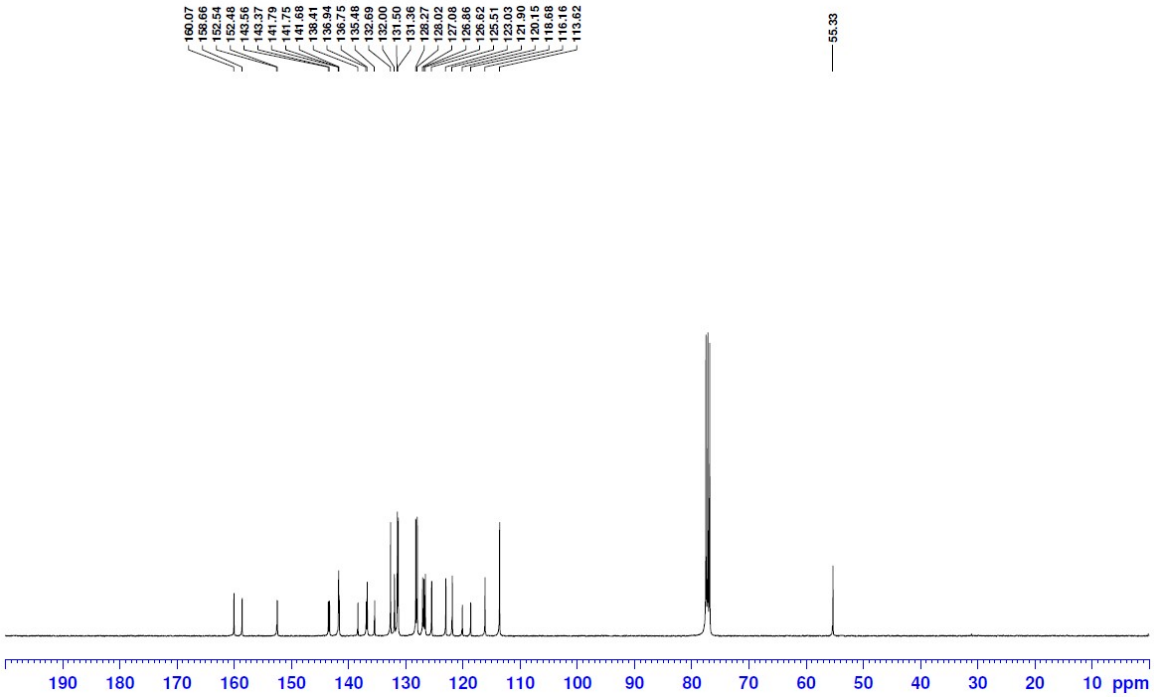

Fig. S21.2 ^{13}C-NMR of ***gem*-OMe-TPE-*1*CUM**.

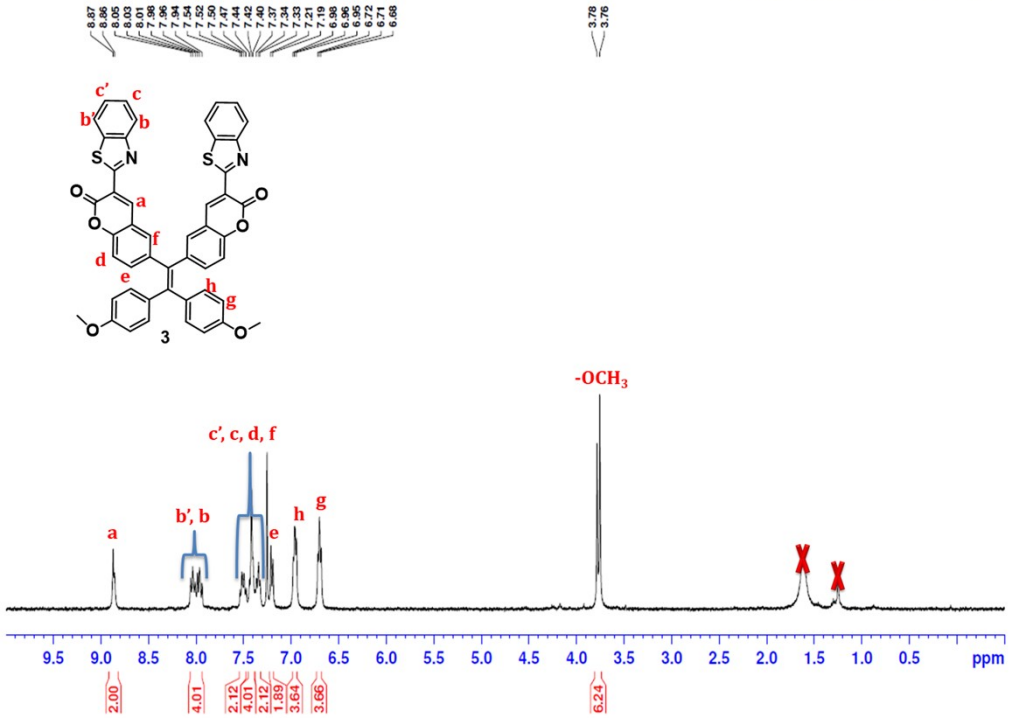

Fig. S22.1 ^{1}H-NMR of ***gem-2*OMe-TPE-*2*CUM**.

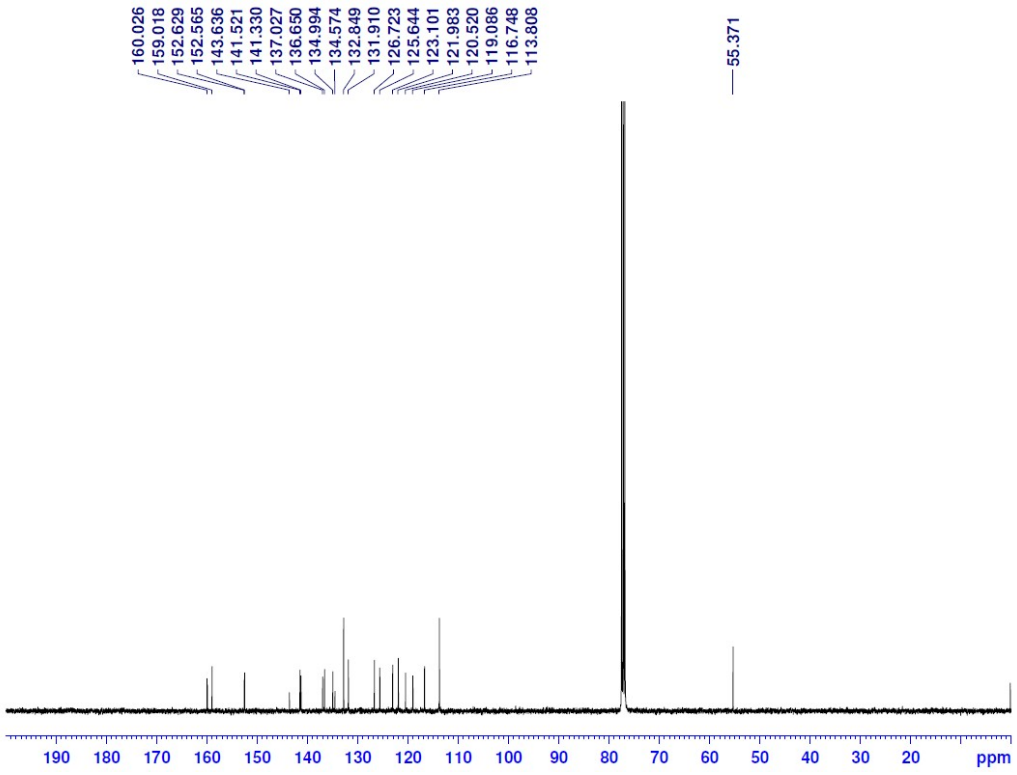

Fig. S22.2 ^{13}C-NMR of ***gem*-*2*OMe-TPE-*2*CUM**.

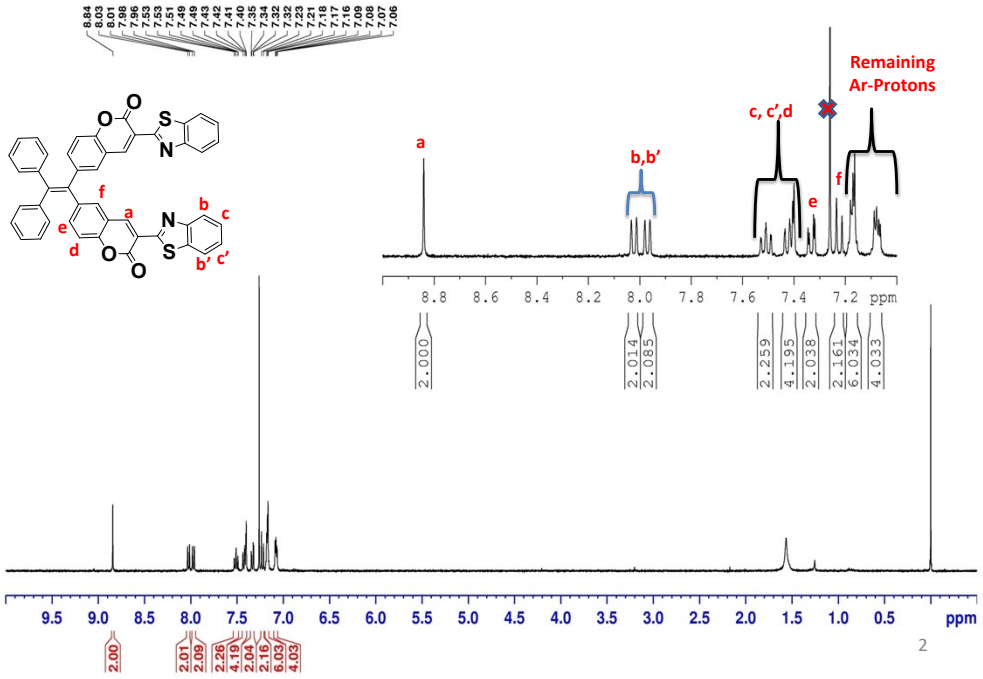

Fig. S23.1 ^{1}H-NMR of ***gem*-TPE-*2*CUM**.

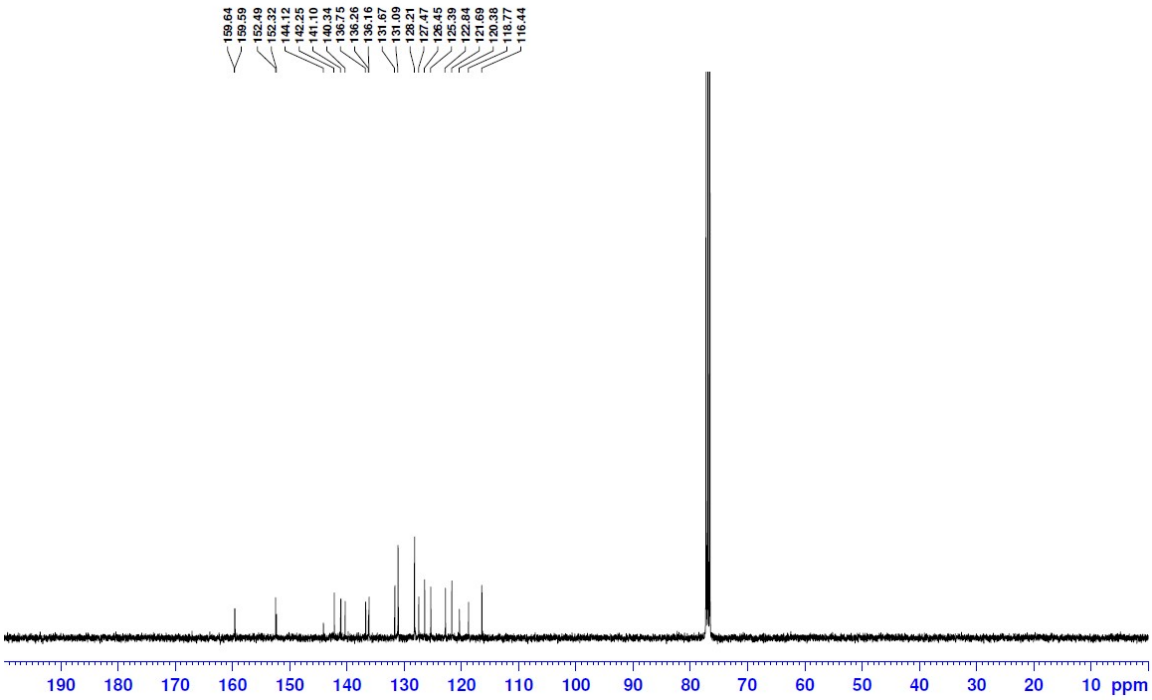

Fig. S23.2 ^{13}C-NMR of ***gem*-TPE-*2*CUM**.

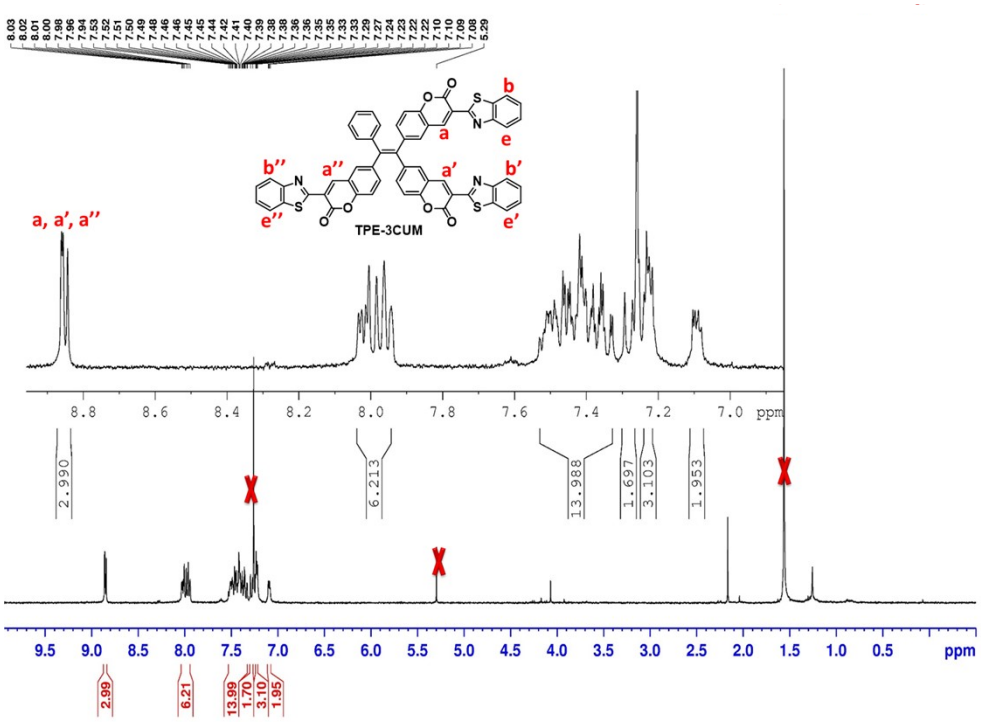

Fig. S24.1 ^{1}H-NMR of **TPE-*3*CUM**.

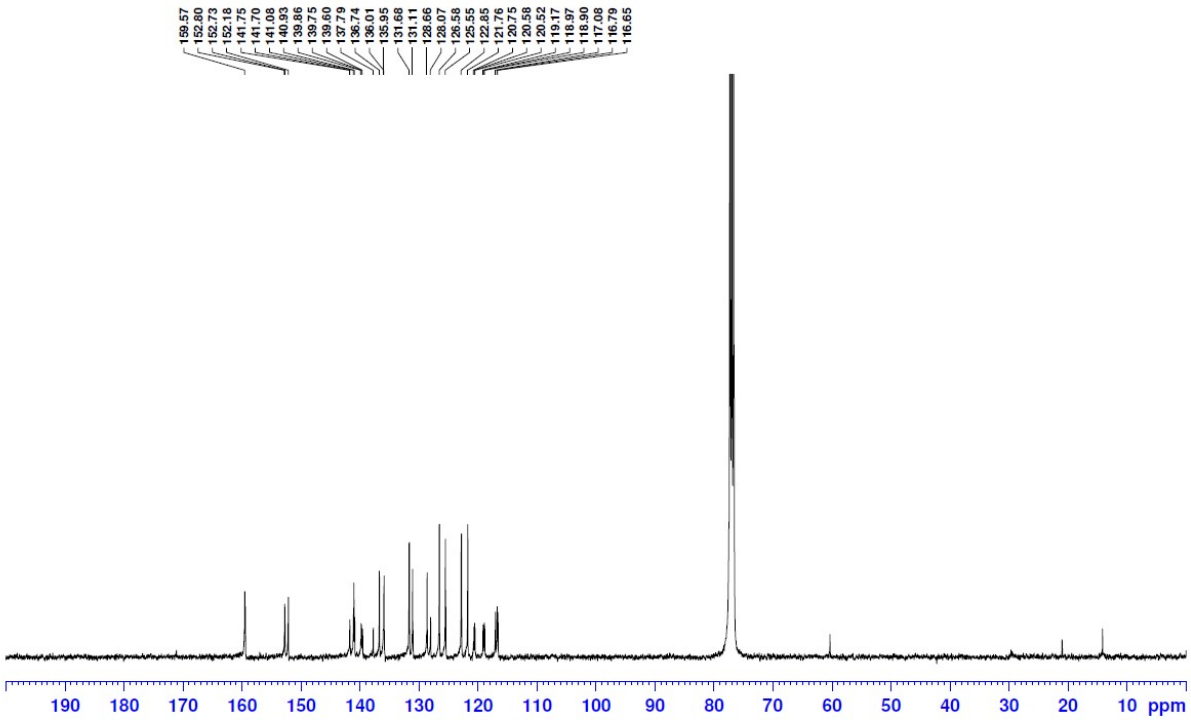

Fig. S24.2 ^{13}C-NMR of **TPE-*3*CUM**.

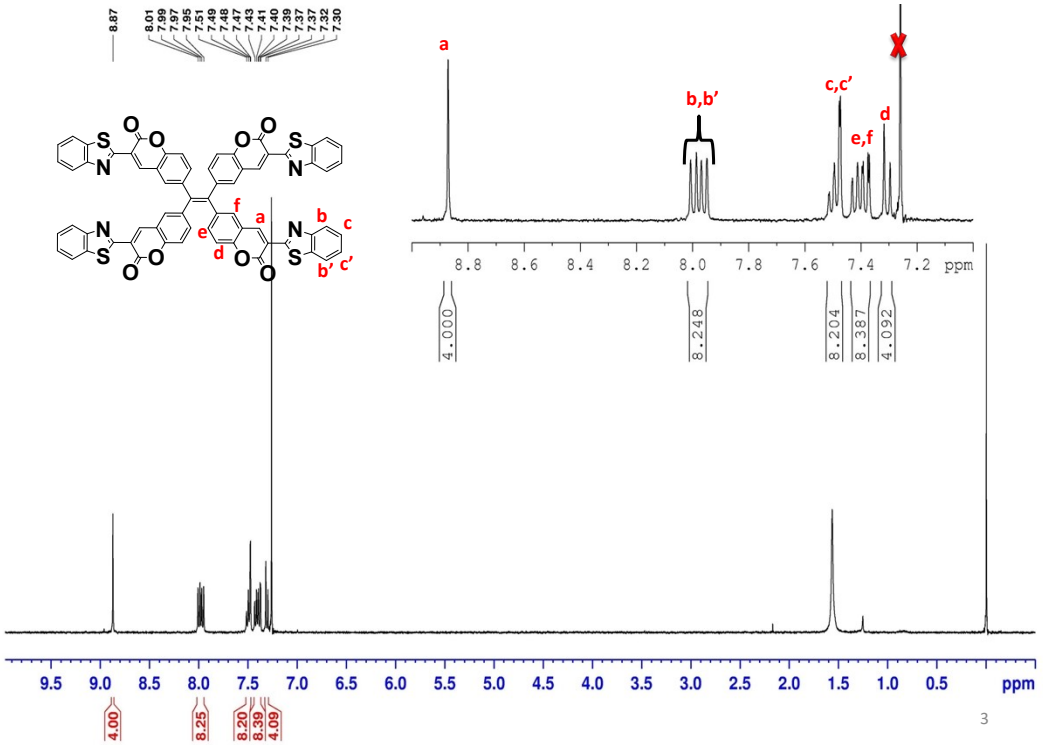

Fig. S25.1 ^{1}H-NMR of **TPE-*4*CUM**.

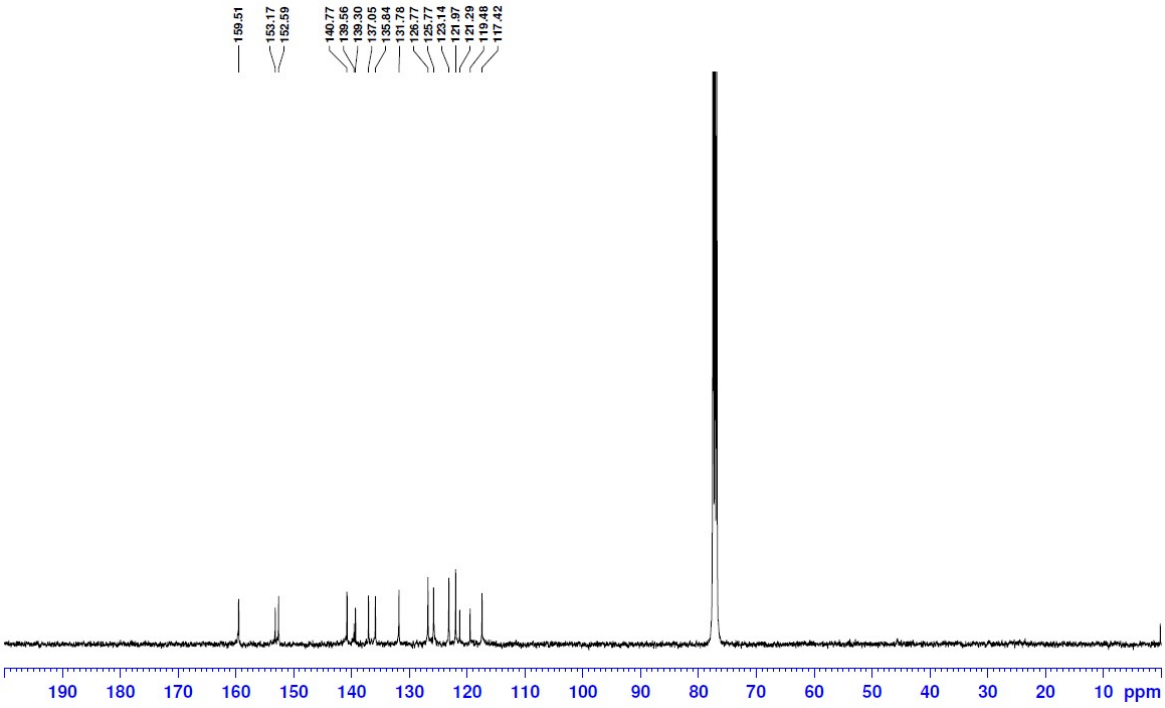

Fig. S25.2 ^{13}C-NMR of **TPE-*4*CUM**.

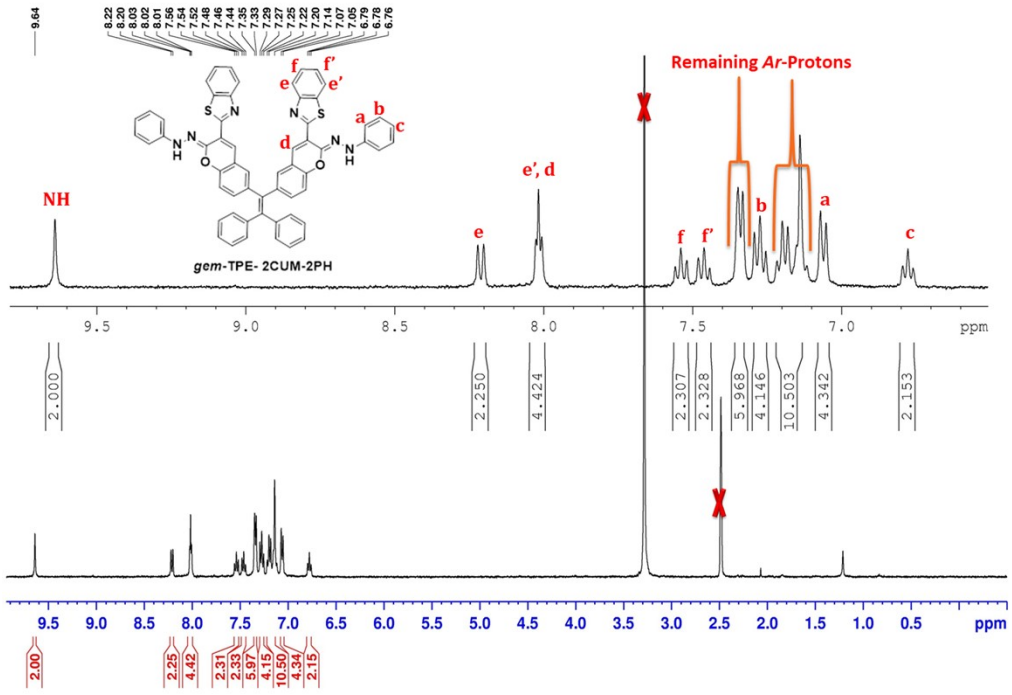

Fig. S26.1 ^{1}H-NMR of ***gem*-TPE-*2*CUM-2PH**.

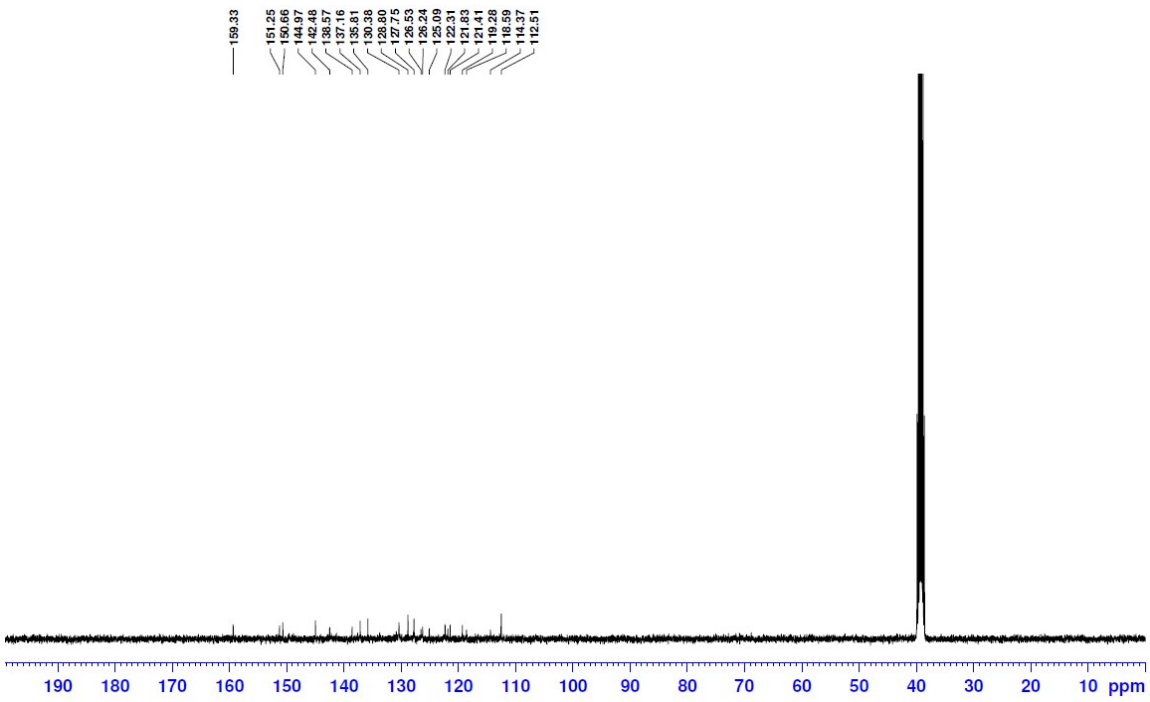

Fig. S26.2 ^{13}C-NMR of ***gem*-TPE-*2*CUM-2PH**.

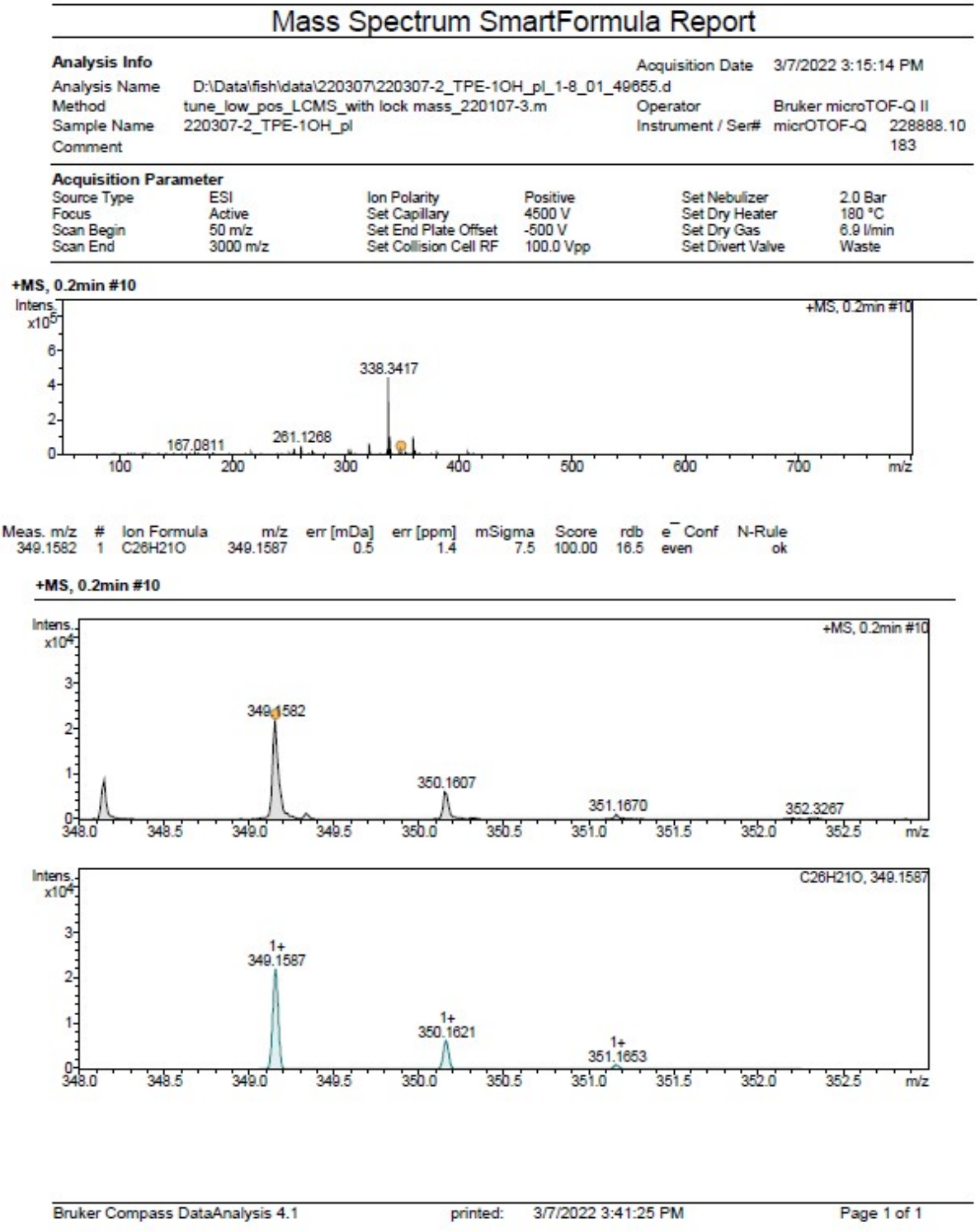

Fig. S27 HRMS data of **1a**.

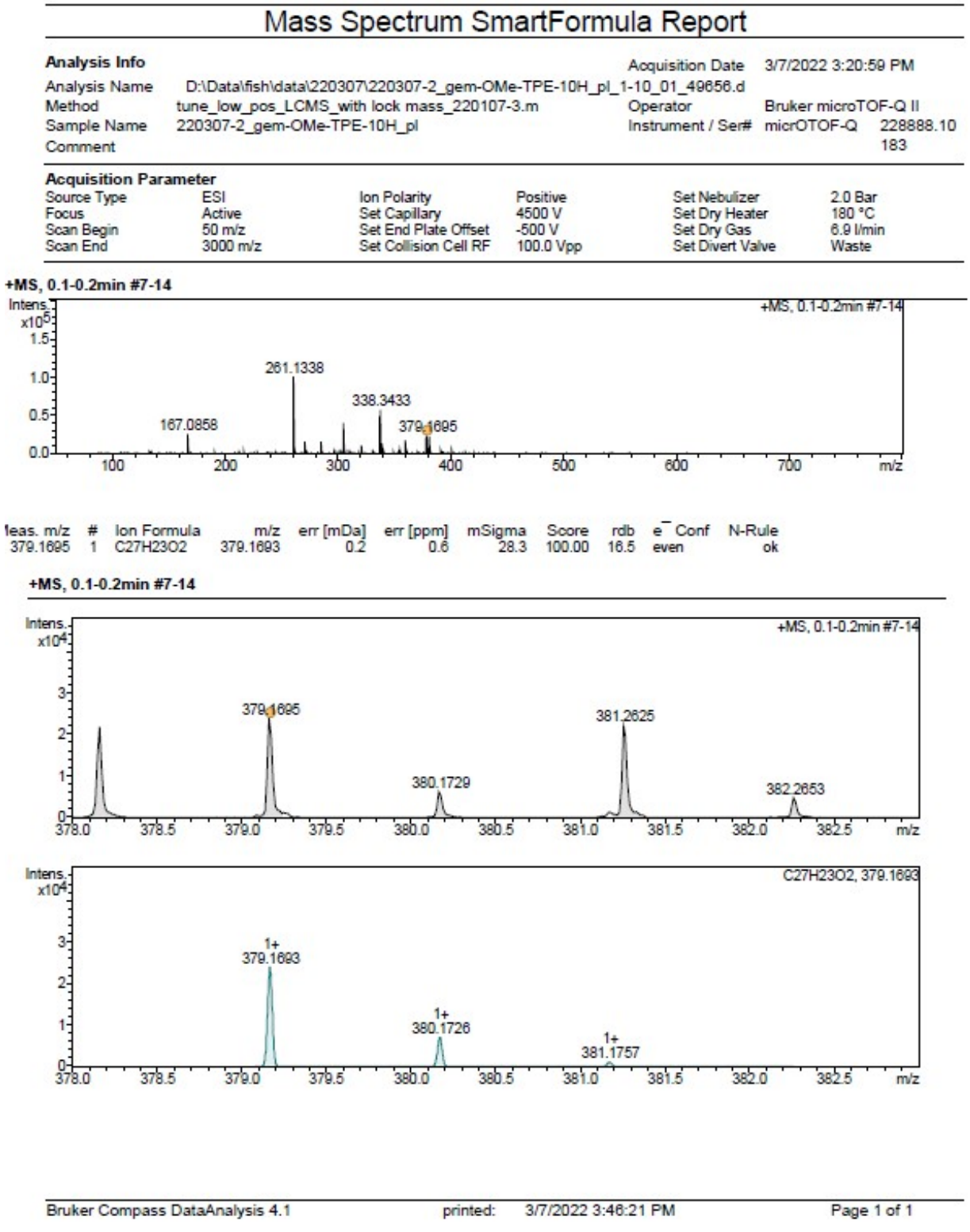

Fig. S28 HRMS data of **1b**.

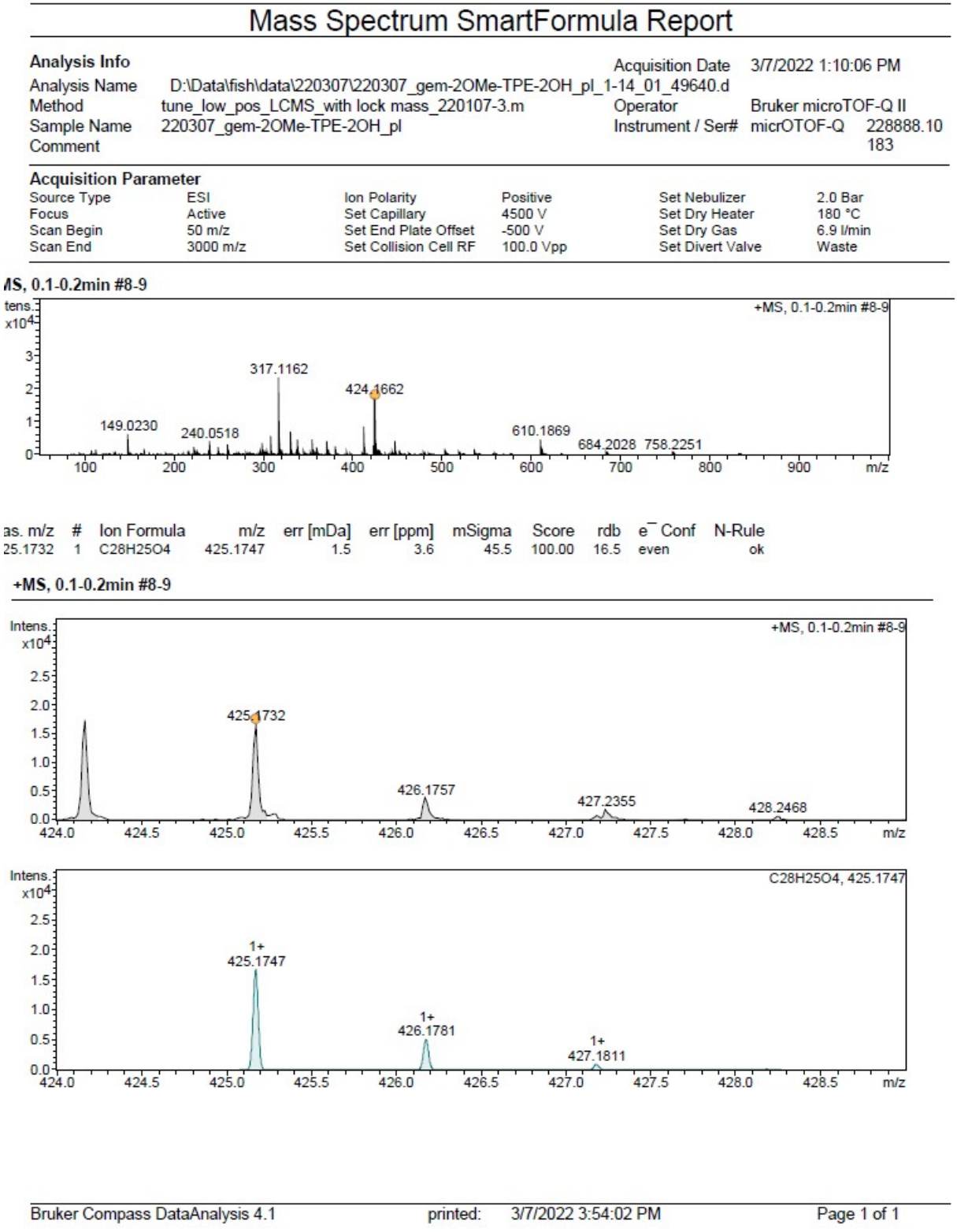

Fig. S29 HRMS data of **1c**.

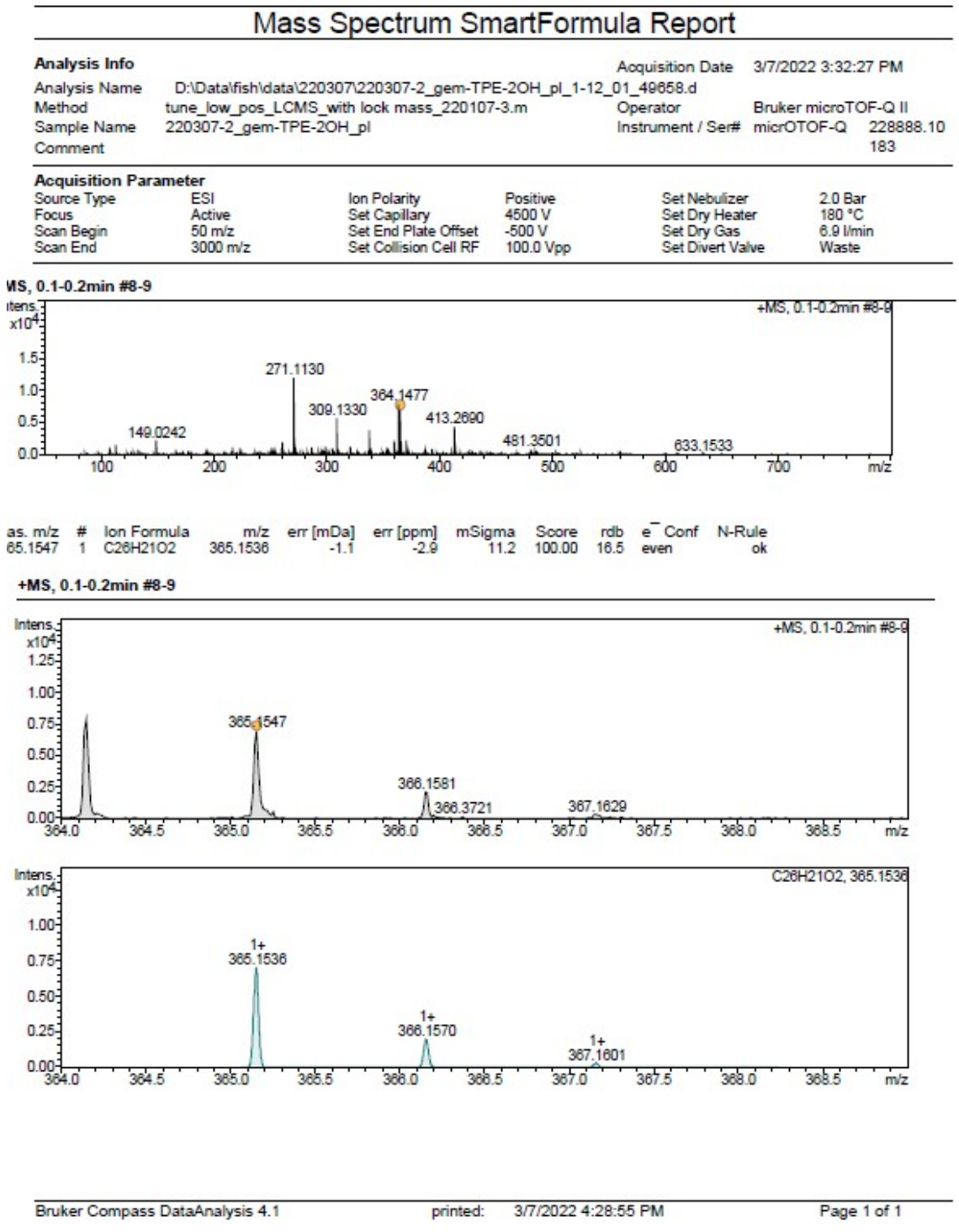

Fig. S30 HRMS data of **1d**.

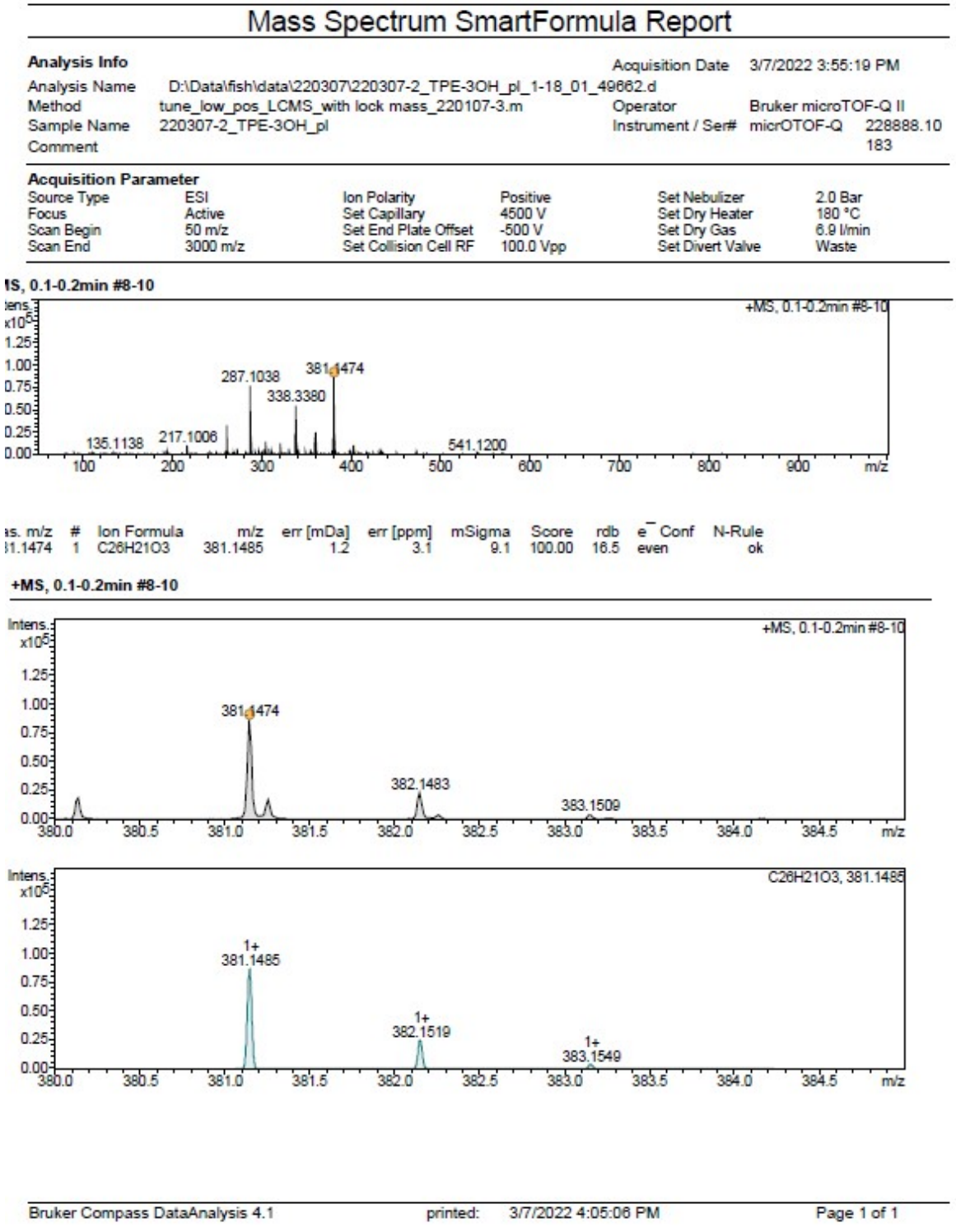

Fig. S31 HRMS data of **1e**.

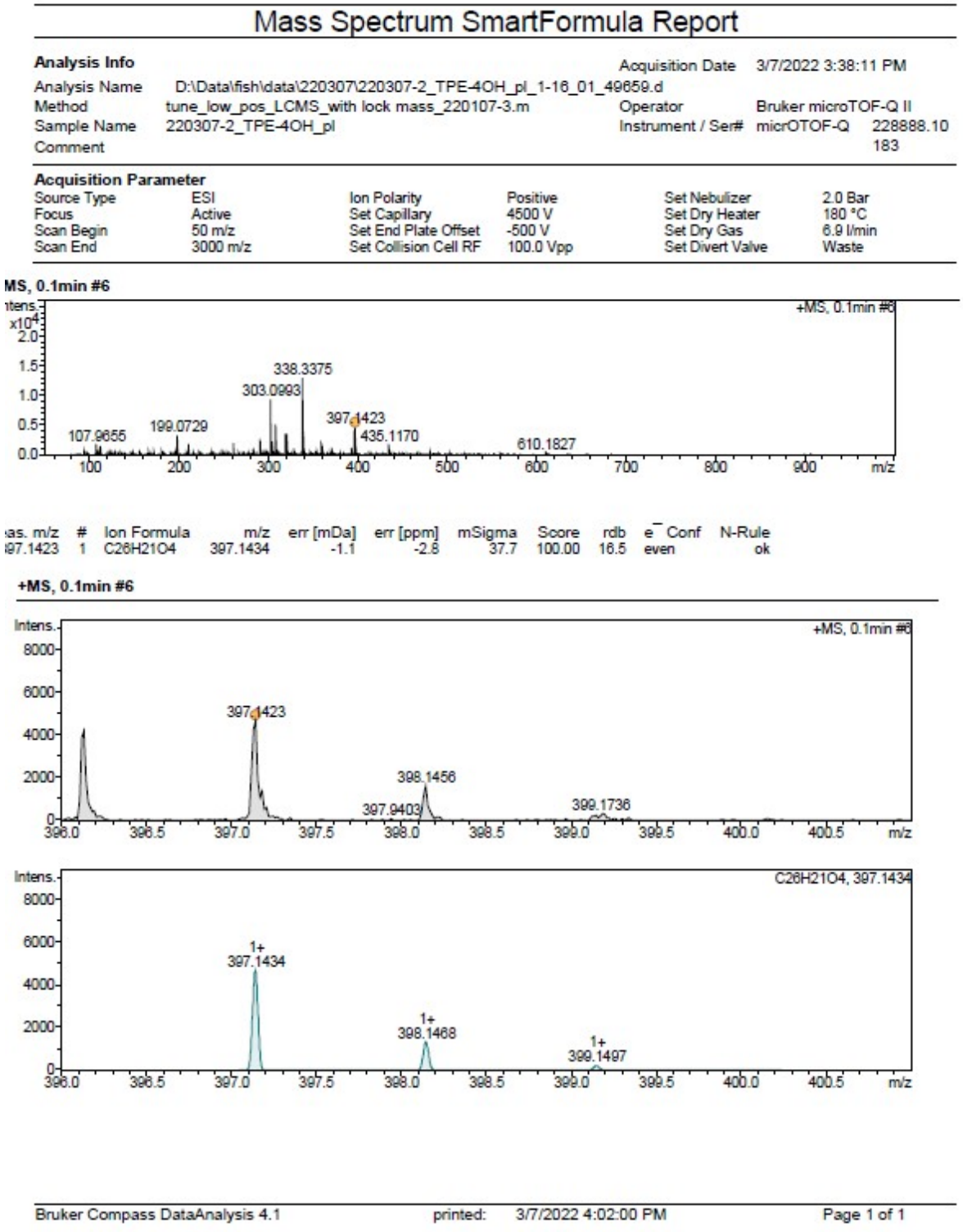

Fig. S32 HRMS data of **1f**.

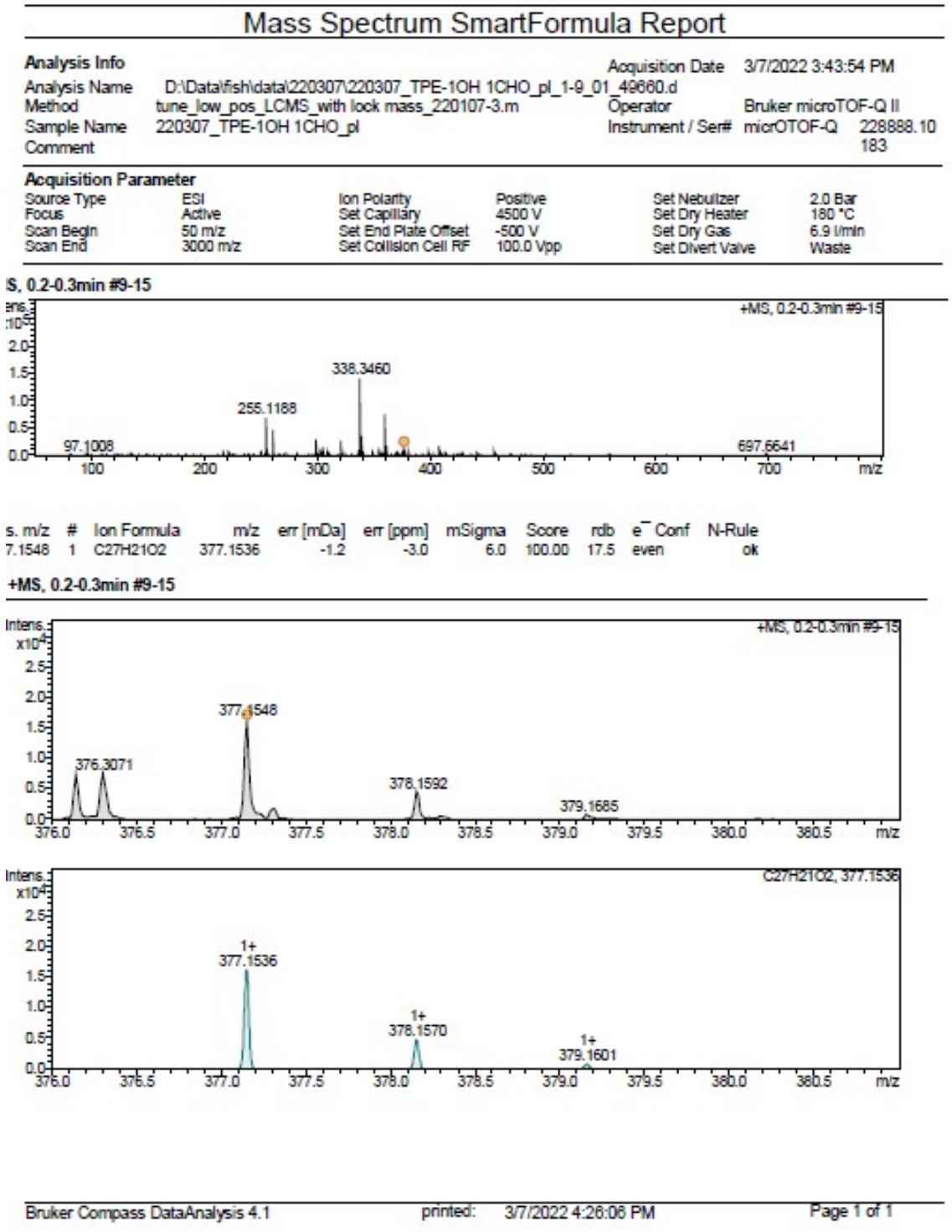

Fig. S33 HRMS data of **2a**.

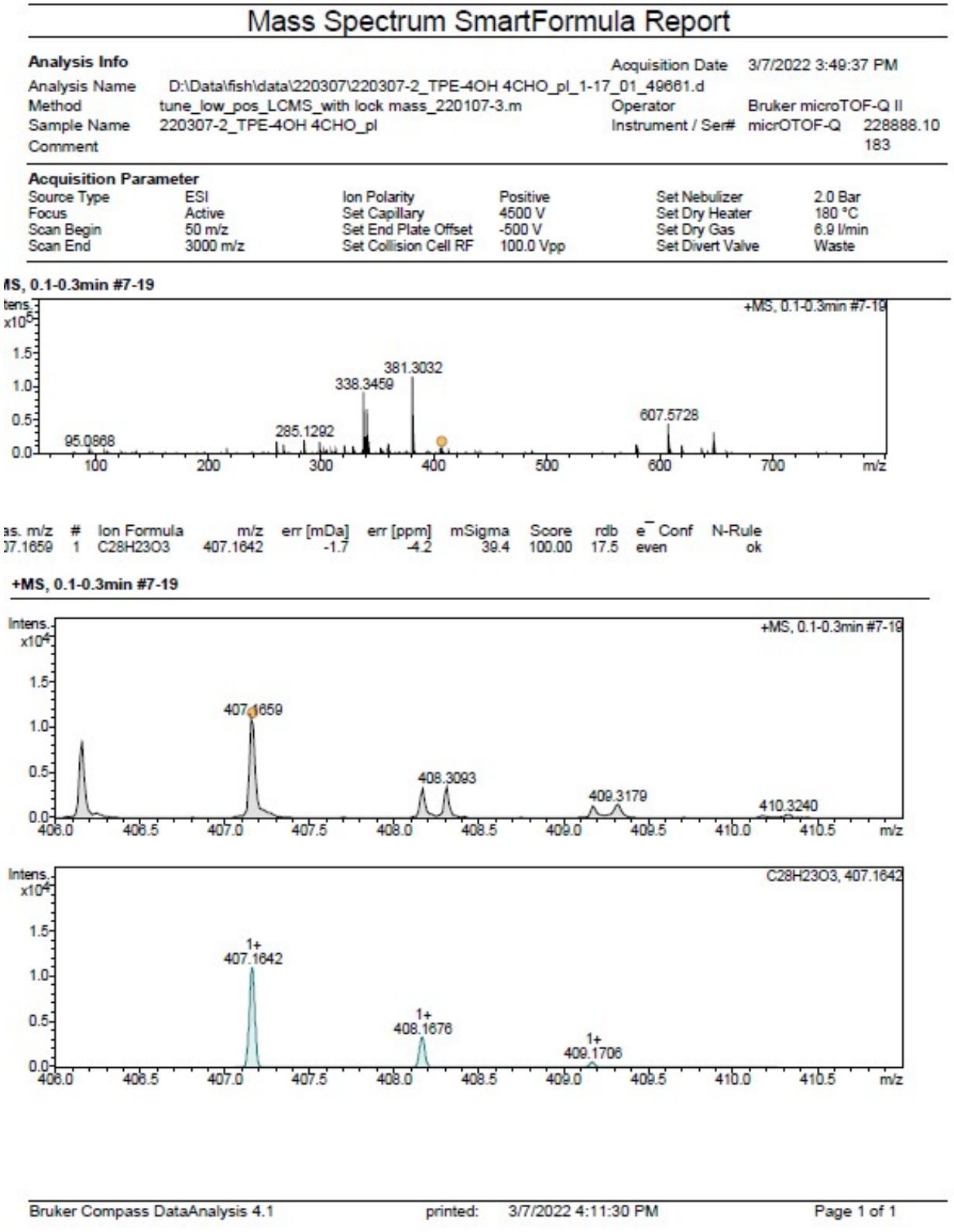

Fig. S34 HRMS data of **2b**.

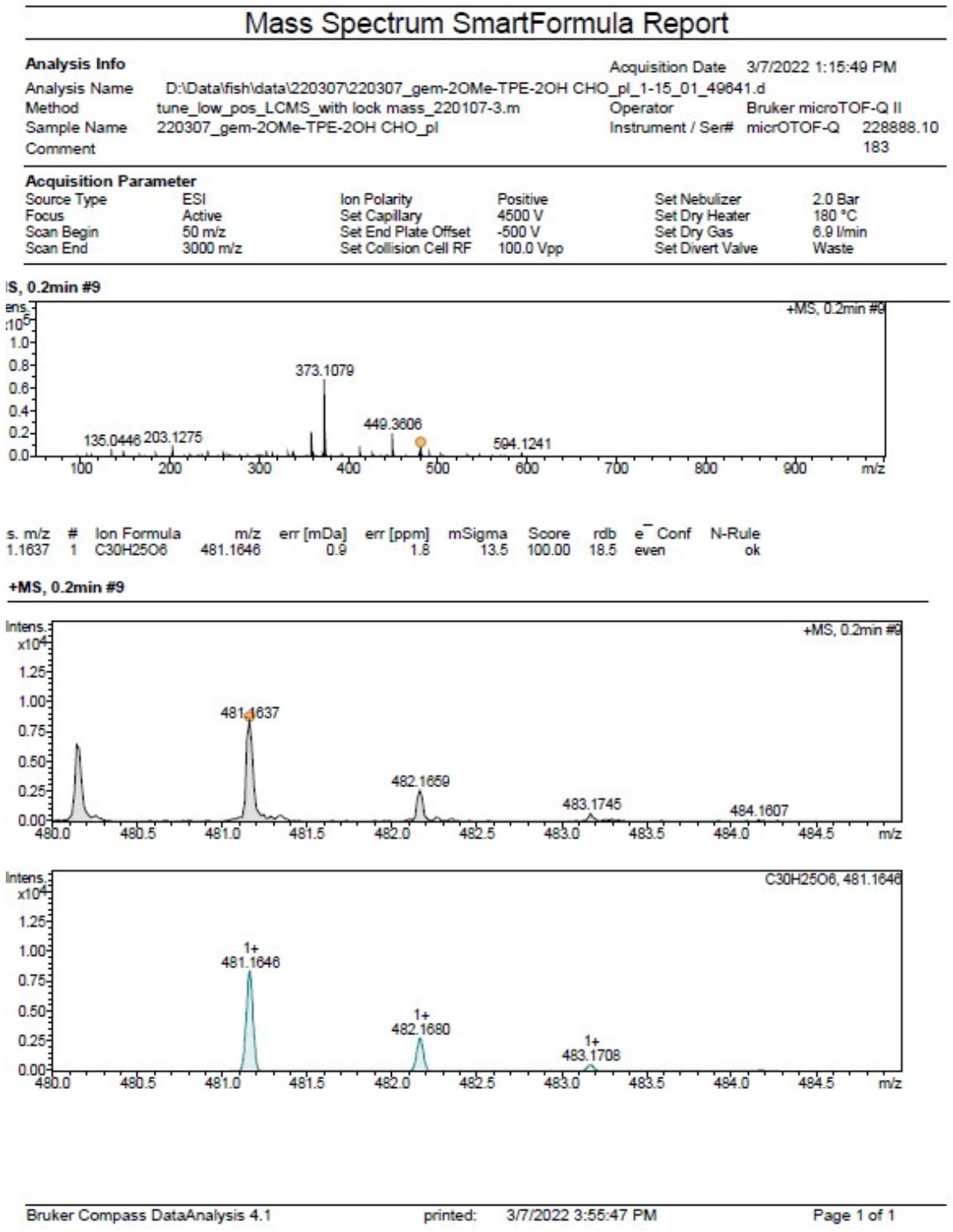

Fig. S35 HRMS data of **2c**.

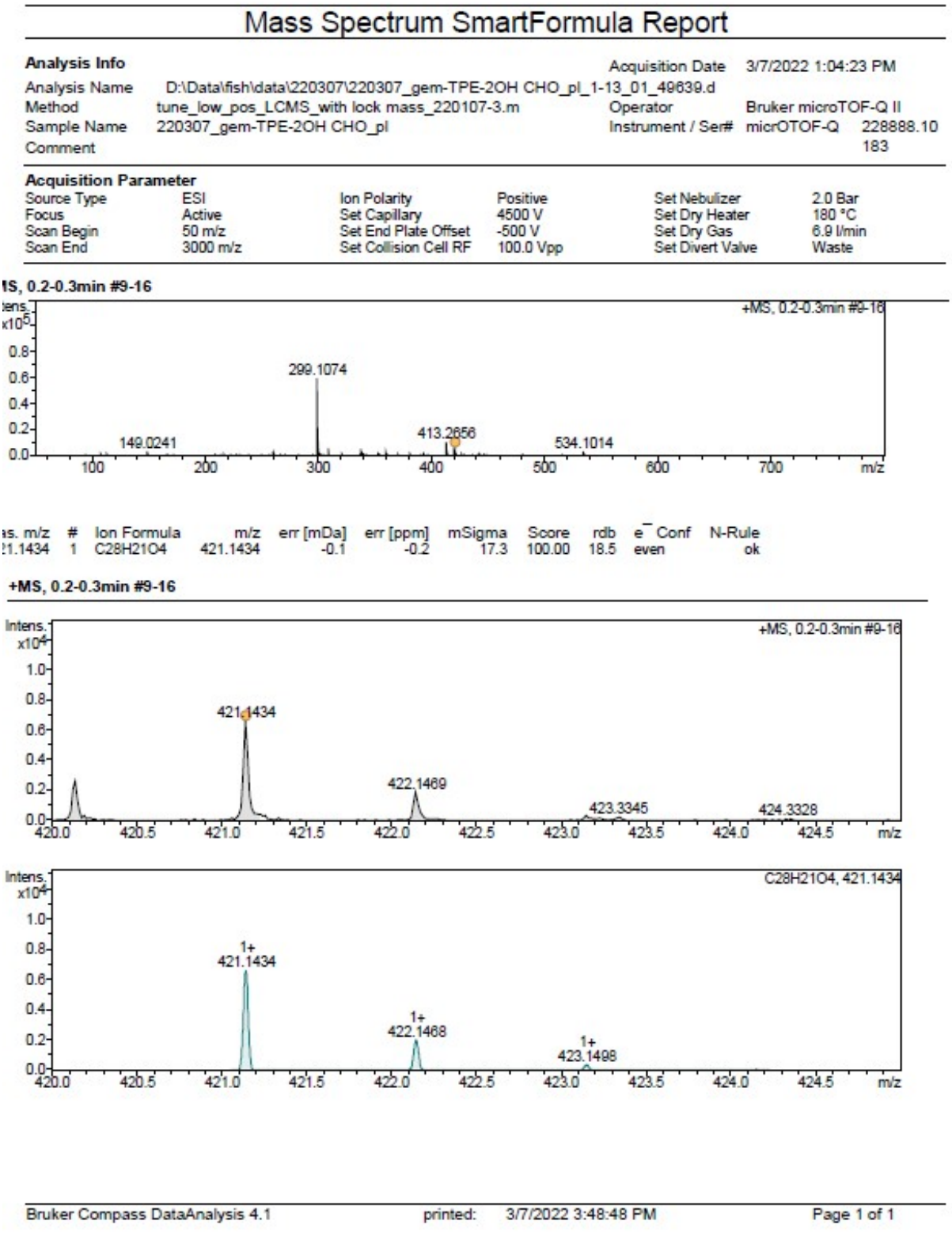

Fig. S36 HRMS data of **2d**.

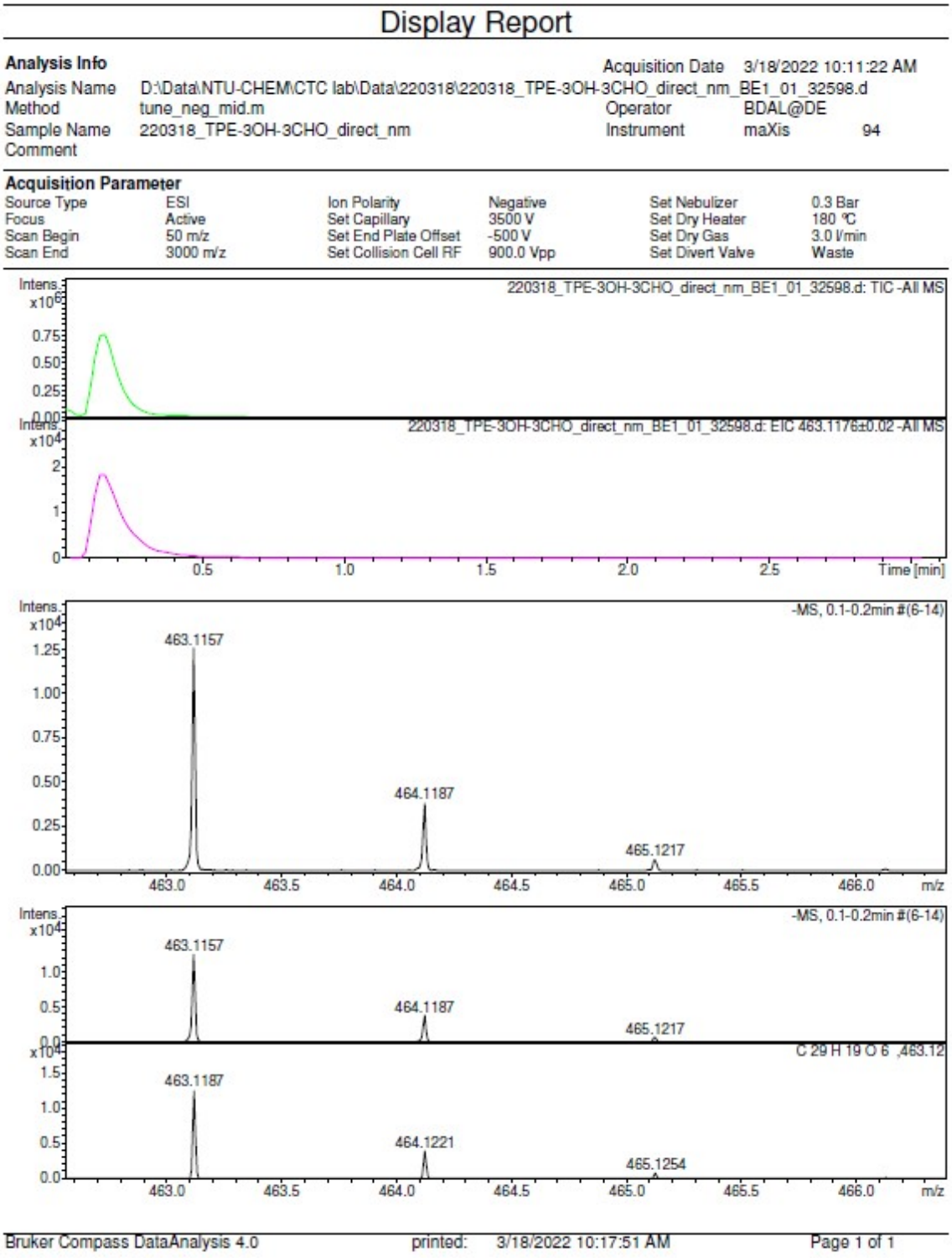

Fig. S37 HRMS data of **2e**.

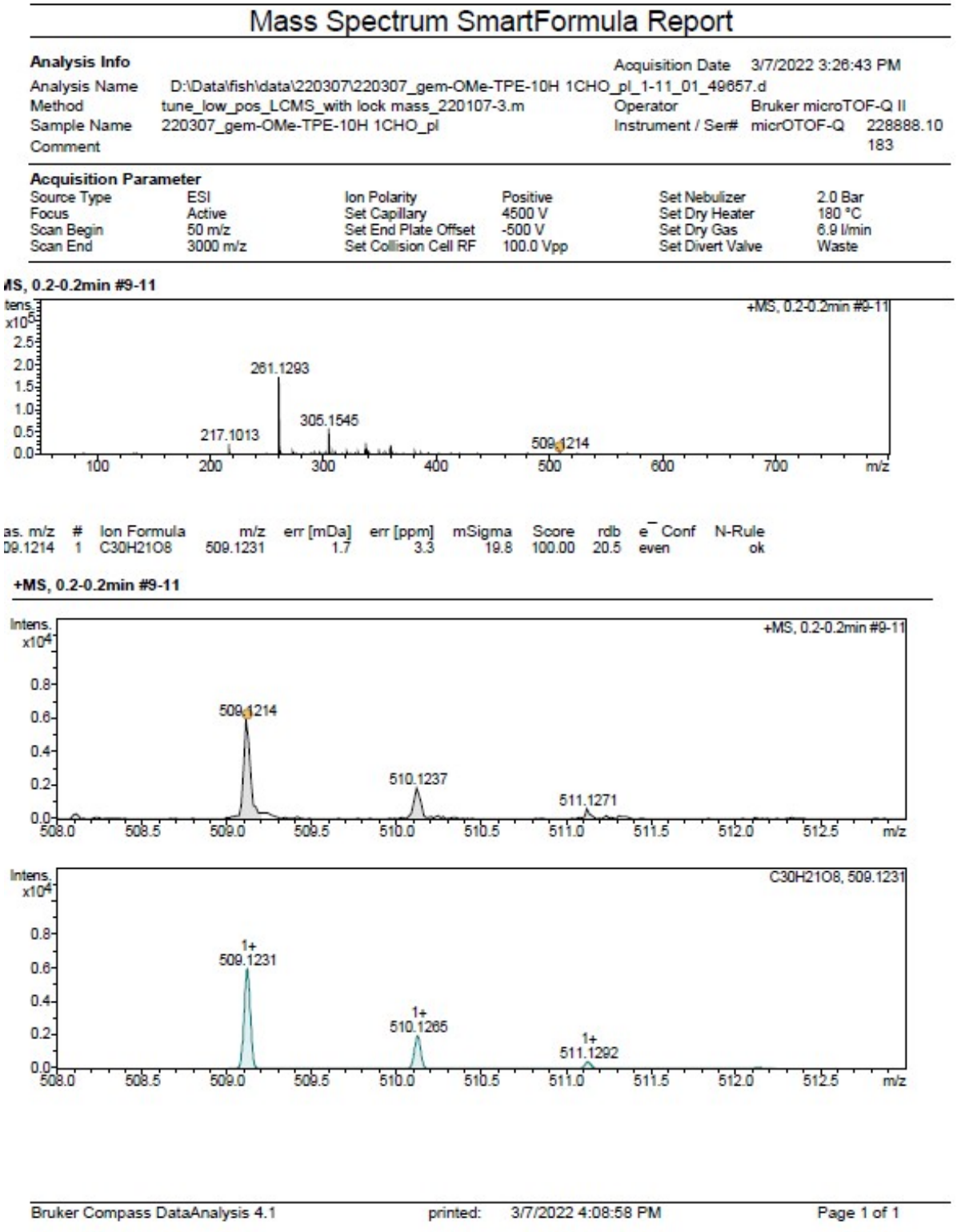

Fig. S38 HRMS data of **2d**.

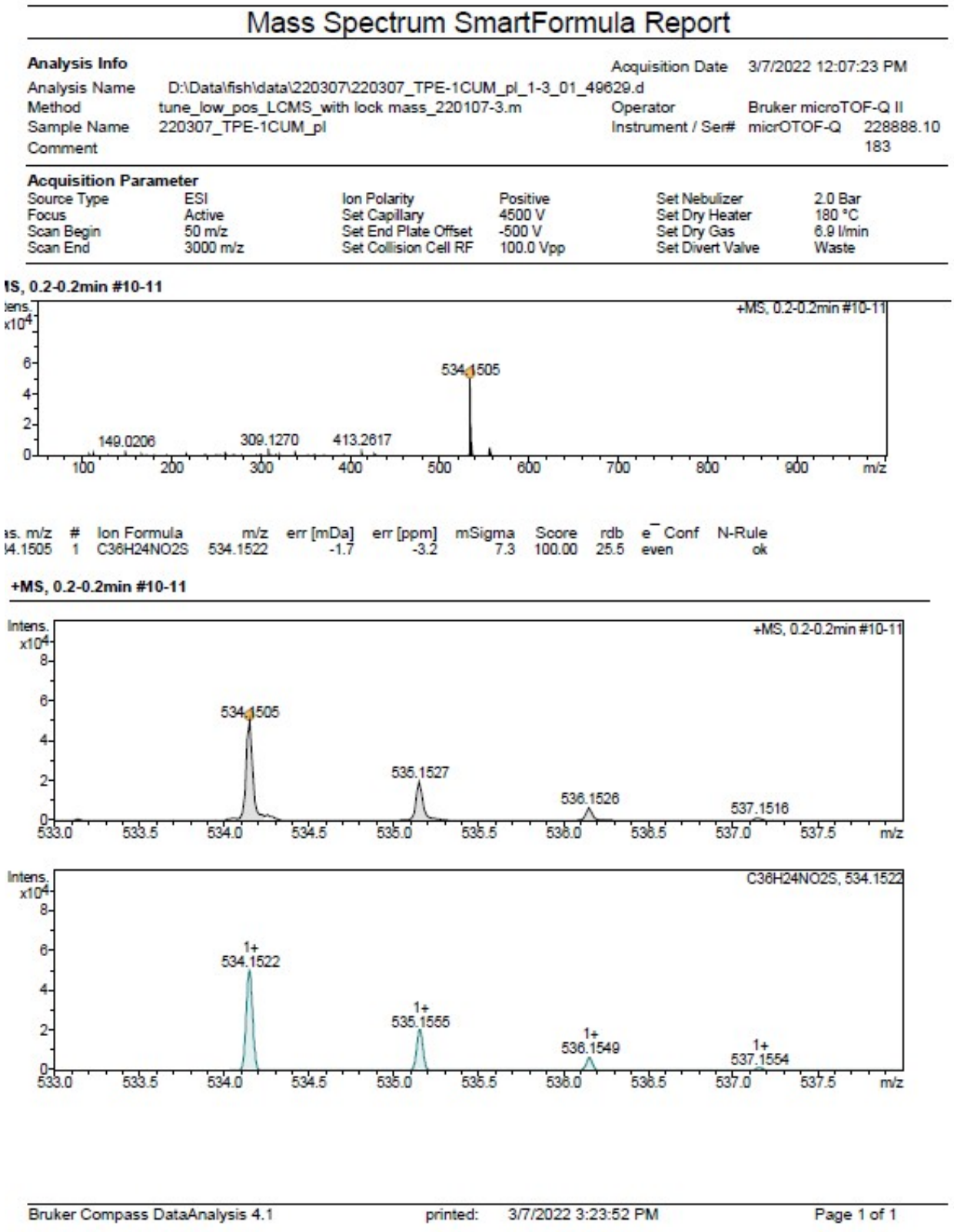

Fig. S39 HRMS data of **TPE-*1*CUM**.

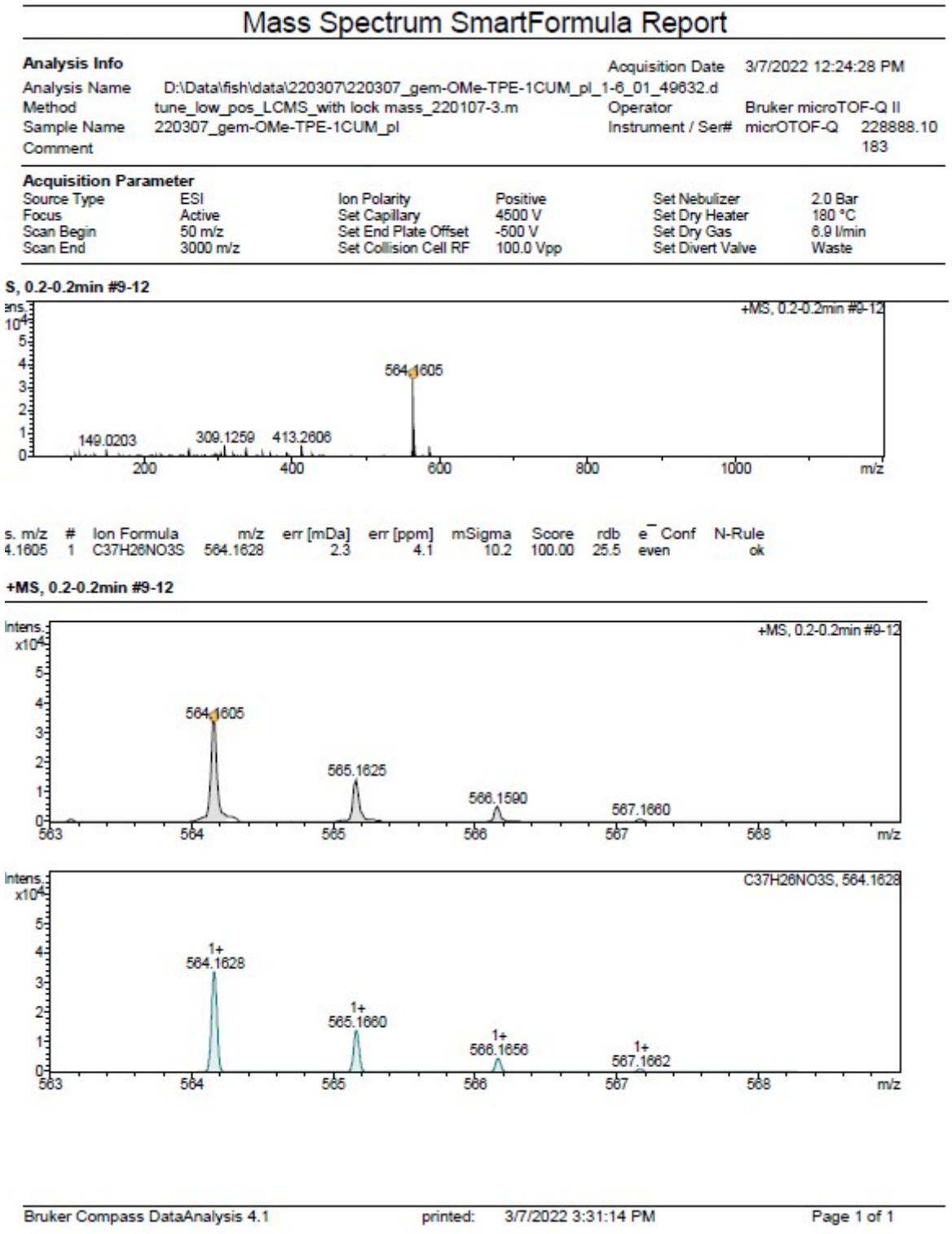

Fig. S40 HRMS data of ***gem*-OMe-TPE-*1*CUM**.

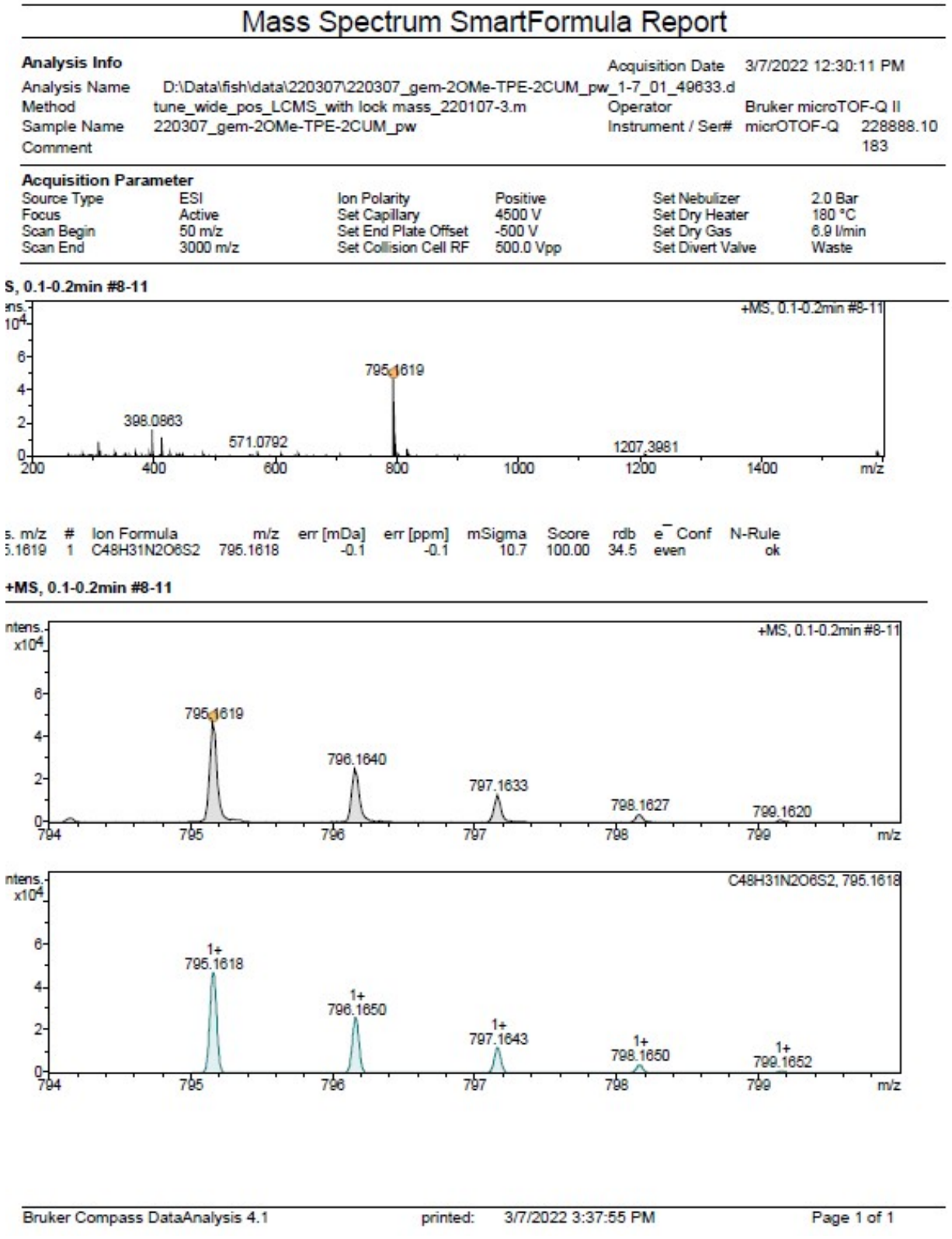

Fig. S41 HRMS data of ***gem*-2OMe-TPE-*2*CUM**.

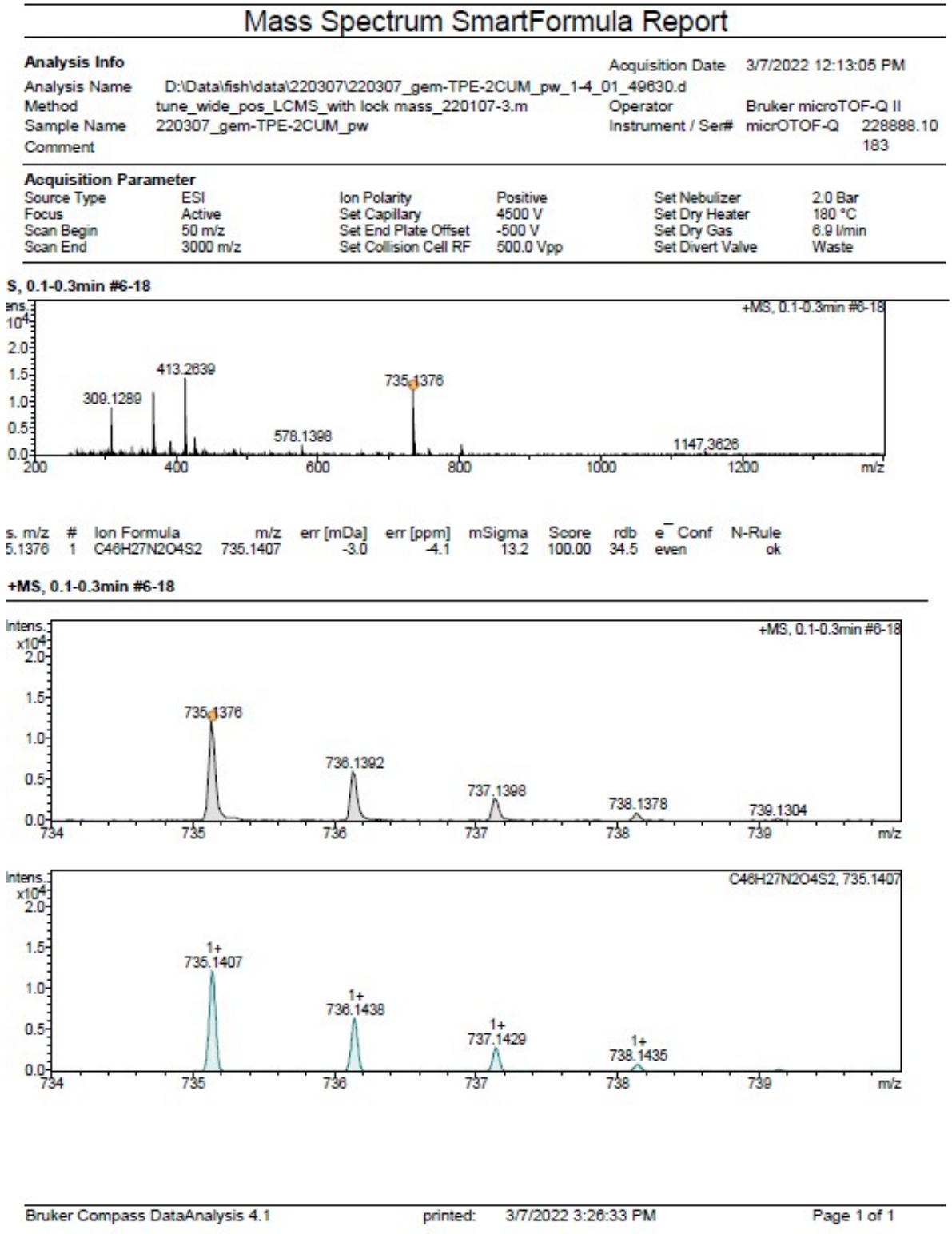

Fig. S42 HRMS data of ***gem*-TPE-*2*CUM**.

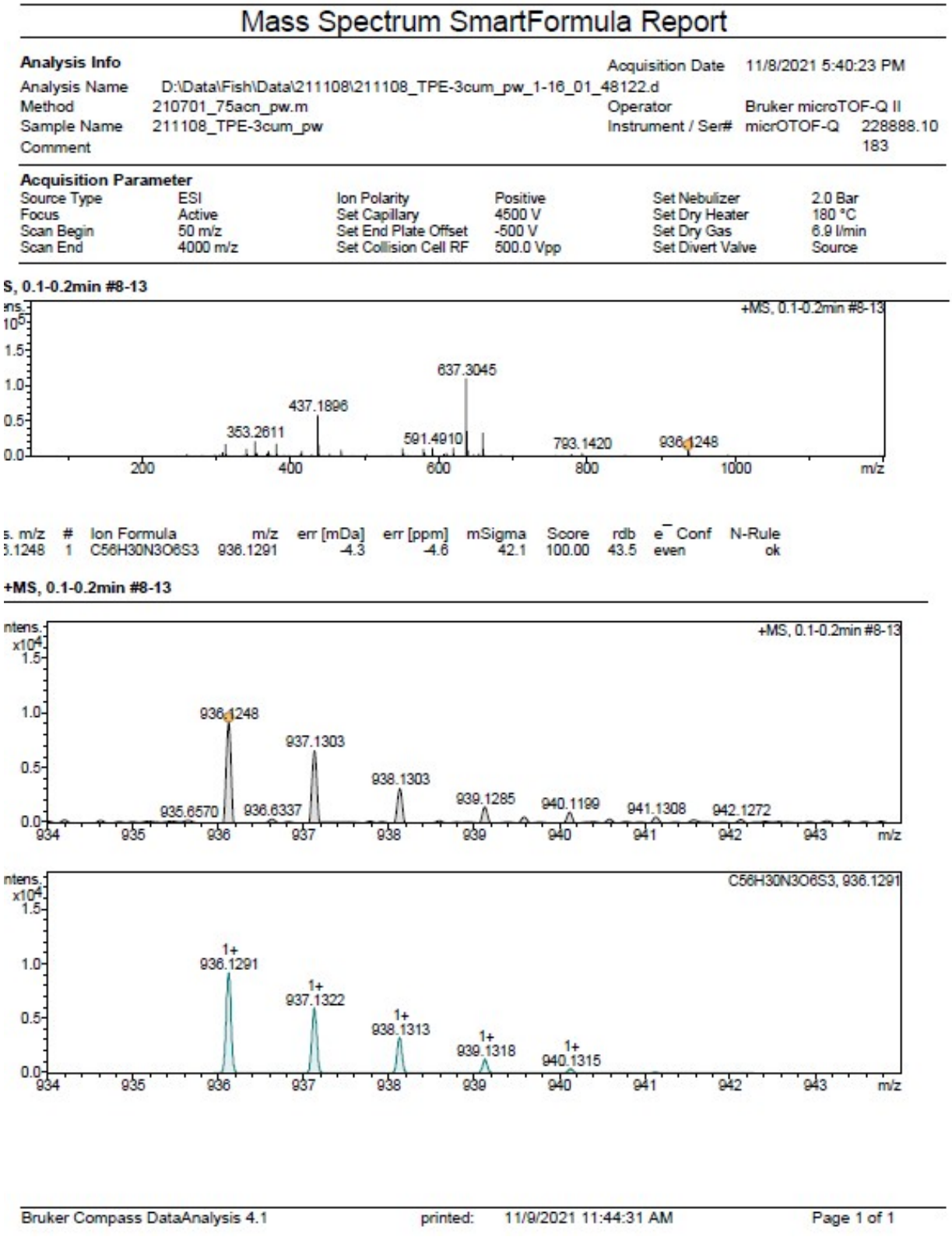

Fig. S43 HRMS data of **TPE-*3*CUM**.

Mass Spectrum SmartFormula Report

Analysis Info

Analysis Name	D:\Data\fish\data\220307\220307-2_TPE-4CUM_pw_1-5_01_49663.d	Acquisition Date	3/7/2022 4:01:04 PM
Method	tune_wide_pos_LCMS_with lock mass_220107-3.m	Operator	Bruker microTOF-Q II
Sample Name	220307-2_TPE-4CUM_pw	Instrument / Ser#	micrOTOF-Q 228888.10183
Comment			

Acquisition Parameter

Source Type	ESI	Ion Polarity	Positive	Set Nebulizer	2.0 Bar
Focus	Active	Set Capillary	4500 V	Set Dry Heater	180 °C
Scan Begin	50 m/z	Set End Plate Offset	-500 V	Set Dry Gas	6.9 l/min
Scan End	3000 m/z	Set Collision Cell RF	500.0 Vpp	Set Divert Valve	Waste

S, 0.4-0.6min #22-33

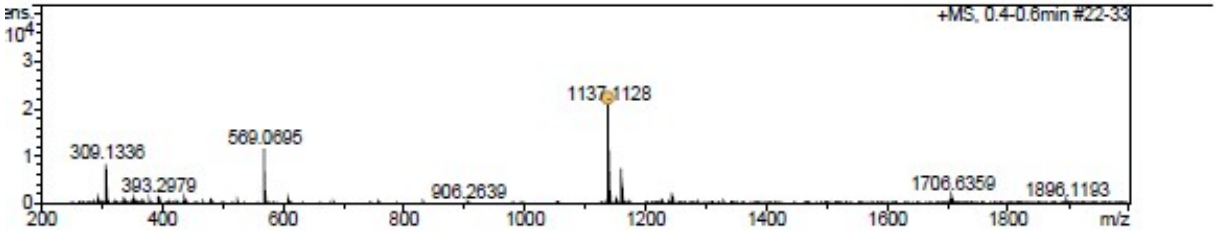

s. m/z	#	Ion Formula	m/z	err [mDa]	err [ppm]	mSigma	Score	rdb	e⁻ Conf	N-Rule
7.1128	1	C66H33N4O8S4	1137.1176	-4.8	-4.2	40.2	100.00	52.5	even	ok

+MS, 0.4-0.6min #22-33

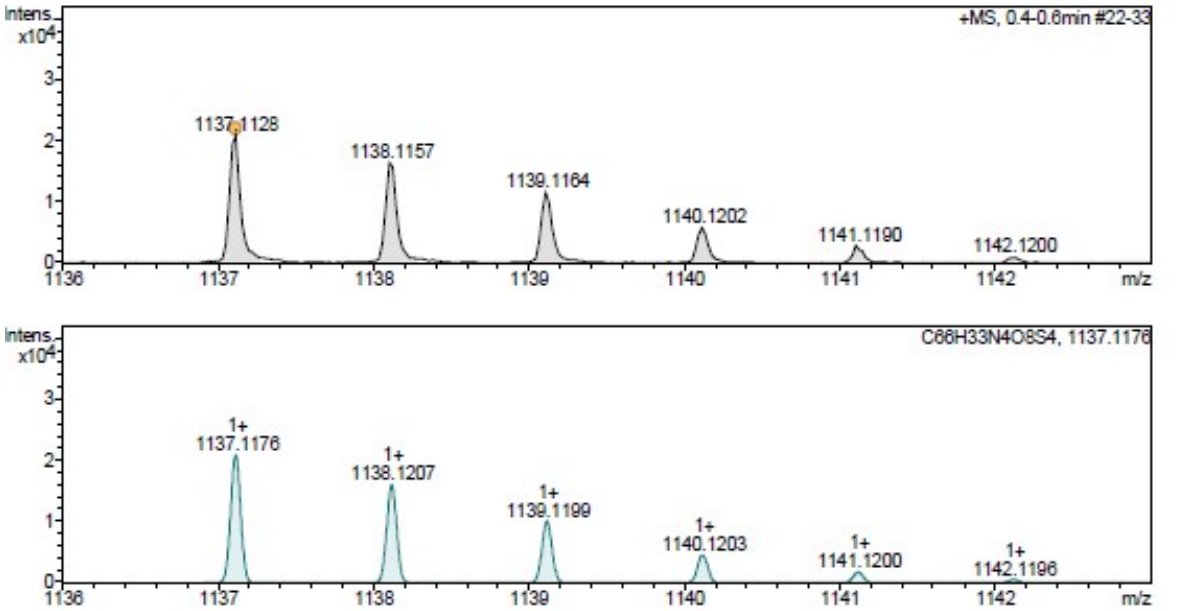

Fig. S44 HRMS data of **TPE-*4*CUM**.

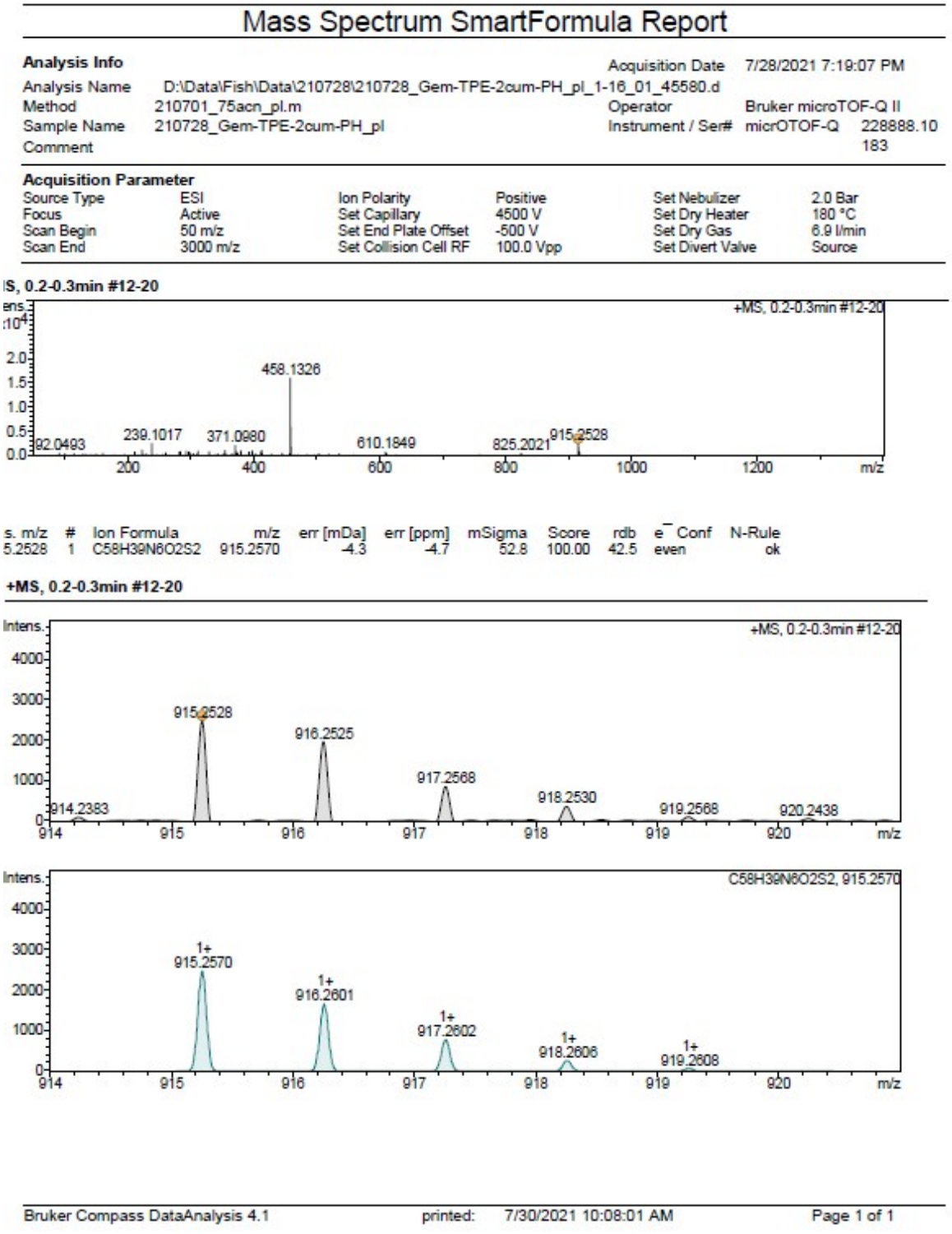

Fig. S45 HRMS data of ***gem*-TPE-*2*CUM-2PH**.

References:

1 G. Signore, R. Nifosi, L. Albertazzi, B. Storti and R. Bizzarri, *J. Am. Chem. Soc*., 2010, **132**, 1276-1288.

2 F. Ercole, N. Malic, T. P. Davis and R. A. Evans, *J. Mater. Chem*., 2009, **19**, 5612-5623.

3 J. Volmajer, R. Toplak, I. Leban and A. M. L. Marechal, *Tetrahedron,* 2005, **61**, 7012-7021.